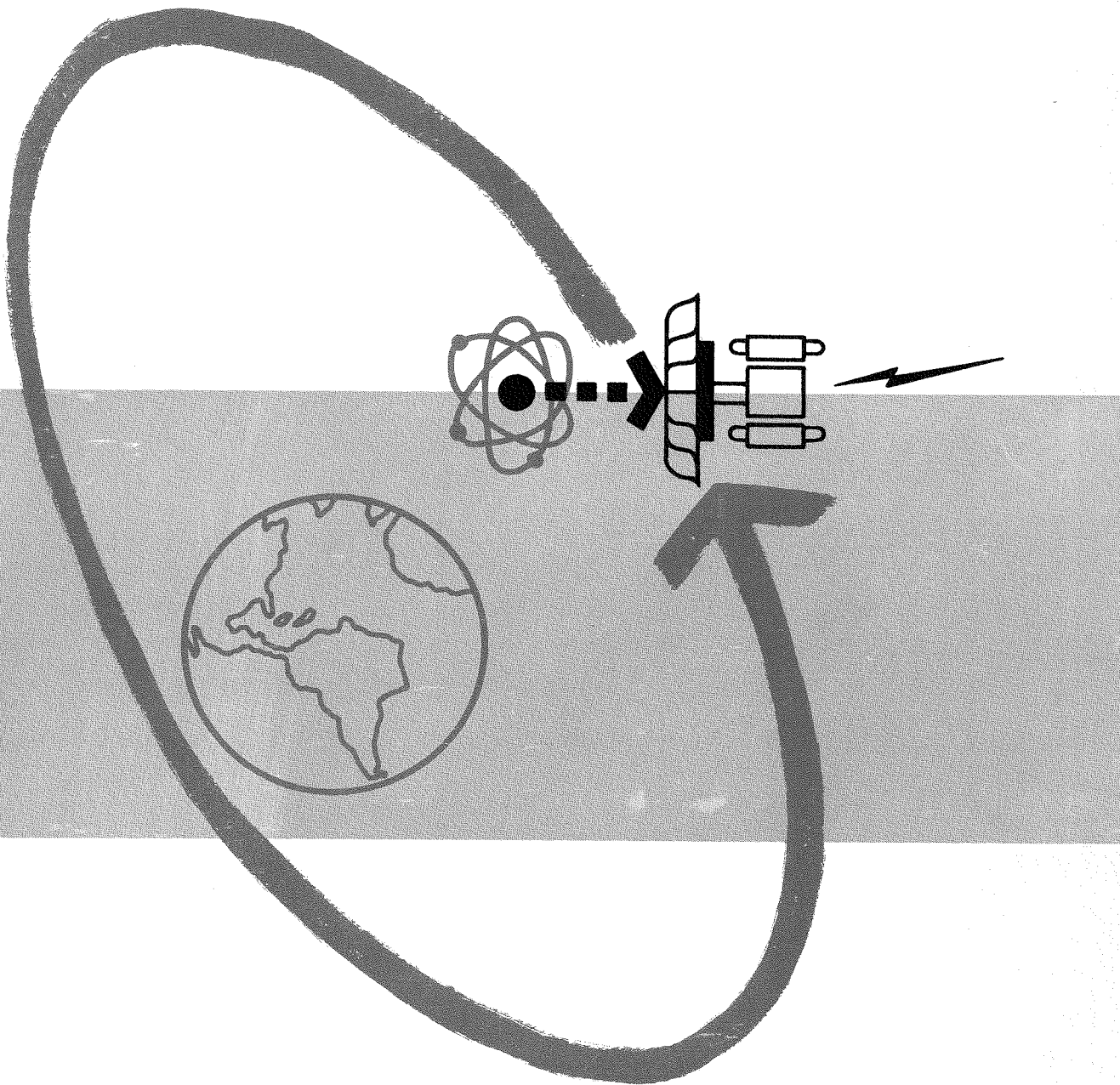REPORT No. ER-4103

THE SNAP II POWER CONVERSION SYSTEM

TOPICAL REPORT No. 7

MERCURY MATERIALS EVALUATION AND SELECTION

STAFF RESEARCH AND DEVELOPMENT
THOMPSON PRODUCTS DIVISIONS
Thompson Ramo Wooldridge Inc.
CLEVELAND, OHIO

PROJECT

562-057252-88

THE SNAP II POWER CONVERSION
SYSTEM TOPICAL REPORT NO. 7

REPORT NO. ER-4103

MERCURY MATERIALS EVALUATION AND SELECTION

PREPARED BY:

James J. Owens
James J. Owens
Engineering Supervisor
Materials Dept.

James F. Nejedlik
James F. Nejedlik
Research Engineer

J. Wm. Vogt
J. Wm. Vogt
Research Engineer

CHECKED BY:

G.J. Guarnieri
G. J. Guarnieri, Manager
Materials Development

Donald L. Southam
Don L. Southam
Project Manager

APPROVED BY:

W.A. Johnson
W.A. Johnson, Manager
Materials Engineering,
Research and Development

DATE

26 October 1960

DEPARTMENT

LEGAL NOTICE

TABLE OF CONTENTS

Page

LIST OF FIGURES

LIST OF FIGURES (Cont'd.)

LIST OF TABLES

ABSTRACT

SNAP II is the designation for a 3 KW nuclear auxiliary power unit to be used in a satellite vehicle. The SNAP II system consists of a reactor heat source, a mercury Rankine engine, and an alternator. The problems involved in selecting materials for the SNAP II mercury system have been under study for the past two years. This report presents the results of this study and discusses the corrosion mechanisms involved in a system in which mercury is the working fluid. The problem resolves itself into selecting materials with the best combination of engineering properties for the application and highest resistance to mercury corrosion at the anticipated temperature. This work was performed under a subcontract to Atomics International as part of the Atomic Energy Commission Contract AT(11-1)-GEN-8.

SUMMARY

The SNAP II auxiliary power unit for 3 KW of electrical output consists of an Atomics International reactor heat source and a Thompson Ramo Wooldridge power conversion system. The power conversion system is a mercury Rankine engine which is composed of a mercury boiler heated by a sodium heat transfer loop, an axial flow impulse turbine which extracts energy from the superheated mercury vapor, a condenser which returns the vapor to a liquid state and a mercury pump which returns the condensate to the boiler. The turbine directly drives the alternator, the mercury pump, and a permanent magnet induction sodium pump which is designed to circulate the sodium between the mercury boiler and reactor.

The SNAP II Materials Program is concerned with the selection of materials for use in the high-temperature mercury region of a high-speed compact power conversion unit. This involves the evaluation of materials for corrosion, fabrication and engineering properties. Corrosion in mercury environments at temperatures up to 1150°F is the least understood aspect of the problem and has received the most attention under this program.

This report presents the mercury corrosion data collected during the past two years under this program. The data is analyzed and conclusions are drawn. An attempt has been made to correlate the data with known theories. Admittedly, there are discrepancies in the correlation. However, it is believed that such attempts at correlation can be rewarding and cannot be disregarded.

The magnitude of the mass transfer problem has been pointed up by this study. Contaminants resulting from mercury attack can be generated in a quantity which presents a hazard of seizure of high speed rotating members and of plugging of small passages carrying mercury to bearings. Various approaches to the control of contaminants have been considered and are being investigated. The uncovering of materials highly resistant to mercury corrosion would be the most acceptable solution to the contaminant problem. Other approaches are the reduction of corrosion by additives and the control of contaminants by traps.

A new testing device, the bent reflux tube, was developed by Thompson Ramo Wooldridge Inc. and used to advantage in the studies under the SNAP II program. This device was responsible for the accumulation of a large quantity of valuable data at relatively low cost. The effects of time, composition, stress, additives, surface treatment, pretreatment and bimetallic interactions on corrosion have been evaluated by this device.

The relative corrosion of over sixty materials has been evaluated and reported. The effect of time has been investigated for some representative materials and found to vary depending on the mode of corrosion attack. Stress effects were not discernible for most materials at 900°F. Titanium when added to mercury was found to reduce corrosion for most materials. The gases oxygen, nitrogen and hydrogen are beneficial in reducing

mercury corrosion.

An attempt to remove contaminants from mercury in a loop by locating a trap in a cool region was unsuccessful.

1.0   GENERAL INTRODUCTION

The demand for achieving maximum thermal efficiency in conversion of heat into electrical energy by means of a turbine alternator system, or in heat transfer applications (especially with low vapor pressure requirements), has directed attention to liquid metals as working fluids.

1.1   The Problem

The materials problems of liquid metal systems are due primarily to corrosion and other related phenomena of interaction (2)(3)(7)*. Consequently, materials which are in contact with the liquid metal must resist corrosion and other interactions. Liquid metal systems operate generally at high temperatures and are subject to large thermal gradients. Structural requirements, oxidation resistance, fabricability, weldability and all other problems encountered in fabrication are important considerations in any evaluation for practical application. These requirements limit the number of materials to a relatively few metals and alloys. Other special physical property requirements also may further limit the choice of available materials, such as magnetic properties, thermal expansion, and conductivity.

In power conversion equipment the presence of either dissolved material or "crud"**in the heat transfer liquid may seriously hamper the functioning of the rotating package and limit its life expectancy severely. The probability that some dissolved material will exist in the liquid system is extremely strong. Since most of the dissolved material may exist with a particle size no larger than a colloid, conventional filters may be inoperative. New methods of filtering may have to be found if "crud" generation cannot be reduced to tolerable levels for available engineering materials.

1.2   Liquid Metal Corrosion Mechanism

Liquid metal attack is generally dependent upon solubility and solution rate unless chemical interaction occurs (2)(3)(6)(7). However, solubility and diffusion barriers may be developed in the form of surface films of various nature (2) (3).

---

* Figures appearing in parentheses pertain to the references appended to this report.

** "Crud" The insoluble corrosion products formed in the mercury.

The known types of liquid metal attack are:

1. Simple solution of solid metal into liquid metal.

    a. Uniformly
    b. Intergranularly
    c. Leaching of an alloy constituent

2. Alloying between liquid metal and solid metal.

3. Temperature gradient mass transfer.

4. Concentration gradient (or dissimilar metal) or isothermal mass transfer.

    a. Alloying between solid metals, one or both of which may have some solubility in the liquid metal
    b. Solubility effect of one constituent upon another

5. Energy gradient mass transfer.

Variables which may affect the corrosion process are:

1. Temperature and heat flux.

2. Temperature gradient and cyclic temperature fluctuations.

3. Ratio of surface area of solid metal to volume of liquid metal.

4. Flow velocity of liquid metal.

5. Purity of the liquid metal.

6. Surface condition and treatment of the solid metal.

7. The type and kind of materials in contact with the liquid metal.

8. Metallurgical effects.

    a. Pure metal
    b. Alloyed metal

        1. Solid solution
        2. Intermetallics and other phases

c. Stress state
d. Grain size
e. Heat treatment

9. Composition of the gas over the liquid metal.

Simple solution is due to the fact that a solid metal may have some finite solubility in a liquid metal. Table 1 lists reported (17) equilibrium solubilities of various metals in mercury at room temperature, which are extremely small (ppm) for most metals. The solubility increases exponentially with temperature in accordance with the Arrhenius equation as shown in Figure 1.

The dissolution may be uniform or intergranular. In a solid solution type alloy, a leached zone may develop if one constituent has a greater solubility or rate of solution. Intergranular penetration may result from preferential attack on secondary phases segregated in the grain boundaries. It may also be due to the higher diffusion rates found in the grain boundaries. The solid metal-liquid interfacial energy relationships at the grain boundary also favor preferential wetting at the grain boundaries.

Under static, isothermal conditions, dissolution is generally a function of time, temperature, and solid surface-to-liquid volume ratio. The solution rate decreases as the solution approaches saturation. At saturation, equilibrium may be reached and attack then ceases. However, attack may continue along with deposition or mass transfer in order to reach a more stable solid metal geometry, or if certain crystal faces (12) in contact with the mercury are less resistant to attack than others (in fulfillment of interfacial liquid - solid energy requirements). This dissolution and desposition process is known as energy gradient mass transfer.

Under dynamic conditions, severe corrosion may be due to temperature gradient mass transfer. A small difference in the solubility of the solid metal in the liquid metal at temperatures differing on the order of only about 10°F (or less) is sufficient to cause solution in the hotter regions and deposition in the colder regions of a system due to supersaturation of the liquid metal (2). Generally, the rate will increase to a maximum with a larger temperature gradient.

The rate of attack increases exponentially with temperatures because diffusion, reaction rates, and solubility all increase exponentially with temperature. Temperature fluctuations may produce alternate solution and deposition.

The mass transport process is dependent upon:

1. Dissolution-transfer of atoms from the metal surface across the liquid-solid interface into the boundary layer.

2. Diffusion of atoms through the boundary layer into the bulk liquid metal.

3. Transport of dissolved metal from hot to colder regions by the liquid flow.

4. Nucleation and growth of the dissolved metal into crystals.

The process may be diffusion controlled if a barrier film is present, or if leaching of one component has resulted in the formation of a new phase or composition which is more inert to corrosion.

Precipitation of the supersaturated solution of solute metal in the liquid metal may not necessarily occur in the coldest region of the system. Nucleation and growth of the precipitate will occur only in the region of the system where the temperature range is optimum for these processes. The presence of other solutes in the liquid metal may also influence nucleation and precipitation.

The dissolved metal may also be carried* in wet mercury vapor, probably through the vapor region of the system.   The probability of having a "wet" mercury vapor is high due to thermodynamic considerations summarized by the Gibbs-Helmholtz relationship (vapor pressure vs. droplet size) (19).

Alloying between the liquid metal and solid metal is dependent upon some solubility of the liquid metal in the solid metal. Solid state diffusion into the bulk solid may result in the formation of new phases or intermetallics which can alter the heat transfer characteristics, solubility, and other properties of the solid metal.

Concentration (dissimilar metal) or isothermal mass transfer may occur when different solid metals are in contact with the same liquid metal, even in an isothermal or static environment. Any solubility of one metal or both in the liquid metal will result in the transfer of some metal from the solution to the other metal if there is some affinity between the two metals such as

---

*"---it has been known for over half a century that distillation (of mercury) carries over appreciable amounts of less volatile, but more easily oxidizable, metals with the mercury ---"(1).

compound or solid solution formation. A solid diffusion zone may build up on the solid metal surface or reaction products may be formed and precipitated in the liquid metal.

The purity of the liquid metal is an important variable which may affect the corrosion rate in a number of ways. First of all, the activity of the liquid metal is likely to be affected, which will manifest itself in changing the vapor pressure of the mercury (and consequently the boiling and condensing temperature). Secondly, the wetting tendency (forces which give rise to the phenomenon of wetting are identical with those which cause chemical reaction and solution) may be increased, since the liquid-solid interfacial energy between the liquid and solid metal may be reduced. The liquid-solid interfacial energy is known to decrease with increasing solubility of a solute in the liquid according to Gibb's adsorption isotherm equation, since the interface of the liquid metal may contain a different solute solubility limit from the interior.

The increase in corrosion rate of a solid metal by a liquid metal in the presence of a dissolved metal in the liquid metal (6)(8)(16) may be similar to that found in other corrosion environments where there may be an induction period during which some metallic material may go into solution and then be deposited on the solid metal surface, thereby causing increased or accelerated attack by increasing the wetting tendency and possibly by causing cell concentration action. For instance, in gold amalgamization it is well known that mercury with some dissolved gold is a considerably better amalgamator then pure mercury(13).

The corrosion rate may also be accelerated by a nucleation phenomenon of some sort such as intermetallic formation (12).

The surface condition of the solid metal is undoubtably of considerable importance in determining the solution behavior, especially at lower temperature. The presence of a Beilby* layer, impurities, imperfections and discontinuities, occluded gases in varying quantities, and the stress state may all have a considerable affect on corrosion, by introducing other reactions, by interferring with metal removal or by changing the wetting tendency.

It is highly probable that electron transfer occurs across a solid metal-liquid metal interface, resulting in an electrical double layer. This layer has important consequences on the surface properties and is undoubtably affected by the presence of dissolved constituents.

*Harder, more soluble and anodic, and is able to dissolve other metals.

Surface roughness is of secondary importance, for if a material resists wetting, surface roughening would reduce the wetting tendency and attack since the valleys would tend not to be filled with liquid. On the other hand, if the material is wetted, then a smooth surface is best to reduce the amount of surface area exposed to attack.

Alloys may be more or less resistant to corrosion than pure metals. The former may be true if alloys form intermetallic compounds or if some measure of passivity is achieved by a change in electronic structure of the solid solution. The strength of the bonds which must be broken for solution to take place is increased in either case. On the other hand, the presence of multiphase or inhomogeneous metal results usually in a reduction in solid interfacial energies, which means that the liquid-solid wetting tendency may be enhanced. Thus, if corrosion is controlled at the metal surface, a homogeneous metal would resist attack better than a multi-phase metal. Grain orientation exerts an effect since various crystal faces have diverse solution rates and stability. Also, the grain size should have some effect, since the wetting tendency is increased along with diffusion rates with decreased size. Lattice type should be relatively unimportant in determining corrosion rate or resistance.

The gas composition may alter the corrosion of a material by preferential oxidation of the solid metal surface as in the case with oxygen, or may cause sludge if dissolved material is preferentially oxidized. The wetting tendency is also affected by the presence of a gas, the smallest contact angle usually occuring in a vacuum.

1.3 Objectives

The primary objective of this program was to help select optimum materials for the SNAP II mercury system, considering minimum corrosion products and appropriate strength for the intended application.

Information considered to be essential in the pursuit of this objective was the determination of the following:

1. The determination of the resistance of various materials to liquid mercury corrosion.

2. The effect of time and temperature upon corrosion.

3. The effect of heat treatment and/or metallurgical condition.

4. The effect of stress.

5. The effect of surface treatment.

a. Cleaning
b. Passivation
c. Oxidation
d. Miscellaneous

6. The effect of additives to the liquid mercury.

a. Inhibitors
b. Accelerators
c. No effect

7. The effect of dissimilar metals on corrosion.

1.4 Approaches to Problem Solution

The current practice for material selection is first to choose materials which appear satisfactory in laboratory corrosion tests. It is then assumed that satisfactory performance will be achieved in system operation if component design is also satisfactory. This empirical method must be used until more operating experience has been gained in the actual system and until more fundamental information is available on liquid metal corrosion mechanisms and corrosion rate. The methods of laboratory testing are qualitative and comparative only, and do not permit a prediction of actual corrosion rates in a system, since no laboratory test is capable of duplicating all existing conditions anticipated in service. Considerable interpretation is required and a corrosion rate given in terms of weight loss or gain per unit area and time cannot be used exclusively in design to predict component life or amount of crud generation.

Material screening and solid-liquid interaction studies may be conducted by a number of testing methods.

1. Static Capsule. The solid and liquid metals are maintained in contact under isothermal conditions. They are relatively in-expensive tests and are useful in determining solubility data primarily; and secondly, for screening materials with considerable uncertainty since corrosion may be of low intensity for most materials.

2. Dynamic Capsule. Motion between liquid and solid is maintained by tilting, by convection or stirring. Some hetero-thermal conditions may be created, resulting in some mass transport. Cost and com-plexity of equipment is variable.

3. Bent Reflux Tubes. In this method, developed by Thompson Ramo Wooldridge Inc., the mass transport characteristics may be studied by maintaining dynamic contact between the solid and liquid with an evaporation-condensation process as described later. The test method is relatively inexpensive and simple and yields more reliable information than the static capsule test since the corrosion extent is generally more severe.

4. Loop Test. The liquid metal circulates through a system containing a temperature gradient. This method yields the most reliable data on mass transport since system conditions are generally approached. However, the method is the most costly and is, therefore, used for more intensive study of materials which appear to be promising in simpler tests.

An evaluation of corrosion damage could include a study of the following material changes:

1. Dimension
2. Weight
3. Composition of liquid metal
4. Composition of solid metal surface
5. Crystal structure of the solid metal surface
6. Nature and depth of attack
7. Hardness
8. Mechanical properties
9. Physical properties

Of these, the weight changes and a metallographic study of the nature and depth of attack were considered to be of the greatest, immediate value in assessing severity of corrosion.

1.4.1 General Materials Screening

Most of the available data on relative resistance of materials to mercury corrosion is meager and based for the most part on static tests, except for some low alloy steels and a few Type 300 series stainless steels (7)(35). Little new information, based on recent laboratory scale studies, has appeared. Consequently, determination of material behavior in dynamic liquid mercury was considered to be of paramount importance. The bent reflux tube capsule method was chosen for preliminary material screening, with loop testing to be conducted on the most promising material or material combinations to serve as a corroborator.

1.4.2 Environmental Effects

Material screening results in situ are not an adequate basis for material selection without an understanding of environmental effects such as those arising from the presence of stress, dissimilar metal combinations, and contaminants or additives. Thus, supplementary information concerning environmental influence is necessary so that material choice will result in minimizing possible malific interactions.

1.4.3 Component Parts Study

Examination of mercury power conversion test system components for location and severity of corrosion, crud deposits and structural performance undoubtably offers an invaluable opportunity to verify material behavior prediction by laboratory tests and to reveal other areas of possible malfunction. Advantageous use may be made of the information obtained to serve as a guide for present and future material selections as well as to suggest additional laboratory tests to clarify perplexing behavior. Therefore, microscopic examinations and chemical analyses were performed wherever possible on tested component parts.

2.0 EXPERIMENTAL METHODS

2.1 Bent Reflux Tubes

Many of the mercury-metal compatability tests were performed in a simple glass apparatus which has been named the "Bent Reflux Tube" (Figure 2). It provides a means for exposing specimens to pure mercury for protracted times at temperatures considerably above the normal boiling point. (26)

The bent reflux tube is made from 5/8 inch OD, heavy-wall Pyrex tubing, and is designed to include a partial inward collapse of the tube wall at the bend. After mercury and metal specimen coupons are inserted, the tube is evacuated to one millimeter of Hg or less and sealed off. The tube is then mounted in a vertical holder in a furnace heated only at the bottom to produce a temperature gradient that causes mercury to distill from the lower boiler compartment to the upper horizontal condenser compartment. The inward projection of the glass wall at the bend serves as a dam to retain a small pool of distilled mercury in the condenser compartment. In operation, freshly condensed mercury is supplied constantly to the pool while overflow at the dam occurs to return the mercury to the boiler. One metal specimen is located in the pool of condensed mercury, and in some instances, another may be placed in the boiler. The condenser specimen is thus exposed to continually replenished, distilled mercury while the non-volatile materials acquired from the specimen accumulate in the boiler.

Modifications of the original bent reflux tube design have been introduced to improve its performance in several respects. Tendency of specimens to float on mercury was counteracted by indenting the glass walls to restrain the specimens (Figure 2A). When it became apparent that attack occurred mainly at the surfaces submerged in condensed liquid mercury, attempts were made to modify the condenser shape to provide a deeper pool of mercury in which the entire specimen could remain submerged. However, it was soon established that the inability of liquid mercury to penetrate narrow channels between non-wetted surfaces prevented liquid-solid contact over the entire specimen surface. Therefore, the simpler condenser shape was adopted and attempts were made to evaluate specimen weight losses in terms of submerged area.

Another design of the bent reflux tube was used in testing the influence of other metals on the mercury attack on a given specimen. The bent reflux tube condenser section was made longer and a second dam was provided about one inch above that at the bend (Figure 2C). Specimen tabs were then located one above each dam. The upper specimen was thus exposed to pure mercury only; the lower specimen was bathed in mercury, part of which had descended from the upper pool with its burden of solutes from the upper specimen.

When mutual interactions of specimens were to be tested, both specimens were placed together in the same simple bent reflux tube condenser compartment.

An improvement in the bent reflux tube design was adopted to minimize entrainment of non-volatile contaminants from the boiler back into the condenser with the distilling mercury. Above the mercury surface level, a pattern of indentations was made in the boiler wall (Figure 2B), in the manner of the Vigreaux reflux condenser, to act as a baffle system for the rising vapors. Although this type of reflux column will function properly only with surface-wetting liquids, the design was incorporated into many of the later tests because it was feasible, and it at least presented some degree of impediment to the free rise of mercury vapors. Tubes of this design have yielded results which are mutually consistent, but as a group, apparently somewhat different from those obtained from simple tubes.

The furnace in which the bent reflux tubes were heated was a simple rectangular chamber heated electrically at the bottom only. An asbestos-board lid covered the top opening. Located directly above the heaters were stainless steel bars (3 inches high x 1 inch thick and running the length of the chamber) into which vertical holes had been bored to receive and support the bent reflux tubes. The boiler compartment was heated by the surrounding metal bar, while the condenser compartment, extending above and away from the bar, was maintained at the furnace chamber temperature. A controlling thermocouple was located in the furnace chamber near the tube condensers. A schema is presented in Figure 40.

Preliminary exploration of temperatures within the furnace revealed that with the chamber controlled at $900^\circ F \pm 10^\circ F$, temperatures within the steel bar holes were about $970^\circ F$. Thus, ambient temperature for the condensers was about $900^\circ F$ while that for boilers was about $970^\circ F$. Because of the low thermal conductivity of the thick glass walls, the actual condensed mercury temperature must be above the condenser ambient temperature by an amount determined, in part, by the rate of mercury distillation. The mercury temperature in the boiler will be slightly greater than that of the condensed mercury. Although some thought was given to the use of a special tube incorporating thermocouple wells to measure actual internal temperatures, it was decided that other unavoidable variables (characteristics of individual tubes, and temperature variation with respect to position in the furnace) created uncertainties of at least comparable magnitude. The temperatures stipulated for bent reflux tube tests are to be regarded, therefore, as representing an approximate level rather than a closely defined value.

Bent reflux tubes made from Pyrex heavy-wall tubing are limited to service

below 950°F; consequently, with this material maximum test temperatures have been at the thermal limit. Internal mercury vapor pressure is approximately 100 psi at 900°F, but only very few failures have occurred.

Several tests of other glasses at higher temperatures have been performed. A bent reflux tube was made from Pyrex combustion tube, a glass designed for higher temperature service, but available only with relatively thin wall. It exploded at about 900°F. Similar tubes were made from Vycor combustion tube (the thickest wall available), but these failed below 1100°F. Another tube, of slightly modified design, was fashioned from Vycor combustion tube by a professional glass blower; this tube survived many hours at 1200°F, at which temperature the mercury vapor pressure approaches 500 psi. The relative inertness of Pyrex (to 900°F) and Vycor (to 1100°F) glass test capsules in mercury was amply demonstrated in preliminary compatibility tests and during the course of material screening. Glass inertness to mercury has also been reported in the literature (7).

Specimen Preparation and Handling

Preliminary handling of the various alloys tested was necessarily adapted in many respects to the nature of the specific alloy. Specimens were cut to size by shearing, sawing, or grinding, followed by an appropriate heat treatment. Surfaces were then cleaned in several alternative ways – pickle in HNO_3–HF solution, pickle followed by electropolish in phosphoric acid–glycerine solution, or by mechanical polish. After a final rinse in pure acetone to remove surface oils and water, the specimens were air dried and weighed. Specimen size was approximately 0.065 in. thick x3/8 in. wide x 1 in. long, or equivalent size to yield a surface area of about 0.9 square inches.

When the specimens were being sealed in the bent reflux tube, appropriate care was exercised to avoid heating the specimen to temperatures at which oxidization occurs. When the particular design of certain of the tubes made excessive heating of the specimen unavoidable, the tube interior was flushed with pure argon gas.

After removal from the furnace, the specimens were examined for wetting by the mercury. The tubes were then cracked open, the mercury was reserved for analysis, if desired, and the specimen was then washed clean of any surface adhering mercury. After an acetone rinse and drying in air, the specimen was weighed. It was then heated (500–700°F) in vacuum to remove all adhering or absorbed mercury, and weighed again. From these three weights were derived the net weight loss by the specimen and the weight of mercury incorporated in any porous depleted surface layer formed by the mercury attack. The specimen was then prepared for metallographic examination. It was so mounted that the edge exposed for polishing and examination included regions both submerged in liquid mercury and exposed only to vapor.

2.2 Loop Tests

2.2.1 Fabrication, Assembly, and Design

Loop tests are generally preferred for the evaluation of the corrosion resistance of materials, if the anticipated application is dynamic and non-isothermal. This is true because the loop test reproduces the conditions of the final application better than any other known type of corrosion test. The SNAP II program had the advantage of the work done under the SNAP I program to develop testing techniques and to design loops.

The loops (see Figure 3) used are fabricated from 0.5 inch outside diameter tube. The general shape of the loops is a parallelogram. The overall height of the loop is 76 inches, and the overall width, 14 1/2 inches. The loops are two-phase, natural circulation type, that is, the mercury is boiled and condensed, giving circulation to the liquid and vapor. A subcooler located in the bottom horizontal leg increases the temperature gradient in the loop. The boiling section is located in the lower vertical leg. The superheater is located in the top horizontal section, followed by the condenser in the higher vertical leg.

The boiler heaters have a capacity of over one kilowatt. However, this power has never been completely utilized because liquid carry-over occurs at less than 800 watts. The highest flux sustained during test is 6,500 Btu $Ft^{-2}-Hr^{-1}$. This gives a mercury circulation rate of about 12 pounds per hour and a vapor velocity of 213 feet per minute. A line heater is located between the boiler and superheater. This heater prevents large heat losses from the mercury and helps dry the mercury vapor before it enters the superheater. The condenser consists of an air duct which surrounds a section of the loop. The condenser is connected by air lines to a blower which can circulate approximately 40 cfm of air. The subcooler is similar, but smaller, with less air flow.

Temperatures are measured at ten locations on the loop and recorded on a null-balance type, multiple-point recorder each at five minute intervals. The heaters on the boiler, line, and superheater are controlled by individual on-off type temperature controllers which indicate but do not record the temperatures. Ammeters are located on each heater to indicate the current and to aid in regulation of the system. The power level to each heater is controlled by an auto-transformer. The air flow to the condenser and subcooler is indicated on an inclined manometer and manually controlled by a valve in each

line. The mercury pressure inside the loop is indicated and recorded on a single-point continuous recorder connected to the loop through a diaphragm.

Since the loops are unattended a large number of hours each day, two safety devices are provided. First, the pressure recorder is equipped with an over-pressure device which controls a relay. The power to all heaters passes through this relay. An over-pressure results in an interruption of power to all heaters. A second safety device consists of an over temperature relay connected to the temperature recorder so that the power to the heaters is also interrupted in case of an over-temperature. The loops are located in a small room with an independent ventilating system. Past experience has indicated that the safety precautions are sufficient.

The fabricating procedure is to cut the 0.5 inch tube into four lengths required for the loop. Two of the lengths are then bent to form the top and bottom sections. The sections are stress relieved and welded together with the connections for the pressure recorder and fill line. The loop is then cleaned and leak tested. The leak test consists of pressurizing to 200 psig with helium and checking with a mass spectrometer-type leak detector. The loop is leak tested again just before operation by standing evacuated to less than one inch of mercury for sixteen to eighteen hours. If no observable pressure rise occurs, the loop is assumed to be free from leaks.

2.2.2 Operating Conditions

The mercury is boiled and condensed at 900°F and superheated to 1150°F. The subcooler temperature is about 400°F. Temperatures are recorded at ten locations on the loop as follows:

(1)	Boiler inlet	(6)	Condenser midpoint
(2)	Boiler outlet	(7)	Condenser outlet
(3)	Superheater inlet	(8)	Subcooler inlet
(4)	Superheater midpoint	(9)	Subcooler midpoint
(5)	Condenser inlet	(10)	Subcooler outlet

The mercury pressure is recorded continuously and maintained close to 100 psi.

2.2.3 Observations

Before and after each test the loop wall thickness is checked at 86 points by the use of an ultrasonic thickness gauge. Unfortunately,

this method of checking changes in wall thickness is not as satisfactory as anticipated. Only general attack is detected by the ultrasonic tester, and frequently the results obtained have been misleading in interpretating the amount of corrosion. However, these readings do provide one source of numerical data for use in evaluating the mercury attack. The thickness gauge results are reported, when available, and should be evaluated with discretion.

The loop is split open and examined for areas of attack and distribution of deposit resulting from mass transfer. Loose deposit is removed and tight scale on the tube wall is scraped from the surface, when possible. Deposits from various areas are kept separate. Tube specimens are taken regularly from four areas: the boiler, superheater, condenser and subcooler. Additional specimens are taken if the visual inspection reveals additional questionable areas. All tube specimens are given a metallurgical examination, the results of which are reported.

The deposits removed from the loop are analyzed by spectrographic means, followed by wet chemical analysis if sufficient sample is available. The mercury removed from the loop at the end of a test is also chemically analyzed. The mercury is removed from the loop under vacuum and observed for oxides on the surface. If a quantity of "scum" or oxides is present, it is analyzed separately from the mercury.

2.3 Chemical Analysis Problems

Many kinds of specimens were submitted for chemical analysis – quantities of mercury, large and minute quantities of metallic solid mixed with mercury, and barely visible quantities of solid wiped from apparatus surfaces with filter paper. Each specimen was analyzed by an emission spectrograph for qualitative information and in many cases a very rough quantitative estimate could be made on the basis of spectral line intensities. However, it was impossible to establish a standard procedure for the various kinds of specimens, and a truly quantitative analysis was not feasible. When quantity of specimens permitted, quantitative analysis by wet methods and spectrophotometer was performed.

At first, the method recommended by K. S. Bergstresser (27) was followed in analysis of mercury for admixed and dissolved metals. The metals were extracted by extended treatment of the mercury with hot, dilute HCl, and the extract was analyzed by appropriate gravimetric, volumetric, and spectrophotometric methods for Fe, Ni, Cr, and Mn. When these methods were applied to specimens from loops and other apparatus, there was no basis for a check on the validity of results. However, when applied to the

mercury and residues of a bent reflux tube test, the analytical totals usually fell far short of the measured weight loss for the specimen. Evaluations of the analytical procedure with artificially prepared solutions were satisfactory. The possibility of a concealed adverse influence of small amounts of mercury ion on the analytical reliability was also disproved. Therefore, doubt was cast on the efficacy of the HCl extraction.

On one occasion, attempt was made to remove, by HCl extraction, a large burden of suspended and admixed metals from a small quantity of mercury. Only a long series of extractions with fresh portions of dilute HCl succeeded ultimately in producing a colorless extract. However, the mercury still showed evidence of contamination. When 10% nitric acid was added to the mercury, a suprisingly large quantity of metals quickly separated, some of which was obviously an agglomerate of small particles, but there were also some rather large pieces of metal.

In another analytical test, weighed quantities of Fe, Cr, Ni and Mn, singly and in mixtures, were heated at $900°F$ in sealed tubes with mercury. When the metals wetted and were incorporated into the mercury (although un-dissolved) the subsequent extraction with 6 N HCl, and even treatment with hot dilute HNO_3, was unable to effect a separation from the mercury. Nickel was especially resistant: wetted chunks of the metal could be seen floating under the mercury surface, but hot dilute HCl failed utterly to extract it. It was necessary to dissolve with HNO_3 the entire mass, including the mercury, to get the nickel into ionic solution. Manganese presented a similar problem.

It seems evident, then, that HCl extraction alone cannot be relied upon to remove suspended and dissolved metals from mercury.

Determination of the nature and quantity of contaminents in the mercury by chemical analysis is an invaluable aid in evaluating corrosion damage and dissolution mechanism.

3.0 MATERIAL SCREENING RESULTS

3.1 General

A large number of material screening tests were conducted in bent reflux tubes. The nominal composition of the alloys tested along with the heat treatments utilized are listed in Tables 2 and 3, respectively. Special surface treatments are listed in Table 4.

A condensed summary of resistance of materials to mercury corrosion is presented in Table 5. The relative corrosion of some materials in mercury at 900°F – based on 12 day tests – is presented in Table 7.

In general, reproducibility is only fair. The scatter in results may possibly be due to invisible oxide films, adsorbed gases, grease films or other kinds of surface contamination, the size of the liquid mercury pool in contact with the test coupon, and rate of mercury distillation. The scatter probably is also a characteristic of the corrosion process related to the corrosion mechanism as discussed later.

A plot of weight loss (or weight loss per unit area of total specimen surface) yielded the most reliable and predictable curves with exposure time. Plot of weight loss per unit area of observed wetted surface showed wide scatter and appeared, in general, to follow the same pattern with time that weight loss plots followed.

Mercury corrosion was classified into the following observable types:

1. Layer – a depleted or leached zone.
   The leached zone may be intergranular or uniform in progression. Intergranular cusps, or slight advance of layer in grain boundaries over bulk grains, may be seen in some layers.

2. Crevice – removal of metal resulting in irregularly shaped fissures. The crevice may be intergranular or may run parallel to the surface just under the surface.

3. Pitting – semi-circular depression caused by metal removal.

4. Wedge – a wedge-shaped fissure caused by metal removal.

Kinetics of Corrosion

Some of the practical questions to be answered are how much crud is generated and what penetration of the metal wall by corrosion may be expected. An accurate knowledge of the corrosion kinetics is necessary to answer these

questions so that accurate predictions may be made. Some idea of the corrosion kinetics that existed in the bent-reflux tube test may be obtained by plotting the experimental data on log-log coordinate paper. The logarithm of the weight loss plotted against the logarithm of the elapsed time results in a characteristic slope depending upon which corrosion law is obeyed. Using analogous concepts concerning empirical growth laws applicable to oxidation, a number of corrosion laws may be derived. When a corrosion product is nonporous and adherent, contact is maintained between the solid metal and liquid mercury by diffusion, and the parabolic law

$$-W^2 = Kt$$

is applicable where W is the weight loss, K is the rate constant and t is the elapsed time at a given temperature. This equation is characteristic of a decelerating rate of corrosion.

When corrosion is unaffected by growth of a corrosion layer and the attendant increase in diffusion resistance, the linear law

$$-W = Kt$$

is observed, where K is the linear rate constant. If corrosion follows this law it is usually concluded that:

1. The corrosion layer is porous or channeled.

2. Reaction rate is controlled not by diffusion but by rate of solution.

However, this law is also applicable if a thin, non-porous corrosion layer next to the base metal is constant in thickness while the porous or channeled corrosion layer on top of it is attacked by a combination of diffusion and channel formation.

The characteristic slope on log-log paper for the parabolic law is 1/2 while the characteristic slope for the linear law is 1.

An accelerating rate of corrosion may be found if the presence of a corrosion layer or products of corrosion actually stimulate a greater rate of attack. This type of behavior may be summarized by

$$-W^n = Kt$$

where the exponent is less than 1. The characteristic slope on log-log paper is greater than 1.

Wettability

Wetting was indicated as positive when liquid mercury was observed to adhere to the specimen surface before opening the tube at the end of test. Incidence of wetting correlated generally with severity of attack, as might be expected

inasmuch as wetting is a consequence of liquid-surface adhesion. For apparently unwetted materials there probably was some adhesion or attraction between the liquid metal and the solid at temperature. The degree of wettability and mutual attraction would best be defined by actually measuring the angle of contact between the liquid metal and solid at the test temperature.

3.2 Elemental Metals (Tables 8, 12, 16 and 17)

The elemental metals have exhibited the widest range of corrosion resistance of all the materials tested. Some have been highly soluble in mercury at 900°F, while others have been inert within the limits of the measuring methods. No weight change has been observed in testing tantalum and tungsten. On the other hand aluminum, platinum and manganese were found to be non-resistant to mercury at 900°F. At the same temperature titanium, zirconium, nickel and chromium were found to have poor resistance. Fair resistance was exhibited by cobalt and beryllium. Iron gave good resistance and molybdenum and columbium gave very good resistance (see Tables 8 and 12).

A plot of the iron (low carbon steel) weight losses as a function of time (Figure 4) indicates that the linear corrosion rate is followed, as would be expected if no diffusion barrier or accelerated attack results from reaction product formation. The same holds true for chromium (not plotted) (see Tables 8 and 12).

The slight weight gains for molybdenum, columbium and cobalt (12 days) at 900°F and the rather large weight gain for zirconium at 700°F are all indicative of mercury penetration and bond formation with the element (Tables 12, 16 and 17).

Several theoretical approaches have been studied, none of which gives a complete explanation of the observed data. These approaches are discussed in the following paragraphs. As more data are obtained and the problem is better understood some of these approaches may become more meaningful.

Comparative resistances of metals to liquid mercury corrosion at 900°F are summarized in Table 6 in a periodic chart form, along with a calculated tendency of each element for solubility. This calculated solubility is another approach towards the corrosion problem which depends upon determining the tendency towards liquid immiscibility or miscibility of metals with mercury based on thermodynamic considerations. Using the Hildebrand-Scott relationship (5) as modified by Mott, a correction factor for the tendency towards chemical bonding, the index of miscibility or immiscibility was calculated for the elements at 1200°F. The miscibility index indicates the extent of mutual attraction and interaction and, therefore, gives an indication

of solubility. In no case was an element calculated to be miscible found to be insoluble or resistant to attack by this method. Of the elements which were calculated to be immiscible or to resist attack and which were found to be attacked, these elements generally had probably a strong tendency towards chemical bonding with the mercury, as evidenced by the mention of known intermetallics for most of these elements with mercury in the literature (7)(17)(18).

It is also interesting to note that all the metals which exhibited a strong resistance to mercury attack were those with unfilled "d" electron energy bands (18). The metals favorably disposed to the formation of chemisorbed films are those with unfilled "d" electron energy bands (19) and with high heats of sublimation, since they can form stronger electron-shared bonds with the adsorbate. Another important factor in chemisorption is the necessity for a high affinity of the adsorbate for the metal, accompanied by a high activation energy for chemical reaction with the metal, so that the adsorbate has a relatively stable life.

The resistance to corrosion shown by tantalum, columbium, tungsten and molybdenum may have been due to some sort of passivity which depended upon chemisorption and its relation to electron structure, since it is well known that all metal surfaces are covered by an adsorbed layer of gases.

The metals with relatively high resistance to mercury corrosion are also those which have relatively high activation energies for high temperature creep and self diffusion. This suggests that dissolution is controlled by the same crystallographic mechanisms which control diffusion, creep, and other thermally activated processes.

Some measure of the tendency toward amalgamation may be obtained from half-wave potentials used in polarographic analysis. The cathodic half-wave reduction potential minus the normal potential measured in an acid or neutral solution corresponds to the standard potential (E) of the cell

Metal/metallic solution/metal-amalgam.

E is a measure of the free energy of amalgamation (ΔF) according to

$$\Delta F = -nEF$$

where n is equal to the valance change and F is the Faraday (21). The calculated free energy of amalgamation for some metals is summarized in Table 20 in order of increasing resistance to amalgamation. The large, positive values for the iron group are due to the fact that deposition is associated with marked irreversible polarization (large overpotential).

This may be connected with the corrosion resistance of these metals, perhaps a result of some kind of passivity.

3.3 Low Alloy Steels (Table 8)

A log-log plot of corrosion weight loss at 900°F as a function of time, presented in Figure 4, suggests that most of the low alloy steels (alloy content under 10 percent) show constant rate of attack (curve slope of 1) losses after an initial period which may show either accelerated corrosion (curve slope>1) as in the case of 1010 steel, or decelerated corrosion (curve slope of 1/2) as in the case of quenched and tempered 1095 steel. Vascojet 1000 data showed considerable scatter, making any deductions as to rate difficult.

Carbon, chromium and silicon additions seemed to reduce corrosion slightly relative to 1010 steel or Armco iron composition. Heat treated 1095 steel showed a slightly higher weight loss than the annealed material whereas the Vascojet 1000 showed a reverse effect.

Penetration data, Figure 6, indicated linear (Sicromo and 1010 steel) or accelerated (Tran-Cor) penetration for most of the low alloy steels. Microscopic examination revealed that dissolution occurred by surface roughening and formation of pits and crevices.

3.4 Moderately and Highly Alloyed Steels (Tables 8 and 16)

Weight loss versus time plots for moderately alloyed steels at 900°F, Figure 5, showed that Neatro dissolution obeyed the parabolic rate law, while quenched and tempered 18-4-1 tool steel obeyed the linear rate law and Chromewear showed accelerated corrosion (slope greater than one).

Quenched and tempered Neatro, and to a lesser extent Chromewear, showed less attack than the annealed stock, whereas the 18-4-1 tool steel suggested the reverse. Plot of penetration data, Figure 6, suggests that 18-4-1 and Neatro followed linear penetration while Chromewear showed accelerated penetration. Penetration occurred in the form of pit and crevice attack.

The effect of composition at 900°F may be noted in the higher corrosion rates for the high nickel-bearing materials, Kovar, Carpenter Low Expansion "42", and Sylvania No. 4 (Figure 4). It is interesting to note that Sylvania No. 4 which contains chromium with, however, a nickel content identical to that of Low Expansion "42" indicated a linear corrosion rate while the latter indicated a decelerating corrosion rate. Kovar also followed a decelerating corrosion rate.

The cobalt containing Hyperco 27, on the other hand, exhibited a constant

corrosion rate. Alnico showed a very low corrosion loss (Table 8). This was probably due in part to the partial tie-up of the soluble constituents in compound form (Ni-Al-Co) dispersed throughout the alpha iron matrix.

Microscopic examination indicated a crevice or intergranular attack on the non-nickel-bearing steels, whereas the nickel containing steels exhibited a depleted or leached zone similar to that formed by the 300 series stainless steels.

Penetration data at $900^\circ F$, plotted in Figure 6, suggests linear penetration for the nickel-bearing materials (Carpenter 42 and Kovar) and accelerated penetration for the cobalt-bearing materials (Hyperco 27).

Results of tests at $700^\circ F$ on Kovar and Hoskins 875 show weight losses which were, as suggested by Kovar results, on the order of about one quarter of those at $900^\circ F$ (see Tables 8 and 16). On the other hand, Kanthal A-1 and Alfenol showed a slight weight increase at $700^\circ F$. Microscopic examination revealed a corrosion layer and crack-like penetration on the Kovar surface. Some attack was also noted on Alfenol and Kanthal A-1 as pit and crevice formation. The Kovar weight loss at $700^\circ F$ appeared to follow a linear law as compared to the parabolic law followed at $900^\circ F$ (see Figures 4 and 7). This more aggressive rate of metal removal is further discussed under the Type 300 series steels results.

Weight loss as a function of the reciprocal of absolute temperature is presented in Figure 8 for 12 and 30 day tests.

3.5 Type 400 Series Stainless Steels (Table 9)

A log-log plot of corrosion weight loss as a function of time for the Type 400 series stainless steels (Figure 9) suggests complex corrosion behavior. In general, an initial accelerated rate of corrosion (dotted line) or linear rate is suggested with a cross-over to a decelerated rate of corrosion occurring very likely after 50 days.

The effect of composition can be seen in the behavior of Type 446 stainless steel which, with a high chromium content, showed greater weight losses than the Type 410 SS and an accelerated corrosion rate.

Upon microscopic examination, corrosion was manifested as a surface roughening or pitting in the early stages, and then as intergranular penetration in the latter stages (Figure 10).

Penetration occurred by diffusion in the Type 446 steel (Figure 11) and linearly for the other Type 400 series steels.

The reason for the improved resistance due to chromium additions is probably that passivity results from electron sharing by the iron and chromium atoms. The division between passive and non-passive compositions occurs at about 13 percent chromium, and this is probably why the Type 410 stainless steel is more resistant than those with higher chromium contents such as Type 446 steels.

3.6   Type 300 Series Stainless Steels (Table 10)

A log-log plot of weight loss versus time at 900°F for the various Type 300 series stainless steels is presented in Figure 12, where the various straight lines which are drawn suggest that corrosion may follow different rates depending upon certain variables. As exemplified by the curve for Type 347 SS the initial rate of corrosion is constant (since the slope is 1), and then becomes diffusion controlled after about 10 days (since the slope equals 1/2). On the other hand, some of the data suggests that corrosion may be diffusion controlled from its inception as indicated by the lower straight line. Also, the initial corrosion rate may be slightly accelerated as exemplified by the upper line (slope - 1.3) for the Type 304 stainless steel before diffusion becomes dominant. The composition effects are noted as an increase in corrosion losses for the alloys (Types 310 and 304 SS) with chromium, or chromium and nickel content greater than that of the Type 347 SS composition.

Microscopic examination showed that corrosion resulted in a leached zone as a result of preferential removal of nickel and chromium, since analyses of the liquid mercury in contact with the test coupons yielded a high percentage of these elements (see Figure 13). Also the layer was ferromagnetic, indicating a partial phase change from austenite to ferrite as would be expected if nickel and chromium were removed. In some cases the corrosion layer appeared to be solid metal and was visible only after etching. In other cases, the layer was easily visible because of penetrations which appeared as fine dark lines. Some penetrations could be traced over fairly long distances or even over almost the entire thickness of the leached zone. The appearance of this zone may explain the difference between diffusion or parabolic and linear or accelerated corrosion behavior. The corrosion occurred intergranularly in some cases (Figure 13), also with whole grain removal in some instances.

It was also noted that crystal deposition occurred lightly on some coupons and more heavily in others. It is believed that this redeposition may result in accelerated corrosion because of concentration cell effects.

A log-log plot of penetration at 900°F as a function of time (Figure 14) suggests that penetration is diffusion-controlled and undergoes a decelerating rate of penetration in most cases. However, the probability of aggressive

penetration is suggested by the straight lines with a slope of 2 for Type 347 (electropolished) and Type 304L stainless steels.

Other austenitic stainless steels tested at 900°F exhibited corrosion behavior (Figure 15) similar to the Type 300 series steels. The sigma-containing steel (XCR) corrosion losses were low, probably due to the protection offered by the ability of the sigma phase to dissolve a third atom (especially that of a transition element like nickel) (23)

Test results on Type 347 steel at 700°F (Table 16) suggest that corrosion proceeds according to an accelerated rate (Figure 7) as compared to the linear and parabolic rates at 900°F (Figure 12), at least between 12 and 30 day exposures. This seemingly more aggressive dissolution behavior at 700°F may be caused by the flocculation which can occur of the soluable elements, allowing the mercury to retain its corrosiveness even when saturated.

Other austentic stainless steels showed weight losses at 700°F which were not particularly in the order found at 900°F (Table 16). The differences may be due to passivity due to oxygen adsorption or oxide film formation. Passivity should become more effective at lower temperatures. At higher temperatures passivity should become less effective and eventually cease to be a deterrent to corrosion.

Weight loss at 1100°F on Type 347 SS appeared to be low (Table 17), probably due to bent reflux tube geometry; however, the data may represent the lower scatter limit, as illustrated in the plot of weight loss as a function of the reciprocal of absolute temperature for 12 and 30 day tests (Figure 8). The 12 and 30 day plots appear to cross at about 1000°F.

3.7   Precipitation Hardening Steels (Tables 11, 16 and 17)

The corrosion behavior of the wrought precipitation hardening grades of steels at 900°F may be classified generally in terms of matrix microstructure, either martensitic or austenitic. The austenitic steel, A286, yielded the highest weight loss for this class of materials (Figure 16). PH 15-7 Mo corroded according to an accelerated rate initially, but later at a decelerated rate. The austenite stabilized condition for this material and for 17-7 PH indicated higher corrosion losses than for the double aged, martensitic matrix. The 17-4 PH steel exhibited diffusion controlled dissolution, whereas the AM350 steel appeared to show accelerated corrosion. Corrosion rates for both steels appeared to be unaffected by heat treatment.

Microscopic examination showed that corrosion was manifested as surface

roughening with crevice or pit formation, intergranular attack, and a depleted layer (Figures 17 and 18). The ferrite colonies in the austenitic matrix in PH-15-7Mo and AM350 steel appeared to resist corrosion (Figure 19). Steels 17-4PH and PH15-7Mo in the heat treated condition indicated a tendency for a diffusion controlled penetration rate whereas AM350 indicated an accelerated rate (see Figure 20). On the other hand, in the austenitic stabilized condition PH15-7Mo indicated accelerated penetration while AM350 indicated diffusion controlled (parabolic) penetration. In general, penetration was greater for materials with an austenitic matrix.

A 700°F test of A286 failed to show any signs of corrosion after 12 days (Table 16). This apparent corrosion resistance may have been due to surface passivity as mentioned earlier in the case of the austenitic steels.

At 1100°F, PH15-7Mo steel yielded a weight loss about 27 times as large as at 900°F (Tables 11 and 17). A plot of weight loss versus reciprocal of absolute temperature is presented in Figure 8.

3.8 Nickel Base Alloys (Table 12 and 16)

Nickel base alloy weight loss at 900°F suggests complex dependence upon composition, especially the nickel, chromium and iron contents. Weight loss plots suggest diffusion controlled dissolution for TP3, Waspalloy and Rene 41 in the heat treated condition (Figure 21). Accelerated dissolution is suggested for Inconel X, AF1753 and heat treated Waspalloy.

Penetration plots (Figure 22) suggest parabolic rate penetration for all nickel alloys except Rene 41 which suggested accelerated penetration.

Microscopic examination revealed crevice attack, some of which was intergranular, on most of the alloys. In addition, Inconel X contained a corrosion layer with intergranular cusps, and the layer contained cracks. The nickel-aluminum intermetallic in TP3 was not attacked (Figure 23).

Corrosion test results on Inconel at 700°F (Table 16) yielded a weight loss about 1/3 of that at 900°F (Table 10). A plot of weight loss as a function of the reciprocal of absolute temperature is presented in Figure 8.

3.9 Cobalt Base Alloys (Tables 12, 16 and 17)

Diffusion controlled dissolution and penetration is suggested for Haynes Alloy No. 25 (Figure 24 and 25). Stellite No. 6 shows linear weight loss and accelerated penetration and Elgiloy also shows linear weight loss.

Corrosion proceeded usually intergranularly for the cobalt base alloys

(Figure 26) and the weight losses appeared to be primarily dependent upon the nickel content, the alloys containing the most nickel showing the largest weight losses.

Aging of Haynes Alloy No. 25 at 1350°F indicated that some reduction in corrosion loss occurred, probably due to incipient formation of sigma or other intermetallics.

Corrosion loss at 700°F for Haynes Alloy No. 25 was about 1/10 the value at 900°F (Tables 12 and 16) and at 1100°F was about 14 times as large (Table 17) as at 900°F based on one test. Other materials appear to behave similarly.

In Figure 27 is presented a plot of weight loss versus reciprocal of absolute temperature for Haynes Alloy No. 25. The straight line obtained lends credence to the test data, with the lower dot-dash line representing the lower scatter limit. Unfortunately, longer duration tests at temperatures other than 900°F were not obtained; therefore, it is uncertain as to whether or not corrosion rate will decelerate with time.

3.10 Non-Metallics (Table 13)

The resistance of the carbides to mercury attack is probably best approached by considering the nature of the reaction which takes place between the ceramic components and metallic binder during fabrication and the nature of the metallic. The titanium carbides with nickel binder are characterized by a polyatomic structure between the cermet and binder resulting in the formation of a solid solution. On the other hand, the tungsten carbide with cobalt binder results in the formation of an intermetallic (22).

Thus, the tungsten carbide with cobalt binder showed excellent resistance as a result of intermetallic formation, whereas the solid solution type Ferro-Tic with iron binder (which lost weight equivalent to other ferrous alloys) and the titanium carbide with nickel binder showed a poorer corrosion resistance (see Table 13).

The titanium carbide (K150A) with low nickel binder content suffered a lower weight loss than the one (K151A) with the higher content – both being lower than expected due to the protective nature of the solid solution (see Table 13). Penetration and weight losses as a function of time appeared to be linear for the titanium carbides and the Ferro-Tic.

The resistance of alumina, pyroceram and ATJ graphite to mercury attack appeared to be excellent, Table 13.

3.11 Penetration and Weight Loss

An examination of penetration and weight loss plots on log-log coordinate paper, in most cases, indicated that the rates of penetration followed the same rates indicated for weight loss (i.e., 1010, Haynes 25, Siciomo 55, and 18-4-1 tool steel). Where penetration proceeded at a rate in excess of the weight loss rate, penetrations were usually observed to occur as non-uniform attack or with considerable local differences in the rate of attack (i.e., Rene 41, Hyperco 27, Tran-Core T and Neatro tool steel). Penetration behavior would normally be expected to follow weight loss behavior if the attack is uniform and general since the two are related. However, when localized attack or non-uniform attack occurs, then one would expect penetrations more drastic in severity since the dissolution level is still maintained.

Localized attack may be due to the presence of surface films or other kinds of surface contamination, and localized flow of mercury over the sample in the BRT. A non-uniform rate of attack is dependent upon a pronounced tendency for the preferential removal of a component, the rate of diffusion, and the presence of discontinuities, irregularities, segregation and other heterogeneities.

4.0 SURFACE TREATMENTS

4.1 Surface Preparation

Surface preparation effects by picking, electropolishing or grinding on cor-
rosion extent appear to be relatively insignificant for the Type 300 and 400
series stainless steels (see Tables 9, 10 and 16 and Figures 9 and 12). However,
some of the results on Type 347 steel (Figure 12) suggest that polishing may
cause incipient diffusion rate controlled corrosion. In general, none of these
procedures of preparation should be significant, especially at higher tempera-
tures.

4.1.1 Degreasing

Ultrasonically cleaning Types 347 and 446 stainless steels in tri-
chloroethylene, with and without a subsequent acetone wash, showed
some improvement in corrosion resistance for the coupons with acetone
wash, Tables 9 and 10. However, the results suggested no overall
significant changes in corrosion for this method of degreasing.

Degreasing with Oakite, followed by a wash in water and a dip in
alcohol, probably resulted in no overall change in corrosion rate for
18-4-1, Type 410 SS, austenitic steels, 17-4-PH, PH15-7Mo, and
Haynes Alloy No. 25 (Tables 8, 9, 10, 11 and 12, respectively).

4.1.2 Surface Passivation

Passivation treatments using a nitric acid solution or an aqueous
mixture of hydrofluoric acid and chromic acid suggested no improve-
ment in corrosion resistance of the austenitic and ferritic stainless
steels (Tables 9 and 10 and Figures 9 and 12).

4.2 Oxidation

Oxidation of the austentic, ferritic and precipitation hardening stainless
steels and Haynes Alloy No. 25 in air resulted in an apparent reduction of
corrosion; however, attack by the liquid mercury was not eliminated (Tables
9, 10, 11, and 12). The same behavior was evident for chromium and
Thermanol (Tables 8 and 12). Corrosion of Armco iron, nickel and aluminum
appeared to be relatively unaffected (Tables 8 and 12) by the presence of an
oxide coat. Unpolished Haynes Alloy No. 25 showed no corrosion attack
at 900°F possibly because of a protective film (Table 12). On the other hand,
nichrome seemed to suffer an accelerated loss in weight when oxidized (Table
12).

4.3 Nitrided Surface

The nitrided surfaces of Nitralloy and Type 410 stainless steel appeared to suffer greater penetration by the mercury than the parent metals (Tables 8 and 9). The Type 410 stainless steel nitride layer was penetrated by a wedge-like crack which appeared to be filled with an amalgam.

4.4 Pretreating

Pretreating by corroding in mercury and then replacing the specimen into clean mercury showed that some benefit was obtained. This effect was noted for Types 304, 304L, and 347 stainless steels (Table 10) for chromium (Table 12), for Haynes Alloy No. 25 (Table 12) and for 18-4-1 (Table 8) tool steel. The reason may be that gases are adsorbed in the channels left by the mercury in the most readily corroded areas. This adsorbed gas then may serve as a barrier thereby reducing corrosion.

Pretreating by corroding specimens in titanium-containing mercury (2ppm) and then testing specimens in pure mercury also caused a considerable reduction in corrosion loss for austentic steels 19-9 DL and Type 304L (Table 10), PH 15-7Mo steel (Table 11), 18-4-1 tool steel (Table 8) and the bimetallic combination Haynes Alloy No. 25 and Type 410 steel (Table 14). On the other hand, low alloy steel 1095 showed no beneficial effects (Table 8). The above effect is due to the formation of a titanium intermetallic of some sort (iron, carbon, or nitrogen and even mercury) which then serves as a barrier to element removal by the mercury. Gas penetration, as mentioned above, may also be beneficial. The protection offered may be caducous because of erosion and other causes.

5.0 INHIBITORS AND ADDITIVES

5.1 Introduction

The utilization of proper additives or inhibitors in many corrosive media, including liquid metals, has been known to reduce corrosion to low levels. Specifically, in the case of mercury corrosion additions of titanium and zirconium on the order of 10 to 100 ppm have been reported to be beneficial, especially on alloy steels containing free nitrogen (2) (6) (7) (20). The above inhibitors were used with magnesium as a "getter" for oxygen so that the surface was completely wetted. Nickel and chromium have also been reported as reducing corrosion (7), however, to a lesser extent.

If electrochemical phenomena are factors in liquid metal corrosion, then anodic protection may ʰe utilized in certain instances to protect the more noble materials. Bimetallic effects are discussed later.

The use of a cover gas may influence the solid-liquid metal interfacial tension thereby reducing the wetting tendency and, consequently, reduce the attack. Also, the gas may be adsorbed on the container wall surface and serve as a barrier.

Of the variety of materials included with mercury and specimens in many of the bent reflux tubes, some (the additives) were intended to reveal aspects of the mechanism of mercury corrosion, while others (inhibitors) were intended specifically to prevent or reduce corrosive attack. Several of the additives were mercury compounds, selected because of their decomposition at test temperature to mercury and other volatile materials. For example, mercuric oxide dissociates into mercury and oxygen. Others were believed sufficiently volatile, as such, (sulfur, iodine) to be transported as vapors from the boiler to the condenser specimen. Inhibitors were placed either in the boiler compartment, in which case transport to the condenser specimen must have occurred by slight volatilization or by entrainment with the distilling mercury, or they were placed in the upper condenser compartment of a double-dam bent reflux tube, the progressive dissolving of the inhibitor material then regulating the supply to the specimen. Note that in either case, the rate of supply of additive or inhibitor to the condenser specimen is determined by the nature of the material and the method of supply; there is very little prospect of any significant control of the process.

5.2 Experimental Results

Additives used in these tests are listed in Table 18.

5.2.1 Mercuric Chloride

Because of the recognized deleterious effect of chlorides on stainless steel in aqueous systems, and because the distrust of chlorides had been carried into the non-aqueous system, mercuric chloride was tested as an additive. It reacts with mercury at moderately high temperatures to form mercurous chloride, which is sufficiently volatile to be supplied constantly in small concentration to the condenser specimen.

$$HgCl_2 + Hg \longrightarrow Hg_2Cl_2$$
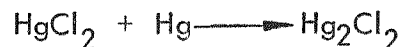
In the first test with Type 347 SS a relatively large quantity of mercuric chloride (about 0.5g) was included in a BRT containing both a boiler and a condenser specimen. The condenser specimen weight loss (37.7 mg) was about triple that observed normally, and the usual depleted layer was absent (Figure 28). The boiler specimen lost 78.6 mg and suffered intergranular attack (Figure 29) whereas usually only a gain of deposited metals is observed. A similar test with Type 304L SS yielded similar results.

To explore the effect of varying concentration of mercuric chloride, four bent reflux tube tests were performed with specimens of Type PH 15-7Mo and weighted quantities of mercuric chloride - 0.5g, 0.005g and 0.0005g. In that order, the condenser specimens suffered a generally declining weight loss to the level to be expected for this alloy without additive in a 20 day test. There is a reversal in the trend of weight losses, and for this no explanation can be offered. The trend of weight change for the boiler specimen is interesting. A change from severe weight loss to weight gain occurs. Evidently, a very small concentration of the mercuric chloride has no significant influence on the cause of interaction between this alloy and mercury.

5.2.2 Mercuric Oxide

Mercuric oxide was selected as a means of introducing oxygen into the closed system of a bent reflux tube. The compound dissociates at elevated temperatures into mercury and oxygen.

$$HgO \longrightarrow Hg + 1/2O_2$$

From available data concerning the degree of decomposition of HgO at various temperatures and the known vapor pressures of mercury, it was computed that in the bent reflux tube containing mercury and mercuric oxide at 900°F, the partial pressure of oxygen must be about 0.03 atm. Therefore, the major part of the quantity of HgO provided

serves as a reserve source of oxygen which is maintained at a low controlled concentration.

Mercuric oxide was tested with Type 304SS, Carpenter 20Cb and PH 15-7Mo. In each instance, the condenser specimen weight loss was reduced to practically zero, and the boiler specimens lost weight. The influence of HgO on the Carpenter 20Cb weight loss is impressive, namely the reduction to 0.4 mg from a normal weight value of 90 mg, and complete absence of a depleted layer (Figure 30).

For the boiler specimens, from the above mentioned bent reflux tube tests, the change from a normal weight gain to a weight loss is interesting. Microscopic examination of many boiler specimens (tested without additive) established a consistent picture - presence on the specimen surface of many well-formed metal crystals evidently grown from the supersaturated mercury solution surrounding the specimen. In the presence of mercuric oxide, or other oxidant, the crystal deposit is absent, and evidence of attack by the mercury is observed. Apparently, the oxygen present converts any dissolved metals in the mercury to oxides which are much less soluble than the corresponding metals and which do not find the specimen surface suitable for nucleation. Moreover, the mercury is maintained nearly freely of dissolved metals and is, therefore, able to attack the boiler specimen insofar as the protective oxide layer will permit.

Apparently, the effects of oxidants in a mercury system are these: a thin oxide layer is formed on metal surfaces and the rate of mercury attack is greatly reduced. Much of the oxidant remains present as a reserve to maintain and reform the oxide layer during long contact with the mercury. Any metals taken into solution are converted to insoluble oxides; and therefore, metal surfaces in the boiler that would normally be the sites of crystalline deposition become subject to solution attack.

5.2.3 Mercurous Sulfate

Mercurous sulfate probably decomposes at test temperatures into mercury, sulfur trioxide, and oxygen, the latter two being oxidants.

$$Hg_2SO_4 \longrightarrow Hg + SO_3 + 1/2\ O_2$$
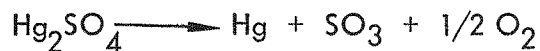
When relatively large quantities of the additive were used (in the initial rough tests) there was a reduction of attack on the condenser specimen to almost the vanishing point (no depleted layer formed (Figure 31), and a slight weight loss by the boiler specimen in most

instances. However, a thin surface deposit was found on one boiler specimen (Figure 32). A slight weight gain was recorded for the Type 304L SS boiler specimen; it may have been due to a layer of mercurous sulfate not adequately removed before weighing. In an attempt to reveal more completely the influence of mercurous sulfate, specimens of Type 304 SS were tested for different times with various weighed quantities of this additive. Although one would probably concede that a general reduction in mercury attack is exhibited, the scatter of results and the lack of correlation with quantity of additive indicate the influence of uncontrolled factors, if not simple error of measurements.

5.2.4 Mercurous Nitrate

Mercurous nitrate decomposes to form mercury, nitrogen dioxide, and oxygen.

$$Hg\,NO_3 \longrightarrow Hg + NO_2 + 1/2\,O_2$$
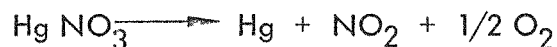
Mercurous nitrate is available as a hydrate, thus water is also present in the system, and it may have an influence on the course of mercury corrosion. Nitrogen dioxide is a volatile and active oxidant.

A test was conducted with Type 304L SS only. Attack on the condenser specimen was reduced somewhat, but the boiler specimen was drastically attacked. Evidently the corrosive properties of nitrogen dioxide predominate, therefore no further tests were attempted.

5.2.5 Barium Dioxide

Barium dioxide was selected as a means of providing a controlled concentration of oxygen lower than the dissociation pressure for mercuric oxide.

$$BaO_2 \longrightarrow BaO + 1/2\,O_2$$
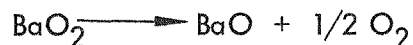
Available data lists equilibrium oxygen pressures for temperatures ranging upward from 1150°F; by extrapolation to 900°F, the partial pressure is estimated to be 0.0003 atm. Both the BaO_2 and BaO are non-volatile solids and would therefore remain in the boiler compartment unless entrainment with the boiling mercury occurs.

Barium dioxide was tested with Type 304 SS. The condenser specimen weight loss was somewhat reduced, but the meager improvement did not justify continued testing. Evidently the oxygen concentration

furnished by barium dioxide is too low to influence the mercury attack significantly.

5.2.6 Water

Water in very small quantity was included in several tests. It, of course, is volatile and does not dissociate appreciably into its elements at 900°F, but direct oxidation of the specimen surfaces is to be expected.

$$2Cr + 3H_2O \longrightarrow Cr_2O_3 + 3H_2$$

Because the critical temperature of water (705°F) is well below 900°F, the quantity of water included in a bent reflux tube must be carefully measured to prevent the attainment of excessively dangerous internal pressure.

Water was tested with Type 304 SS specimens (Table 2). The results disagree too greatly to permit any confident interpretation. It is believed that the water measured into the tubes was partly, or perhaps completely, lost during the pumping and sealing operation. Freezing the injected water during pumping and sealing is the obvious way of minimizing its escape, but the opportunity to pursue this further did not develop.

5.2.7 Boric Acid Anhydride (B_2O_3)

Boric acid anhydride was tested with Type 304 SS. The weight changes recorded indicate a reduced attack on the condenser specimen and a weight gain of the boiler specimen. However, microscopic examination revealed an extremely thin affected layer on the condenser specimen and a significant depleted layer on the boiler specimen. Although the observations are contrary to expectations, the question could not be pursued by further testing.

5.2.8 Other Additives

Of the several other additives tested, iodine seems interesting. The condenser specimen weight loss is reduced to about 5% of what is observed normally for Carpenter 20 Cb, but no depleted layer is observed (Figure 33).

Tellurium powder was tested with Type 304 SS; condenser specimen weight loss was reduced to practically zero, and no depleted layer was observed. More thorough testing of tellurium is desirable.

Ferro-selenium (as a convenient source of selenium) was tested. Although the condenser specimen gained weight, microscopic examination revealed a depleted layer beneath a surface deposit. This additive is, therefore, ineffective as an inhibitor of mercury attack.

Several metals were tested – magnesium, aluminum, cadmium, copper, tin, and titanium. Only the titanium had a distinctly beneficial effect. The condenser specimen weight loss was reduced to practically zero and there was no depleted layer, in spite of complete mercury wetting of the specimen and of the glass walls.

Titanium additions to the mercury on the order of 0.0002% (2ppm), approximately the limit of solubility in mercury at 900°F, reduced corrosion losses and penetration remarkably for the austenitic stainless steels 15-15N, Carpenter 20 Cb, 19-9DL, and 304L and for the precipitation hardening stainless steel PH 15-7Mo (see Tables 10 and 11). The Types 410, 304 and AM350 stainless steels and 1095 steel did not show any beneficial effects (Tables 8, 9, 10 and 11). Haynes Alloy No. 25 and 18-4-1 tool steel also benefited from inhibitor use (Tables 8 and 12).

The diuturnal character of the titanium layer is unknown, for it is believed that titanium replenishing is not necessary in an oxygen-free system since it is probably the preferential formation of titanium oxide which eventually consumes the titanium. Graphite powder has also been observed to lower the corrosion rate on Type 347 steel (Table 10) probably because of coating of the specimen.

The effects of the presence of several gases at 9 mm Hg pressure on the corrosion rate of Type 347 SS were investigated. Oxygen reduced corrosion to the lower (diffusion controlled) scatter band limit illustrated in Figure 12 Hydrogen reduced corrosion somewhat below the lower scatter limit. On the other hand nitrogen markedly reduced corrosion (Table 10). The effect of hydrogen in slightly reducing corrosion of Haynes Alloy No. 25 has also been noted (Table 12).

Summarizing, therefore, titanium additive is most beneficial; oxidants and nitrogen gas are very beneficial, while iodine, tellurium, and boric acid anhydride and the gases, oxygen and hydrogen are moderately beneficial. Other than the use of more refractory metals, it is believed that the use of an inhibitor is the most promising method in reducing corrosion and permitting the utilization of available, readily fabricated materials.

6.0 EFFECT OF STRESS

The effect of stress on the corrosion of Type 304, 304L, 347 and 410 and PH 15-7Mo stainless steel was not decernible for short time tests at 900°F (see Tables 9, 10 and 11). On the other hand, Carpenter low expansion "42" indicated a greater weight loss in the cold rolled condition, (Table 8). Columbium and tantalum (Table 12) showed slight weight losses in the stressed condition. It is possible that the slightly greater weight loss for the quenched and tempered 1095 steel may also be a stress effect (Table 8).

It has been reported that stress does cause an increase in corrosion rate in liquid metals (24) and the phenomenon of stress cracking in more aggressive liquid metals (such as lead, tin and zinc) is well known. However, no such extreme effects occurred in these stress tests. On the contrary, it is possible that the cold working may have actually had some effect in improving corrosion resistance on most metals by obliterating surface defects which would allow mercury penetration and corrosion to begin.

7.0 BIMETALLIC EFFECTS

Since deleterious bimetallic effects have been reported in the literature (3)(6)(8)(16), various combinations of materials anticipated in the Power Conversion System were subjected to testing to determine possible interactions.

7.1 Same Compartment (specimens touching)

The following materials in combination with 17-4PH stainless steel at 900°F did not indicate any appreciable changes in corrosion losses (Table 14)

18-4-1	Type 347 SS
19-9DL	PH 15-7Mo
Titanium Carbide (K151A)	Type 321 SS
Ferro-Tic	

The 17-4PH steel did not lose any weight with Inconel or with Haynes 25, while tungsten carbide (CA8) and Type 431 stainless steel indicated weight losses greater than normal for 12 days at 900°F. Since the tungsten carbide indicated no weight losses even after 30 days when alone (Table 13), this suggests that the presence of the 17-4PH steel caused corrosion by synergistic action.

Tantalum with Types 347 and 410 SS gained weight because of dissolved constituent deposition and diffusion inwards. Haynes Alloy No. 25 with Type 304 and 410 steel showed no appreciable changes. Microscopic examination indicated incipient attack on most coupons along with crystal deposition in varying amounts. On the other hand, Haynes Alloy No. 25 with tungsten suggested a lower rate of corrosion, whereas when coupled with columbium or tantalum, higher weight losses were indicated (Table 14). The latter effect was probably due to alloy formation since the two refractory metals gained weight.

Titanium carbide (K150A) coupled with Type 347 stainless steel showed an increased weight loss at 900°F, while tungsten carbide coupled with Type 347 steel showed no weight loss, but microscopic examination indicated corrosion and a deposit. Tests at 900°F on various welded combinations, listed below,

PH 15-7Mo to Haynes Alloy 25

17-4PH to Haynes Alloy No. 25

indicated no accelerated attack on any of the components. All combinations including the welded area, showed evidence of corrosion about as expected on single material tests under microscopic scrutiny (Table 14).

A Nicrobrazed austentic stainless steel at 900°F showed a high weight loss (Table 10) whereas a Type 410 stainless steel showed a slight increase in weight loss over the parent metal (Table 9). The dilution of the nicrobraze composition by penetration into the base metal during brazing was very likely responsible for the observed modified weight loss in the case of Type 410 SS.

Tests at 700°F on brazed combinations with filler metal AMS 4778, listed below,

> Haynes Alloy No. 25 to Tran-Cor T
>
> 17-4PH to 17-4PH
>
> 17-4PH to Tran-Cor T

indicated slight weight gains probably due to intermetallic formation with the mercury. Microscopic examination revealed slight corrosion as pitting on all coupons in addition to a grey layer on the 17-4 PH steel (Table 16).

7.2   Separate Compartments

To determine the influence of mercury previously contaminated with corroded material upon the corrosion resistance of a second material, test coupons were placed in tandem in separate condenser compartments. Results obtained are presented in Table 15 and suggest the following effects (although open to considerable conjecture).

1. Weight gains by Haynes Alloy 25 and Armco Iron indicated that mercury vapor carried dissolved chromium and nickel, respectively into the condenser compartments.

2. The iron and nichrome picked up nickel, and the Haynes Alloy 25 picked up chromium, due probably to a strong tendency for compound formation.

3. The fine particles of nickel solute carried by the mercury vapor seemed to accelerate nickel corrosion when nickel was placed in the uppermost condenser compartment. Nickel also suffered heavy losses when chromium and iron were located in the upper compartment.

4. On the other hand, iron and chromium did not seem to influence each other's corrosion rate. Haynes 25 was also not affected by Type 410 steel when placed in the lower compartment.

Pretreating mercury with cobalt suggested no appreciable change in Type 347 steel corrodability (Table 10). The presence of 0.1 percent cerrobend or 1/2 percent sodium did not affect weight loss although microscopic examination revealed that more surface was affected by corrosion than normally (Table 10).

8.0 MASS TRANSFER

8.1 Introduction

Mass transfer probably is the most serious aspect of mercury attack in the SNAP II system. Its importance stems from the danger involved in transporting contaminents into rotating components and into small flow passages. Flow passages to critical areas, such as to bearings, if obstructed can cause complete failure of the unit. Contaminants in small clearances of rotating parts can cause seizure and failure. Loop testing is the only testing method available to evaluate mass transfer. Other methods such as bent reflux tubes do not provide the thermal gradient required. The mass transfer tests were conducted in conjunction with corrosion tests in loops described under "Experimental Methods."

8.2 Materials Tested

Nine (9) loop tests have been completed. Six (6) have been reported (28, 29, 30, 31, 32, 33). The seventh report is in progress and the final two loops for the Fiscal Year 1960 are being evaluated.

The following loops were constructed and tested:

Type 347 S.S.

Type 316 S.S.

Type 446 S.S.

Type 316 S.S. (containing different material specimens)

Type 316 S.S. (incorporating a simple trap)

Type 410 S.S.

Type 347 S.S. (interior surface pre-oxidized)

Haynes Alloy #25

Type 347 S.S. (with titanium additive)

The Type 300 series steels were originally tested to evaluate this class of material for corrosion and mass transfer. The more recent tests of Type 300 series loops have been conducted to evaluate an oxidized surface and the effect of titanium as an additive. The Type 300 series materials were used because at 900°F corrosion and mass transfer effects can be observed in 1000 hours. The more

resistant materials, such as the Type 400 series stainless steels and Haynes 25 alloy, are only slightly attacked in the same length of time. Therefore, the more resistant types do not lend themselves to the study of changed surface conditions, heat treatments or additives which may not cause a major change in corrosion resistance.

8.3 Test Results

The results of the various loop tests have been reported as indicated in the paragraphs which follow. The data is summarized here for convenience and for comparison of one loop test to another.

Test G-1, Type 347 Stainless Steel (28)

The first material tested was Type 347 stainless steel. This test was conducted at a mercury boiling and condensing temperature of 900°F and a superheater temperature of 1150°F for a 1000 hour period. At the time of this test the ultrasonic thickness gauge was not available and the test was evaluated on the basis of metallurgical examinations and chemical analyses.

The mercury removed from the loop after the test was fairly clean, but upon standing soon became covered with a dark deposit. The dark deposit was analyzed spectrographically and found to be mostly chromium with small amounts of nickel, copper, tin, iron, vanadium, manganese, and molybdenum. The filtered mercury contained nickel and a trace of copper.

A quantity (48 grams) of "sludge" was found in the subcooler. It is not known whether this "sludge" was in the subcooler during the test or whether it was carried there as the mercury was drained from the loop. Upon heating the "sludge" in a vacuum oven, 6.9 grams of black powder remained. The powder was analyzed by "wet" chemical procedures and was found to be mostly nickel and chromium with a small amount of iron and manganese. There was approximately twice as much nickel as chromium.

The metallurgical examination revealed a corrosion layer in the boiler* and condenser** areas of the loop. There was no attack in the subcooler* or superheater.*** The attack in the boiler and condenser was very similar and consisted of selective removal of nickel and chromium to a depth of about 0.005 inches. A microhardness survey was made across the corrosion layer of the condenser. This hardness survey showed that the layer was softer than the base metal. The corrosion layer was also found to be ferromagnetic.

---

*Liquid phase.

**Vapor and liquid phases.

***Vapor phase.

The general attack of the tube was not great enough to cause concern from a stress standpoint. However, if the leaching of nickel and chromium were to continue at the same rate as observed in the boiler and condenser, a rupture of the tube wall could eventually occur. The amount of transported material found in the loop was sufficient to cause the obstruction of small flow passages.

Test G-2, Type 316 Stainless Steel (29)

This test was conducted at the same temperatures and duration as the Type 347 SS loop. The results were evaluated in the same way. The corrosion layer was the same depth (0.005 inches) in the corresponding locations, that is, in the boiler and condenser.

The microhardness test revealed the same type of softer corrosion layer as that found in the Type 347 SS loop. The corrosion layer was also ferromagnetic.

Analysis of the mercury and "scum" gave the same results as those found in the Type 347 SS loop. The quantity of "sludge" found in the subcooler was greater, in this case being 86 grams. When "baked" in the vacuum oven 18.4 grams of the same type of black powder were recovered. A "wet" chemical analysis revealed the same constituents but in a different ratio. In this case the nickel content was four times that of the chromium. While it is felt that there was a higher percent of nickel in this powder, several points should be kept in mind. First, there is the possibility of small quantities of powder forming a tight scale on the loop wall and being overlooked. A small quantity, if it is primarily made up of one element, could alter the results, because the total quantity of loose sludge is small. Second, a problem is that due to chemical analysis which is discussed elsewhere in this report. Therefore, the chemical analysis of deposits must be considered more qualitative than quantitative.

The results experienced in these first two tests are in good agreement with the bent reflux tube results. That is, in the Type 300 series stainless steels, the alloy with the highest nickel content has the greatest corrosion rate. In the Type 316 SS loop the quantity of black powder was over twice that found in the Type 347 SS loop. The depth of penetration was about the same in each case.

Test G-3, Type 446 Stainless Steel (30)

Type 446 stainless steel was tested because of the apparent effect of nickel in the corrosion of the Type 300 series steels. This material contains less than one percent nickel. Also, Type 446 SS possesses excellent resistance to atmospheric and chemical corrosion. The time and temperature of this test were the same as for the Type 347 SS and Type 316 SS.

The ultrasonic thickness gauge was available for use in this evaluation. The results of the ultrasonic thickness gauge indicate an average general corrosion of less than 0.0005 inches. This is about the limit of measuring accuracy of the thickness tester. The metallurgical examination revealed that there was no penetration or selective removal such as found in the previous tests. The super-heater microstructure showed a definite change with the formation of a substantial amount of sigma phase. Hardness measurements of the boiler and superheater sections showed an increase in hardness of about 10 Rockwell A units between the before and after test specimens.

There was no loose "sludge" in the loop after test and insufficient deposit in the mercury for a "wet" chemical analysis. Separate spectrographic analyses of the mercury and "scum" removed from the mercury indicated that the "scum" was mainly chromium with some aluminum, copper, manganese, iron, and silicon. The mercury contained only traces of some of the above metals.

The results of this test are also in agreement with the bent reflux tube data. The bent reflux tubes indicated that the corrosion rate of the Type 300 series steels is over ten times as high as the Type 400 series steels. The increased hardness in the boiler and condenser should be expected in this (800-1100°F) temperature range. This test indicates the possibility of using another Type 400 series steel having a lower chromium content with less susceptibility to embrittlement.

Test G-4, Type 316 SS Loop with Multiple Specimens (31)

It was realized that it would be impossible to fabricate a unimetallic system for the SNAP II unit. Also, there were data from SNAP I bimetallic tests to indicate interaction between different materials in a mercury environment. Therefore, since many components were in the process of fabrication, it was deemed advisable to combine specimens of the various materials in one loop test. It was believed that if any catastrophic corrosion was going to occur as a result of material combination, it would be revealed by a test combining the anticipated materials in one loop. The Type 316 SS loop used in test G-2 was altered for this test. This loop was used because of its initially high corrosion rate and the desire to determine what would occur in a second thousand hours of test. Specimen holders, each of which contained seven specimens, were placed in the boiling and condensing regions of the loop. The specimens were flat samples 6 inches long, 1/2 inch wide, and 1/16 inch thick. The materials in each holder were: Type 316 SS, Type 347 SS, PH 15-7 Mo, AM-350, Type 420 SS, Type 446 SS and molybdenum.

The major piece of information gained was that no catastrophic corrosion occurred. However, the corrosion of the various materials was more severe than that experienced when tested alone in bent reflux tubes.

The corrosion attack of the sections of the loop from the boiler and condenser area was very similar to the corrosion found in the same areas after the first 1000 hour test. The corrosion layer was about the same depth, but appeared to be more porous. The subcooler was still unaffected. A layer of porous metal was deposited in the superheater. The deposit was diffused intergranularly into the base metal.

It appears from this test that the corrosion of Type 316 SS is much more severe during the first 1000 hours than in the second thousand hours under the test conditions. While the combination of materials tested did not result in catastrophic corrosion, still interaction between the materials did occur (Table 19).

Test G-5, Type 410 SS

This test lasted only one day. The loop failed because of an overheated super-heater section. Type 410 SS was retested under test G-7.

Test G-6, Type 316 SS Loop with a Trap (32)

The previous tests with Type 300 series steels indicated that the major materials problem may be the control of the contaminants generated by mercury corrosion. Three avenues of approach to this problem have been considered. They are as follows. First, the selection of a material which is resistant to mercury corrosion so that contaminants are not generated. Second, use of an additive to reduce or eliminate the generation of contaminants. Third, provide filters, traps, or other methods of removing or controlling contaminants in the system. The desirability of these methods is probably in the order named. However, since the success of any of these approaches can not be predicted, it is felt that all three avenues should be investigated. The first two approaches are under study in the bent reflux tubes. The third can be explored only in loop tests.

This was the first and only test conducted to investigate the feasibility of traps in a flowing mercury system. A simple trap (Figure 39) was fabricated and installed in a Type 316 SS loop between the condensing and subcooling sections. Type 316 SS was selected because in previous tests the largest quantity of contaminants was generated with this material. The trap consisted of a chamber large enough to reduce the mercury velocity to a low value. There were two settling areas one at the top and one at the bottom. It was postulated that a trap located in a cool region of the system would collect solids separated because of temperature changes and density differences.

The test was conducted at the same conditions as the previous loops. However, no deposit was found in the trap. Some deposit was found between the condenser and the trap, and some was found in the boiler. The lack of deposit in the trap was unexpected. The change in solubility of the Type 316 SS alloy constituents in mercury as a function of temperature would lead one to anticipate deposits in the cool areas of the loop, with or without a trap. It was first suspected that the contaminants generated in the condenser had deposited before reaching the trap and the contaminents in the boiler had been generated there. This speculation was contradicted by the following facts: first, there was very little attack in the boiler area. The selective removal of nickel and chromium was not experienced in the boiler as it was in the previous Type 316 SS loop. The condenser did have the expected penetration and selective removal to a depth of 0.005 inches. Second, a chemical analysis of the deposit found in the region following the condenser was primarily chromium with less than one percent nickel. The deposit in the boiler, on the other hand, was mostly nickel, but with over sixteen percent chromium. This indicates rather strongly that nickel from the condenser passed through the trap into the boiler. The low temperature solubility of nickel in mercury is reported to be high enough to account for the transfer of the nickel in solution through the trap.

Unfortunately, very few theoretical studies have been performed in the field of mercury corrosion. There is very little agreement in regard to the solubility of elements as a function of temperature. Colloids in mercury have not been investigated, except very briefly. Therefore, our conclusions must be based on the emperical data obtained here and elsewhere. On this basis, there is no unquestionable explanation for the lack of boiler attack during this test. It is apparent that a simple trap of the kind used will not separate contaminants from the mercury. The low velocity of the mercury in this trap and the large liquid temperature difference (600°F) between the condenser and the trap places the use of any trap, based on the same principles, in question.

Test G-7, Type 410 Stainless Steel (33)

The Type 410 SS material was selected for testing because of the results experienced with Type 446 SS (see G-3 above) under this program, and the results experienced with Type 410 SS at 766°F under the SNAP I program (34). Because data were available at 766°F, it was decided to conduct this test at 1000°F. The superheater temperature could not be increased over 1150°F because of equipment temperature limits. The subcooler temperature was the same as in previous tests.

Samples from the boiler, superheater, condenser and subcooler were examined metallurgically after test. The boiler and condenser specimens displayed a jagged internal surface. The subcooler and superheater had a slightly irregular surface

which was not present in the "as-received" specimen. It is believed that this resulted from oxidation during heat treatment and subsequent acid cleaning.

There was no loose "sludge" in this loop after test. There was a very thin layer of black powder on the subcooler wall. Wet chemical analysis of this powder was as follows:

Manganese	1.76%
Nickel	0.42%
Chromium	36.84%
Iron	52.36%

The balance was probably mercury.

This loop was attacked less by the mercury than any other loop tested except the Type 446 SS. However, this loop was operated at a boiling and condensing temperature 100°F higher than the Type 446 SS. The resistance of this material to mercury is very good considering the maximum attack revealed by metallography did not exceed 0.0005 inches. Based on the assumption that all the black powder came from the boiler and condenser, it was estimated that the general attack was about 0.0001 inches. Extrapolation of corrosion data can lead to erroneous conclusions. However, it is obvious that the rates above would give an average general corrosion of less than one mil per year and a maximum attack of less than five mils per year. The values may be less in the final unit than those indicated because the condenser temperature would be lower than the 900°F test temperature.

Tests Presently Unreported

Three additional loop tests have been concluded but are not completely analyzed or reported. It is felt advisable to indicate the preliminary observations here, realizing that later detailed examination may contradict any conclusions drawn at this time.

One of these loops was Type 347 SS which had been intentionally oxidized internally by heating to 1000°F for three hours. No increase in resistance to mercury corrosion occurred from oxidation of the surface. The depleted layer was about the same as that found in the Type 347 SS loop previously run under Test G-1 and the Type 316 SS loop, G-4. There was a major difference in that the transported contaminants were tightly adhering to the walls of boiler, and condenser. There was no loose deposit or "sludge" in the loop. The mercury removed from the loop after test was relatively clean. Some "scum" formed on the surface of the mercury after standing in air. Separated from the mercury, this "scum" was analyzed by spectrograph and found to contain primarily nickel and chromium.

A second loop, not yet reported, was Type 347 SS in which the mercury contained five parts per million of titanium. After four hundred hours this loop failed because of an overheated superheater inlet. The loop was examined visually and a few metallurgical specimens have been examined. The boiler section does not have a depleted layer, but the condenser section does. This indicates that the titanium may have protected the boiler but did not carry-over into the condenser. There was no loose deposit or "sludge" in the loop. There was adherent deposit between the condenser and the subcooler, in the boiler and in the superheater. Some of the deposit between the condenser and subcooler has been analyzed and is primarily chromium. The balance of the deposit is too adherent to permit removal from the wall, without removing part of the wall itself.

The third loop still being examined is Haynes Alloy No. 25. The mercury removed after test was clean and no scum formed when exposed to air. No loose deposit was found in the loop. Only slight attack has been observed in the boiler and condenser areas. Preliminary observations would indicate that this material has high degree of resistance to mercury corrosion.

9.0 COMPONENT STUDY

9.1 Introduction

Components removed from mercury power conversion test systems were metallurgically examined per request of the various design engineering project groups. Malfunction and corrosion behavior analyses were the primary reasons for evaluation.

Component examination undoubtedly offers an invaluable opportunity to check material performance in a mercury environment under actual system conditions, since this is the only adequate basis upon which to judge material behavior. Advantageous use may be made of the information obtained to serve as a guide for present and future material selections for mercury systems, as well as to suggest additional laboratory tests.

9.2 Results

In general, the corrosion manifested in a mercury system consisted of drastic metal removal, unusually without the formation of a depleted or leached corrosion layer such as that found on the austenitic stainless steels in laboratory screening tests. Crystal deposition of dissolved matter was also practically always noted to some degree along with corrosion.

In the vapor phase portion of the system both corrosion and deposition have been observed. A valve hardfaced with Stellite (and maintained at 1050-1300°F) become inoperable due to heavy deposition of material analyzed to be nickel and chromium evidentally removed from Type 316 stainless steel tubing by dissolution elsewhere. A total of 607 hours of operation (516 hours at a mercury vapor temperature of 1150°F) was accumulated at the time of malfunction. Evidence strongly indicates that the deposited material was carried in the mercury vapor, since no corrosion was evident on the valve (see Figure 34).

Attack manifested as pitting was found on Type 316 stainless steel tubing in one case after an exposure of 290 hours to 1000-1300°F mercury vapor, and in another case after a 75 hour exposure to 940-1500°F vapor. Grain boundary attack with grain removal was evident in a Type 316 stainless steel control valve inlet tube after a 138 hour operation in 950-1330°F mercury vapor.

A Type 304 stainless steel tube exhibited pitting attack after 132 hours in 1300°F mercury.

An Inconel thermocouple sheath failed after a 50 hour exposure in 1080°F mercury because of excessive corrosion.

Turbine wheel blades made of 18-4-1 tool steel after a 40 hour exposure in 1000-1300°F mercury vapor showed evidence of some corrosion on the concave blade side and erosion on the leading edges.

A nozzle blade made of PH 15-7 Mo stainless steel suffered corrosion to a depth of 0.0003 inches along with some surface erosion after a 482 hour operation in 1145°F vapor. The corrosion, which occurred on both convex and concave surfaces, was evident as a leached layer with intergranular cusps (see Figure 35).

The attack noted in the vapor region on various components indicates that the mercury vapor was wet or that partial condensation occurred, since dry vapor is not considered to be corrosive. Wet vapor is to be expected in the turbine region.

In the high temperature liquid region of a prototype boiler, a tube made of Type 304 stainless steel displayed a depleted layer 0.0006 inches thick after exposure to 800-1000°F mercury for 132 hours.

A 17-4 PH stainless steel housing exposed to mercury at up to 600°F for 48 hours showed evidence of corrosion, as did also the Type 347 stainless steel tubes brazed into it. The mercury temperature ranged from 310 to 440°F in the tubes. Corrosion was generally more intense in the vicinity of the brazes. The brazes made with AMS 4775 alloy also were attacked and showed strong indications of corrosion cracking (see Figure 36).

An 18-4-1 tool steel thrust bearing exposed to 400°F mercury indicated that some corrosion occurred on the thrust face and possibly in the lube passages. The bearing thrust surface may have experienced pressures to 1000 psia and temperatures well in excess of 400°F.

In the low temperature regions, an austentic stainless steel (composite of Types 302, 303, and 316) and nicrobraze did not show any attack after 100 hours of operation in 350°F mercury. On the other hand, a Type 302 stainless steel spring immersed in mercury at less than 200°F with a flow rate of 15 to 30 pounds per minute failed because of corrosion fatigue. The spring was pitted on the surface to a depth of about 0.0007 inches. The austenitic ball valve actuated by the spring also was attacked in a similar manner (see Figure 37).

A Type 316 stainless steel tube showed dissolution in 385°F (vapor and liquid) mercury when examined after 85 hours. The dissolution caused malfunction of a Type 316 SS valve because of deposition (see Figure 38).

Inconel "0" rings were corroded to a depth of about 0.0005 inches by what was reported to be relatively stagnant mercury at 350 and 550°F. The corrosion was manifested as depleted areas.

The evidence suggests that all materials which were found to be corrodable in the laboratory screening tests were subject to some degree of corrosion in a dynamic system regardless of temperature in liquid (or liquid containing vapor) mercury. The corrosion found was generally in accord with the order derived from the laboratory screening tests, thus supporting the validity of the testing procedures.

The drastic corrosion at low and higher temperatures, as evidenced by absence of a corrosion layer, indicates that corrosion may be influenced in part by velocity effects which may change the attack from diffusion to solution rate controlled. Also the corrosion in low temperature mercury supposedly saturated with contaminants dissolved from "hotter" areas demonstrates the fallacy of the belief that low temperature mercury saturated with contaminants is non-corrosive. The effect on component strength of a liquid metal which wets and corrodes is pronounced. The endurance limit is probably reduced to a low value (25) decreasing the resistance of a metal to fracture. Component design must compensate for the strength loss so that the desired unit life may be achieved.

The synergistic increase in intensity of corrosion resulting from close proximity of dissimilar metals suggests that electrolytic action may influence mercury corrosion. The pitting attack is also characteristic of concentration cell action. Diversity of component materials should, consequently, be kept to a minimum.

10.0 CONCLUSIONS

1. Of the alloys tested with high strength at elevated temperatures, with exception of the refractory metals and alloys, Haynes Alloy No. 25 was found to have the highest resistance to mercury corrosion at 900°F.

2. Type 410 stainless steel has very good resistance to mercury corrosion at temperatures up to 1000°F.

3. Sicromo 5S,, PH 15-7Mo, Neatro Tool Steel and 17-4PH have very good corrosion resistance to mercury at 900°F.

4. Several materials have excellent resistance to mercury corrosion at 900°F, but their use is limited because of fabrication and other problems. These include tantalum, tungsten, molybdenum, columbium, tungsten carbide, titanium carbide (K150A), alumina, ATJ graphite and Pyroceram.

5. A number of materials a c unusable in mercury at 900°F because of poor corrosion resistance. They include aluminum, nickel, Inconel, chromium, manganese, zirconium, platinum, Sylvania #4, Kovar, Carpenter 20Cb and titanium.

6. A large group of materials have poor resistance to mercury corrosion and probably are unusable at 900°F without additives. Included in this group are the Type 300 series stainless steels, Waspalloy, Rene 41, AF1753, and A286 stainless steel.

7. Chromium, nickel and manganese are the alloy constituents most susceptible to corrosion attack by mercury.

8. Contaminant generation is the major problem resulting from mercury corrosion in the SNAP II application.

9. Some contaminants are transported in the mercury vapor.

10. Liquid mercury supposedly saturated with contaminants can still be corrosive even at temperatures below 200°F in some cases.

11. Separation of contaminants from a dynamic system by thermal gradients or density changes is ineffective.

12. Interaction between dissimilar materials can increase corrosion effects in a mercury system.

13. Titanium, in small quantities, added to mercury greatly reduces the corrosion rate of some materials.

14. The gases nitrogen, oxygen and hydrogen are beneficial in reducing mercury corrosion but not all to the same degree.

15. Surface pretreating with mercury or mercury containing titanium reduces corrosion for periods up to sixty days.

16. Surface treatments are inconsequential in preventing mercury corrosion at 900°F.

17. Surface oxidation reduced the severity of corrosion of most alloys. However, corrosion was not eliminated at 900°F.

18. Deleterious stress effects were not discernable in bent reflux tubes tests for most materials at 900°F.

19. Corrosion fatigue failures can occur in mercury environments at temperatures below 200°F.

20. The mercury corrosion rate increases rapidly with temperature for most materials. However, other effects such as velocity can lead to significant corrosion even at low temperatures.

21. Different effects of time are experienced with different materials, depending on the mode of corrosion attack.

22. Corrosion occurs in a system under conditions of heat flux, even when the contained mercury is saturated with container alloy constituents.

23. Data from bent reflux tube tests correlate well with loop test data and component examination observation.

11.0 RECOMMENDATIONS

The investigation of materials for use in mercury environments, that has been conducted thus far, has indicated areas which require additional study. Also, larger pressure drops are being reported in the mercury boiler than had been anticipated, leading to higher boiler pressures and temperatures, thus making corrosion data at higher temperatures imperative. Therefore, to continue this study in a logical manner, the following recommendations are presented.

1. The material screening tests in bent reflux tubes should be continued at 900°F to accomplish the following:

    (a) Find a bearing material superior to 18-4-1.

    (b) Evaluate the cast Haynes Alloys for use as a housing material for the rotating unit.

    (c) Locate a valve material more resistant to seizing than the Type 316 SS.

    (d) Evaluate the long time corrosion resistance of materials which have been evaluated in twelve (12) day tests.

    (e) Extend the study of inhibitors to more materials and to longer timed tests to increase the number of usable materials.

    (f) Study the interactions of more bimetallic combinations before they are incorporated into rotating units.

    (g) Study the effects of cover gases on the corrosion of a greater number of materials.

2. Continue, but in greater number, the bent reflux tube tests at 1100°F to do the following:

    (a) Determine which materials, satisfactory at 900°F, can be used at 1100°F.

    (b) Find out if inhibitors useful at 900°F are also beneficial at 1100°F.

3. Additional loop tests should be conducted for corrosion, mass transfer, and contaminant separation data. The number of loops run should be kept to a minimum to reduce costs. Therefore, the selection of loop tests should be made as the investigation proceeds. However, the need for several loop tests is apparent at the present time. They are as follows:

    (a) A Type 347 SS loop containing titanium should be run. This loop

should be run up to 900°F for a few hours full of liquid mercury with titanium. Then the mercury level should be lowered and the test conducted in the usual way for 1000 hours.

(b) A loop of a combination of Haynes 25 and Type 316 SS welded together in both the liquid and vapor regions should be tested for at least 1000 hours. This is to evaluate the required Haynes 25 to Type 316 SS connections in the P.C.S. -1 unit.

(c) A Haynes 25 loop with titanium should be run for a long period of time, at least 3000 hours.

(d) Another loop containing a trap should be tested. Type 316 SS or Type 347 SS would provide the greatest quantity of contaminants and is recommended. The trap on this loop should contain a large internal surface area which should be oxidized. The purpose of this test would be to investigate several questions emanating from previous tests. Can the effect, noted in the Type 347 SS oxidized loop be used to separate contaminants? Does the trap in the loop effect the boiler attack as observed in the first trap loop or if good separation occurs will the trap enhance the attack? Can the trap design be modified slightly to give some centrifugal separating action?

4. Continue the component examination to check material performance under actual system conditions. This effort is also expected to uncover any unsuspected problems that may exist.

12.0 ACKNOWLEDGEMENTS

The authors wish to acknowledge the contribution of the various people engaged in this program. Mr. R. Evans conducted a large number of the loop tests and offered many helpful suggestions in regard to the design of the loop system. Mr. V. Timpano conducted the capsule tests and fabricated the bent reflux tubes. Mr. P. Metz prepared the specimens both for the test and for metallurgical examination after the tests. Mr. R. Palmieri conducted the spectrographic and chemical analyses.

13.0 REFERENCES

1. N.K. Adams, The Physics and Chemistry of Surfaces, Oxford University Press, 1952, p. 130.

2. W.D. Manly, " Fundamentals of Liquid Metal Corrosion," Corrosion, July, 1956, 336t.

3. A. de Brasunas, "Liquid Metal Corrosion," Corrosion, March, 1953, p. 78.

4. R.F. Koenig, "New Tests Prove Materials for Nuclear Power Plants," Iron Age, August, 1953, p. 129.

5. O.J. Kleppa, "Thermodynamics and Properties of Liquid Solutions," Liquid Metals and Solidification, American Society for Metals, 1958, p. 56.

6. J.R. Weeks and D.H. Gerrinsky, "Solid Metal-Liquid Metal Reactions in Bismuth and Sodium," ibid, p. 106.

7. Liquid Metals Handbook, United States Atomic Energy Commission and Department of the Navy, 1953.

8. C. Wagner, "Thermodynamic Investigation on Ternary Amalgams," Journal of Chemical Physics, Vol 19, May, 1951, p. 626.

9. H.H. Uhlig, "Metal Surface Phenomena," Metal Interfaces, American Society for Metals, 1952, p. 312.

10. J.B. Hess, "Measurement of Solid Interfacial Energies," ibid, p. 134.

11. H. Udin, "Measurement of Solid: Gas and Solid: Liquid Interfacial Energies," ibid, p. 114.

12. W.D. Robertson, "Structure Dependent Chemistry of Metal Surfaces," Impurities and Imperfections, American Society for Metals, 1955, p. 170.

13. A.M. Gaudin, Principles of Mineral Dressing, McGraw Hill Book Co. Inc., 1939, p. 475.

14. G. Ehrlich and D. Turnbull, "Surface Structure and Chemical Interaction," Physical Metallurgy of Stress Corrosion Fracture, Interscience Publishers, 1959, p. 47.

15. J.M. McKee, "Sodium Corrosion as a Function of Time," Preprint V114-, Nuclear Engineering and Science Conferences sponsored by ASME Joint Council, 1959.

16. A.K. Covington and A. A. Woolf, "Isothermal Mass Transfer," Journal Nuclear Energy, Part B, Reactor Technology, Vol. 1, 1959, p. 35.

17. M. Hansen, Constitution of Binary Alloys, McGraw Hill Book Co. Inc. 1958.

18. J.F. Strachan and N. L. Harris, "The Attack of Unstressed Metals by Liquid Mercury," Journal of the Institute of Metals, 1956-57, Vol. 58, p. 17.

19. W. J. Moore, Physical Chemistry, Prentice Hall, 1955, p. 505.

20. R.C. Reid, "Mercury Boiler Treatment with Titanium and Magnesium Metals," Papers No. 51-S-13, Presented at Atlanta, Ga Spring Meeting of ASME, 1951.

21. G. Kortum and J. O'M. Bockris, Text Book of Electrochemistry, Elsevier Publishing Co., 1951.

22. H. H. Hausner, "Fundamentals of Metal-Ceramic Combinations," Metals for Supersonic Aircraft and Missiles, American Society for Metals, 1958, p. 315.

23. P. Durvez, "Intermediate Phases in Alloys of the Transition Elements," Theory of Alloy Phases, American Society for Metals, 1956, p. 243.

24. G.W. Horsley, "Mass-Transport and Corrosion of Iron-Based Alloys in Liquid Metals," Journal of Nuclear Energy, Part B, Reactor Technology, 1959, Vol 1, p.84.

25. R. Cezand, "Fatigue of Metals," Philosophical Library, 1953.

26. J.W. Vogt, "A Device for Investigation of Corrosion by Mercury," TRW, TM1376CM.

27. K.S. Bergstresser, "The Determination of Ni, Fe, and Cr in Mercury," Technical Information Division, AEC, Oak Ridge, Tenn., pp. 11-23-48-98 and 339.

28. D.B. Cooper, "One Thousand Hour Corrosion Test of Type 347 SS Loop Containing Mercury, TRW, TM1397CM, June, 1959.

29. D.B. Cooper, "One Thousand Hour Corrosion Test of Type 316 SS Loop Containing Mercury," TRW, TM1401CM, June, 1959.

30. D.B. Cooper, "One Thousand Hour Corrosion Test of Type 446 Loop Containing Mercury," TRW, TM1414CM, June, 1959.

31. D.B. Cooper, "One Thousand Hour Corrosion Test of Type 316 SS Loop with Specimen Holders," TRW, TM1476CM, October, 1959.

32. D.B. Cooper, "One Thousand Hour Mercury Corrosion Test of a Type 316 SS Loop Containing a Trap," TRW, TM1512CM, January, 1960.

33. J.J. Owens, "One Thousand Hour Corrosion Test of Type 410 SS Loop Containing Mercury," TRW, TM1513CM, December, 1959.

34. J.J. Owens, "One Thousand Hour Corrosion Test of Type 410 SS Loop Containing Mercury, Run No. 11," TRW, TM1420CM, June, 1959.

35. L.R. Kelman, et al, "Resistance of Materials to Attack By Liquid Metals," ANL-4417, July, 1950.

14.0 BIBLIOGRAPHY

1. L.F. Bates, P.F. Illsley, "The Magnetic Properties of Iron Amalgams," Proceedings of the Physical Society of London, Vol. 49, 1937, p. 611.

2. L.F. Bates, J.H. Prentice, "The Electrical Resistance of Nickel Amalgams," Proceedings of the Physical Society of London," Vol. 51, 1939, p. 419.

3. J.A.R. Bennet, J.B. Lewis, "Diffusion et controle chimique dans la dissolution des metaux dans le mercure," Journal de Chimie Physique, No. 55, 1958, p. 83.

4. J. Jaffrat, J. Cariat, "Thermodynamique – Sur quelque properties physiques des amalgames de nickel," Compte Rendu, No. 231, 1950, p. 1128.

5. F. Lihl, "Untersuchangen an den amalgamen dir Metalle Mangan, Eisen, Kobalt, Nickel and Kupfer," Zeitschrift Metallkunde, April, 1953, p. 160.

6. R.E. Myers, "Results Obtained in Electrochemical Analysis by the Use of a Mercury Cathode," Journal of the American Chemical Society, Vol. 26, 1904, p. 1124.

7. F. Pawlek, "Magnetische Eigenschaften von Amalgamen der Eisenmetalle," Zeitschrift Metallkunde, December, 1950, p. 451.

8. M. Rabinowitsch, P.B. Zywotinski, "Quecksilber als Dispersionsmittel – Die kolloide Natur der Eisenamalgame," Kolloid Zeitschrift, Vol. 52, 1930, p. 31.

9. Carl Wagner, "Thermodynamic Investigations on Ternary Amalgams," Journal of Chemical Physics, Vol. 19, 1951, p. 626.

10. E. Wichers, "Pure Mercury," Review of Scientific Instruments, Vol. 13, 1942, p. 502.

11. E. Wichers, "Pure Mercury," Chemical and Engineering News, Vol. 20, 1942, p. 111.

SOLUBILITY OF SEVERAL METALS IN MERCURY AS A FUNCTION OF TEMPERATURE
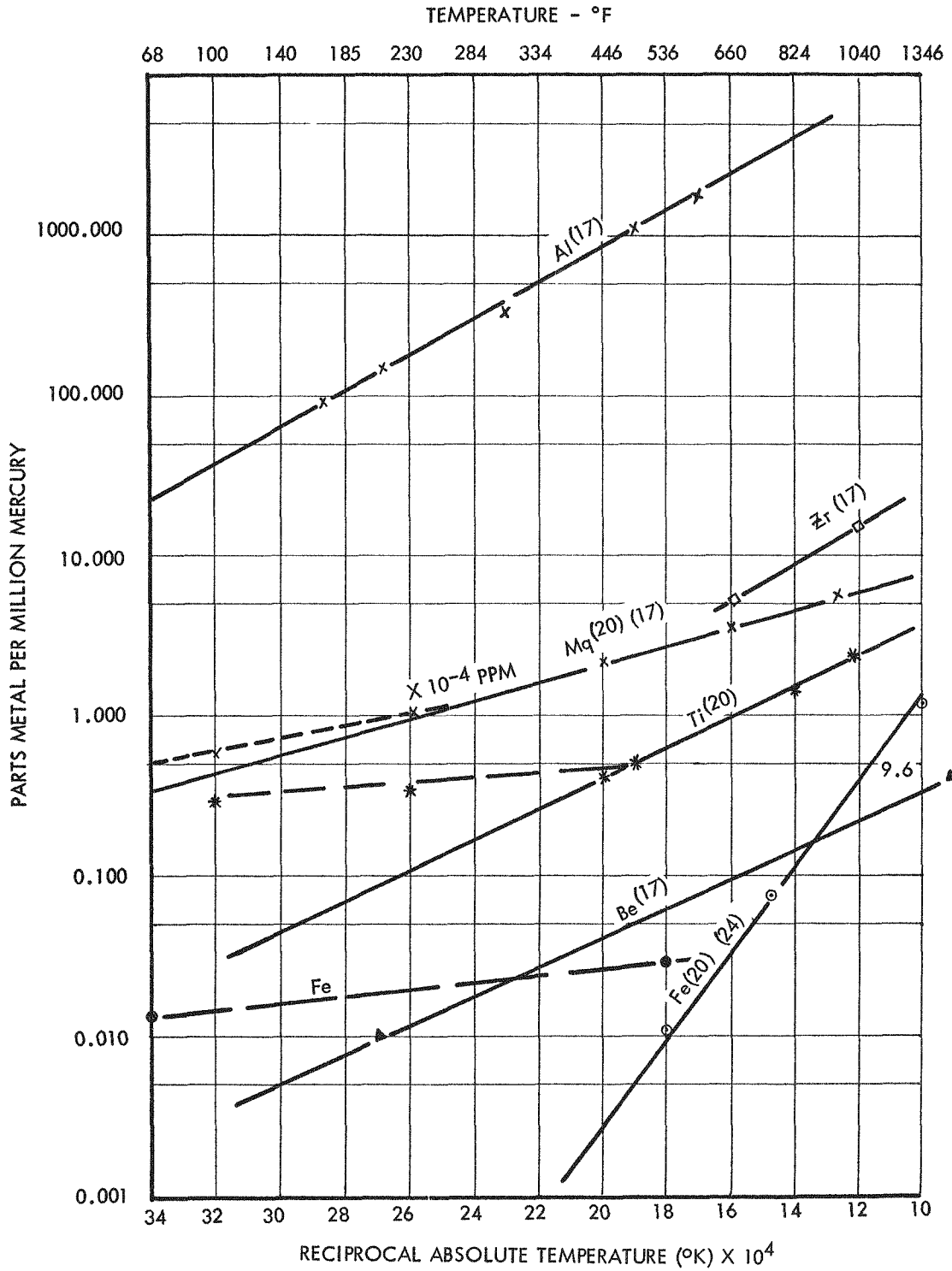
FIGURE 1

BENT REFLUX TUBES

FIGURE 2

516A
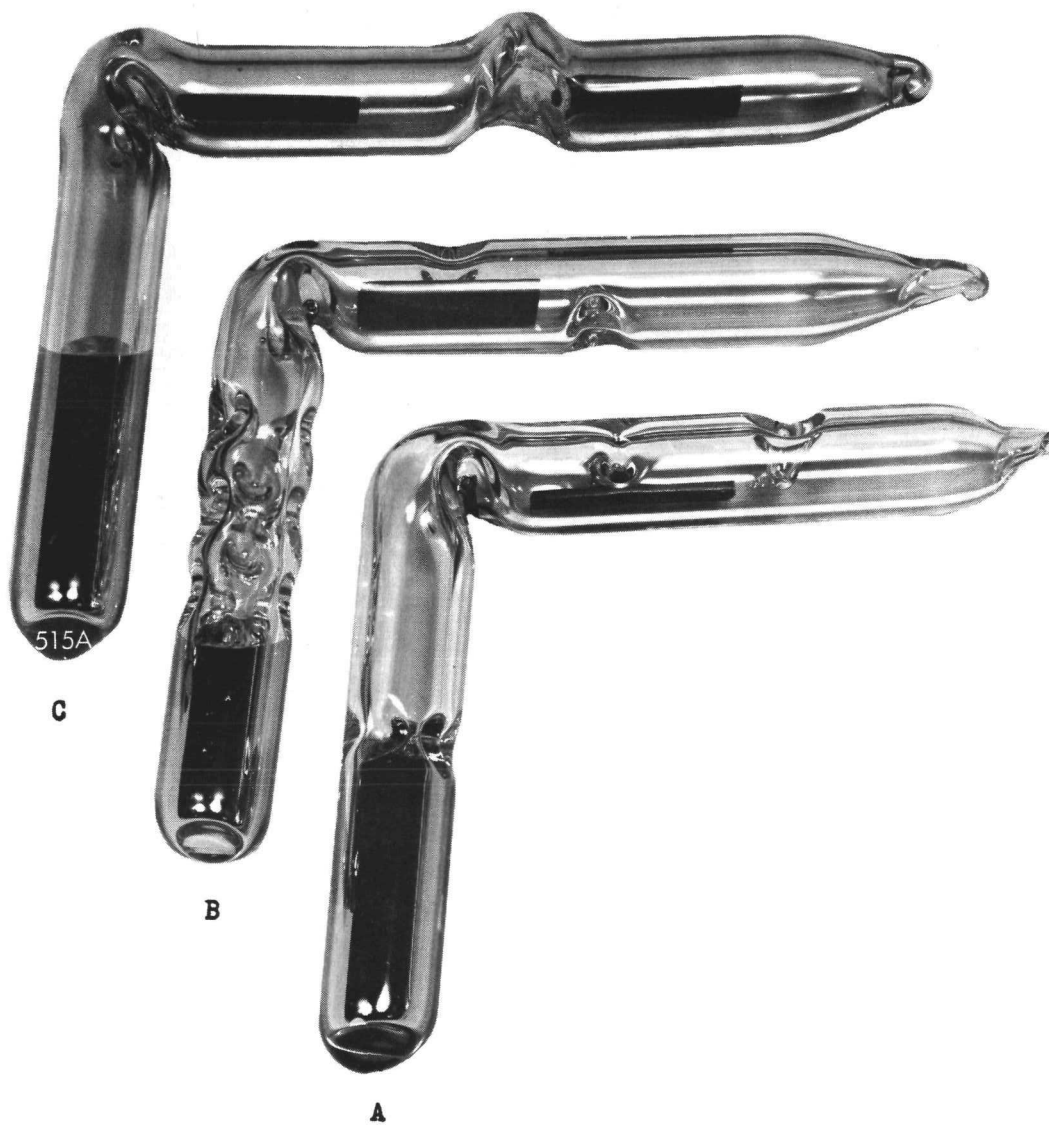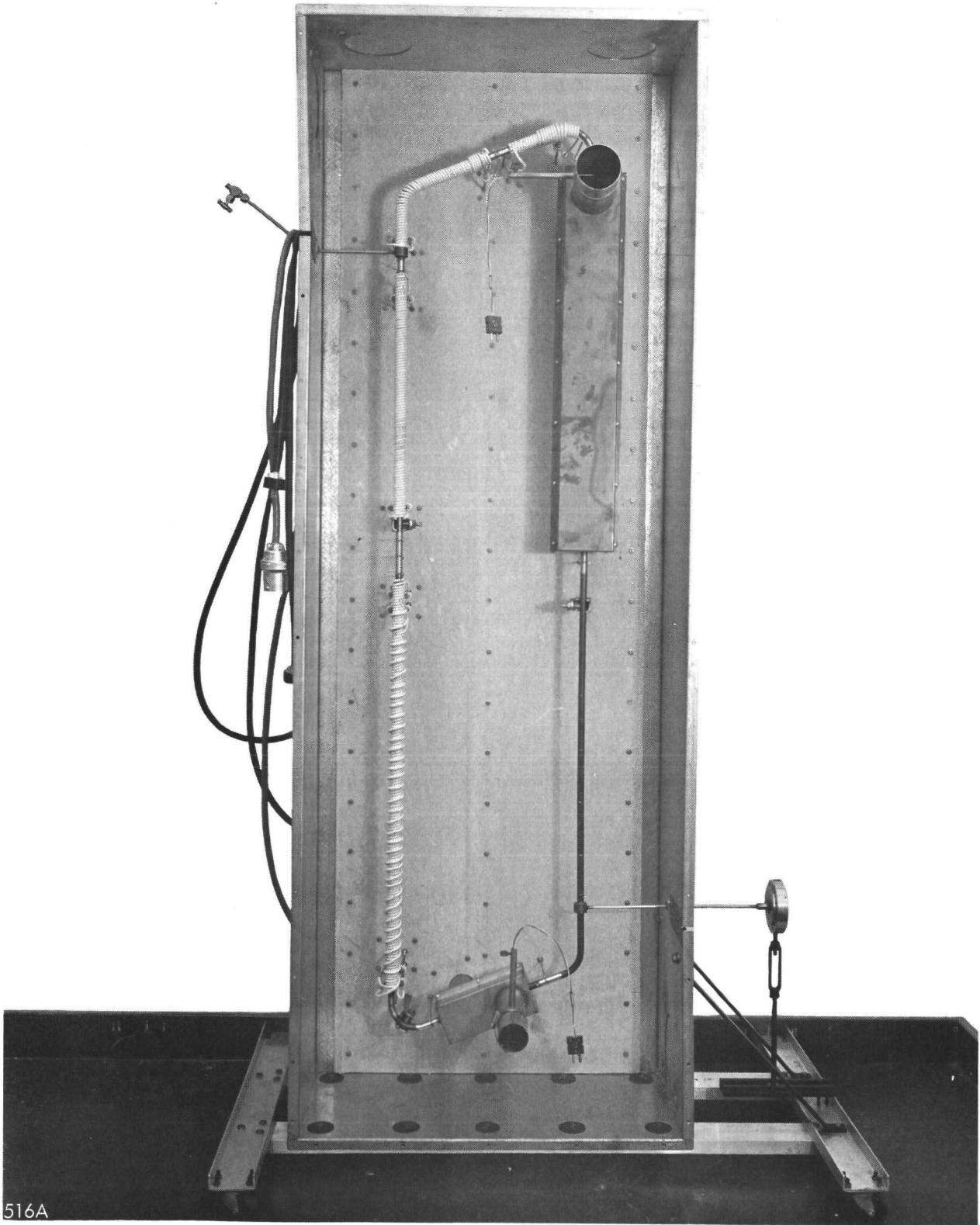
CORROSION LOOP

FIGURE 3

WEIGHT LOSS VS. TIME FOR LOW ALLOY STEELS AND SOME
IRON BASE ALLOYS IN REFLUXING LIQUID MERCURY AT 900°F

Sicromo 5s
×

Armco Tran-Cor T
+

Sylvania No. 4
○

Carp. 42
△ (Cold rolled)

Hyperco 27
●

Kovar
*

Vascojet 1000
D
◗ (QT)

1010 and Armco Fe
〉

1095
◇
◆ (QT)
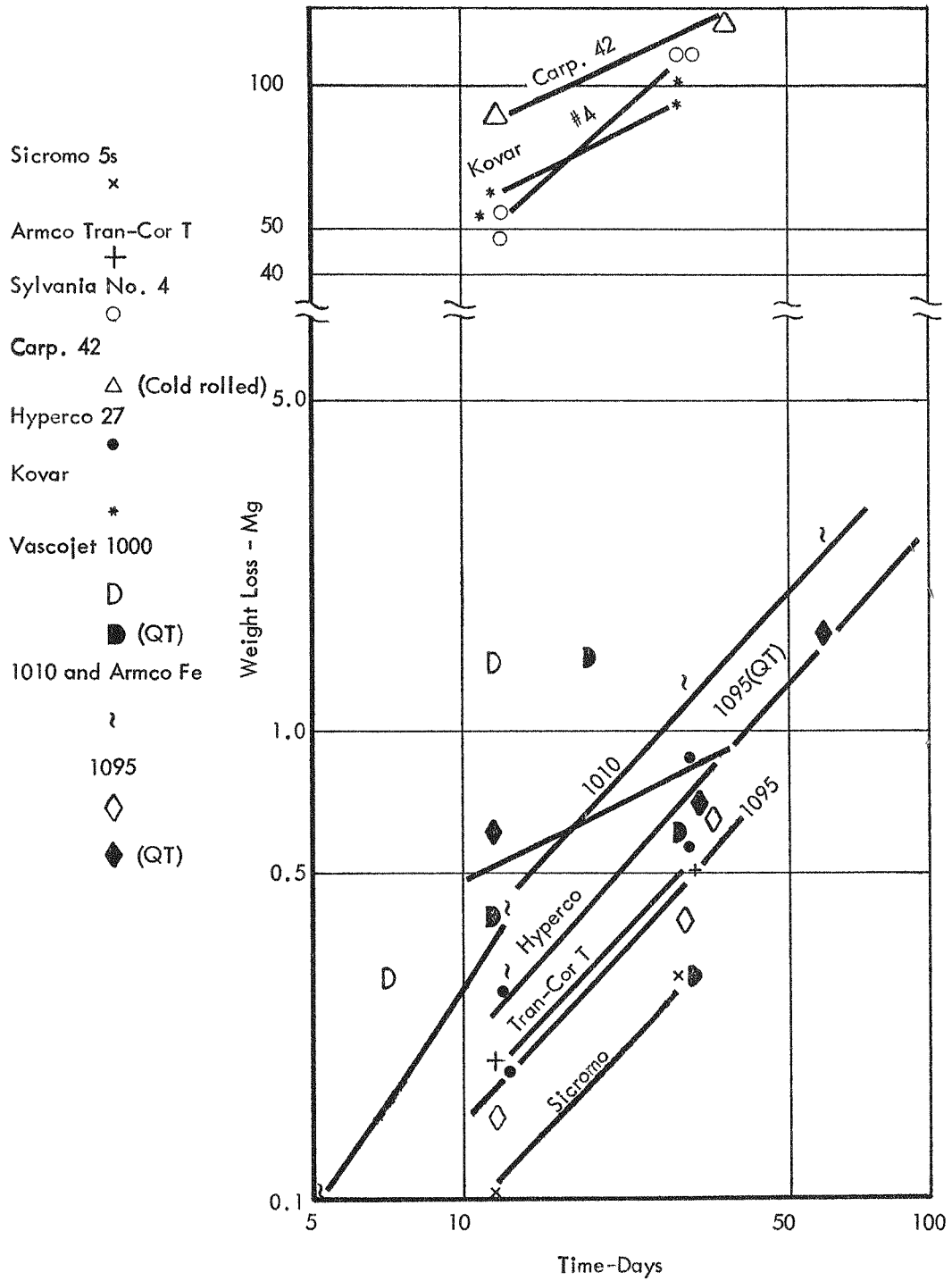
FIGURE 4

WEIGHT LOSS VS. TIME FOR MODERATELY ALLOYED STEELS
IN REFLUXING LIQUID MERCURY AT 900°F.

18-4-1
  ▽
  ▼ (QT)

Neatro
  ○
  ◉ (QT)

Chromewear
  □
  ▧ (QT)

FIGURE 5

64
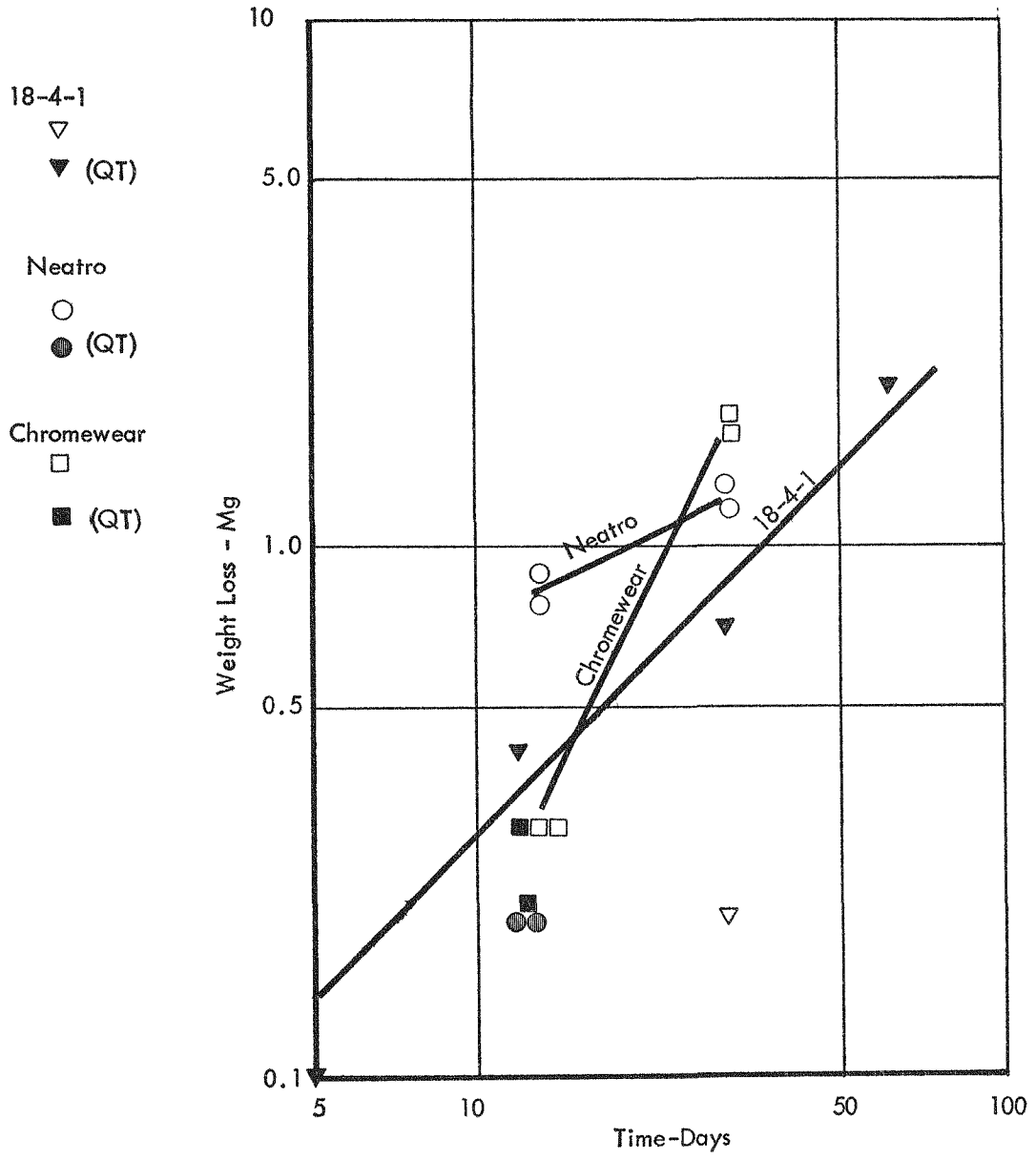
PENETRATION VS. TIME FOR VARIOUS IRON BASE ALLOYS
IN REFLUXING LIQUID MERCURY AT 900°F

FIGURE 6

65
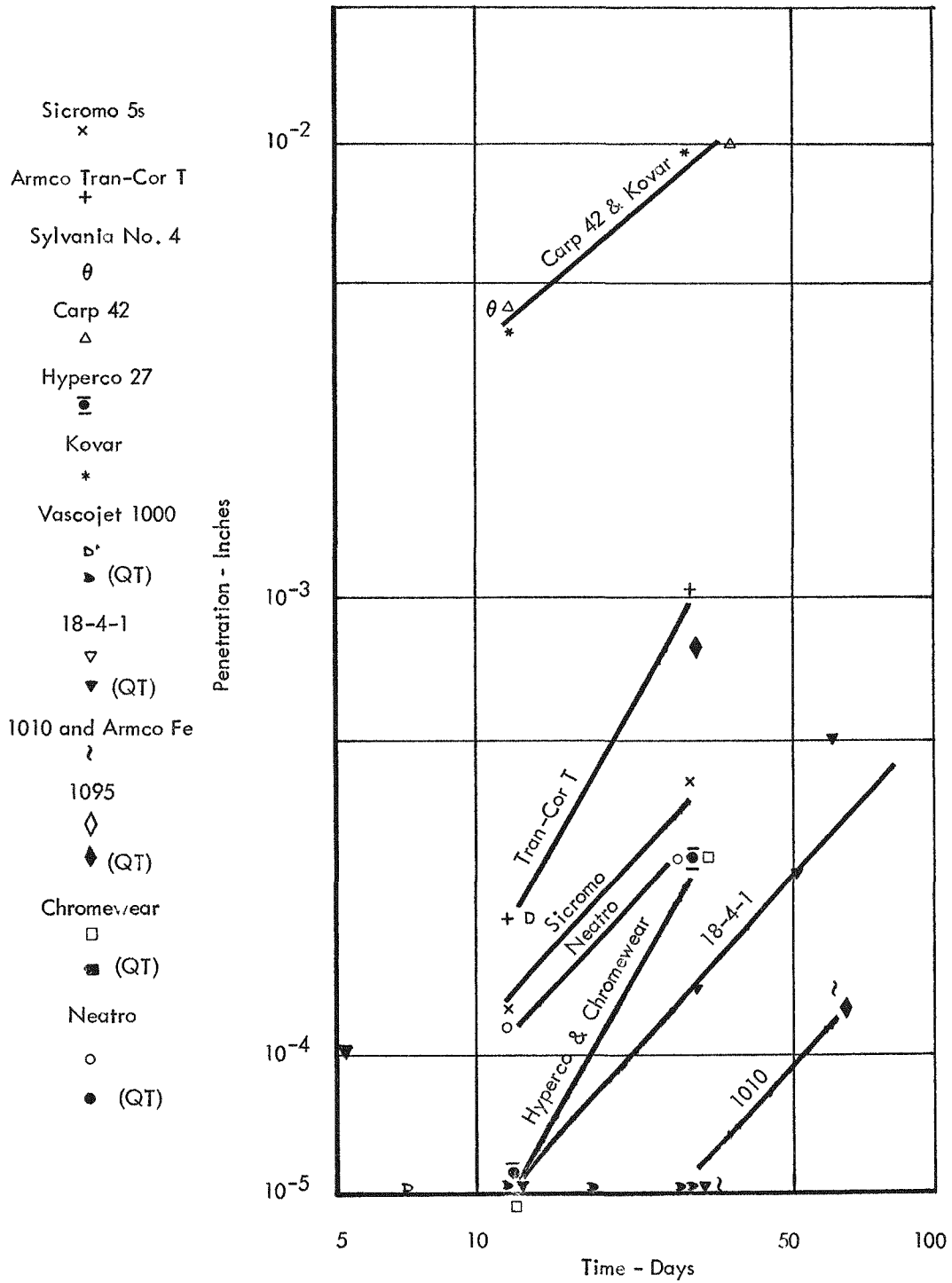
WEIGHT LOSS VS. TIME FOR VARIOUS MATERIALS IN REFLUXING LIQUID MERCURY AT 700°F

347 (Ann)
●

Kovar
×

316
□

310
△

Carpenter 20Cb
+

Haynes Alloy No. 25
∗

Inconel
◇

Weight Loss – Mg

Time – Days
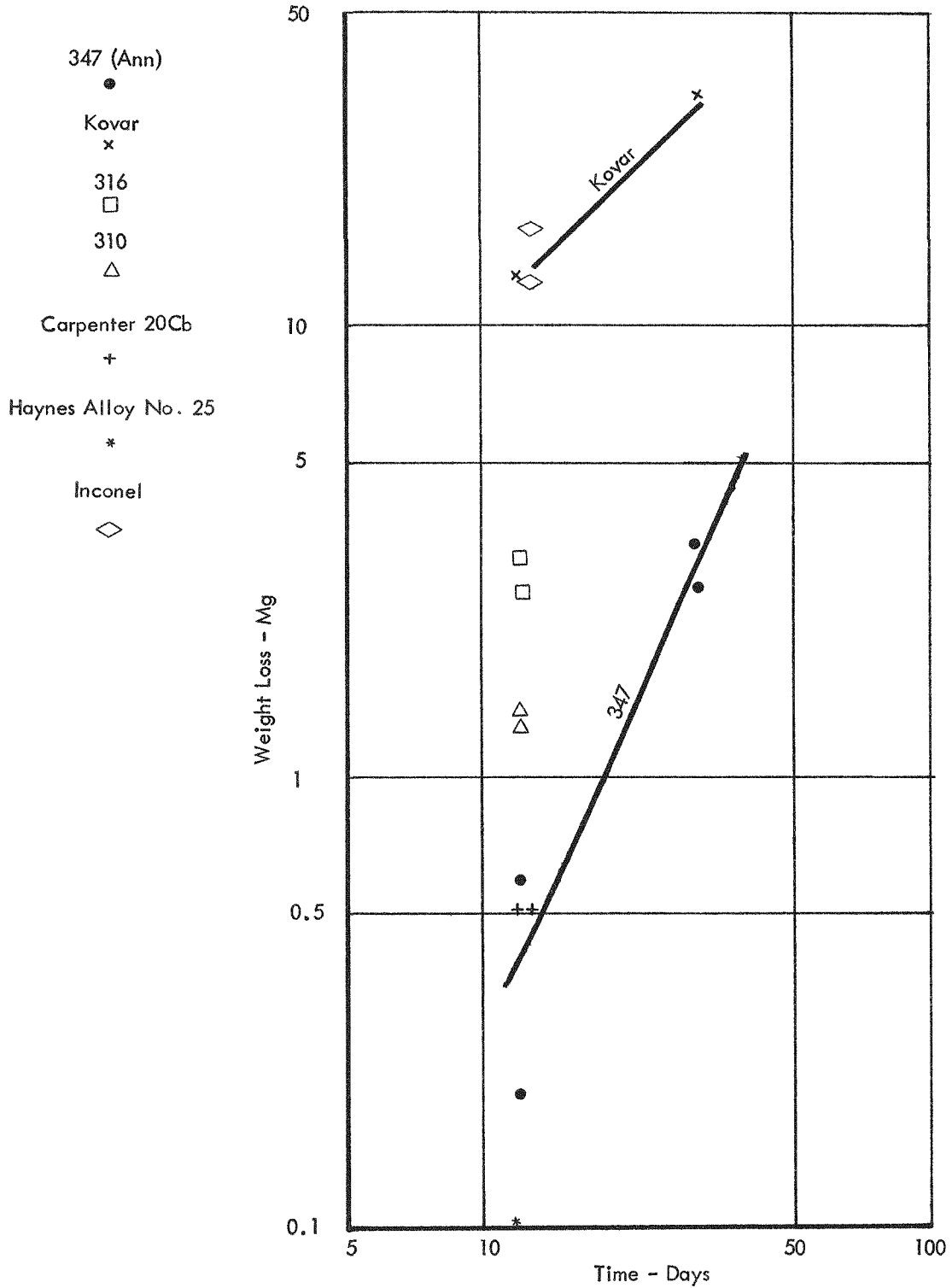
FIGURE 7

WEIGHT LOSS VS. RECIPROCAL ABSOLUTE TEMPERATURE FOR VARIOUS STAINLESS
STEELS, INCONEL, AND KOVAR IN REFLUXING LIQUID MERCURY
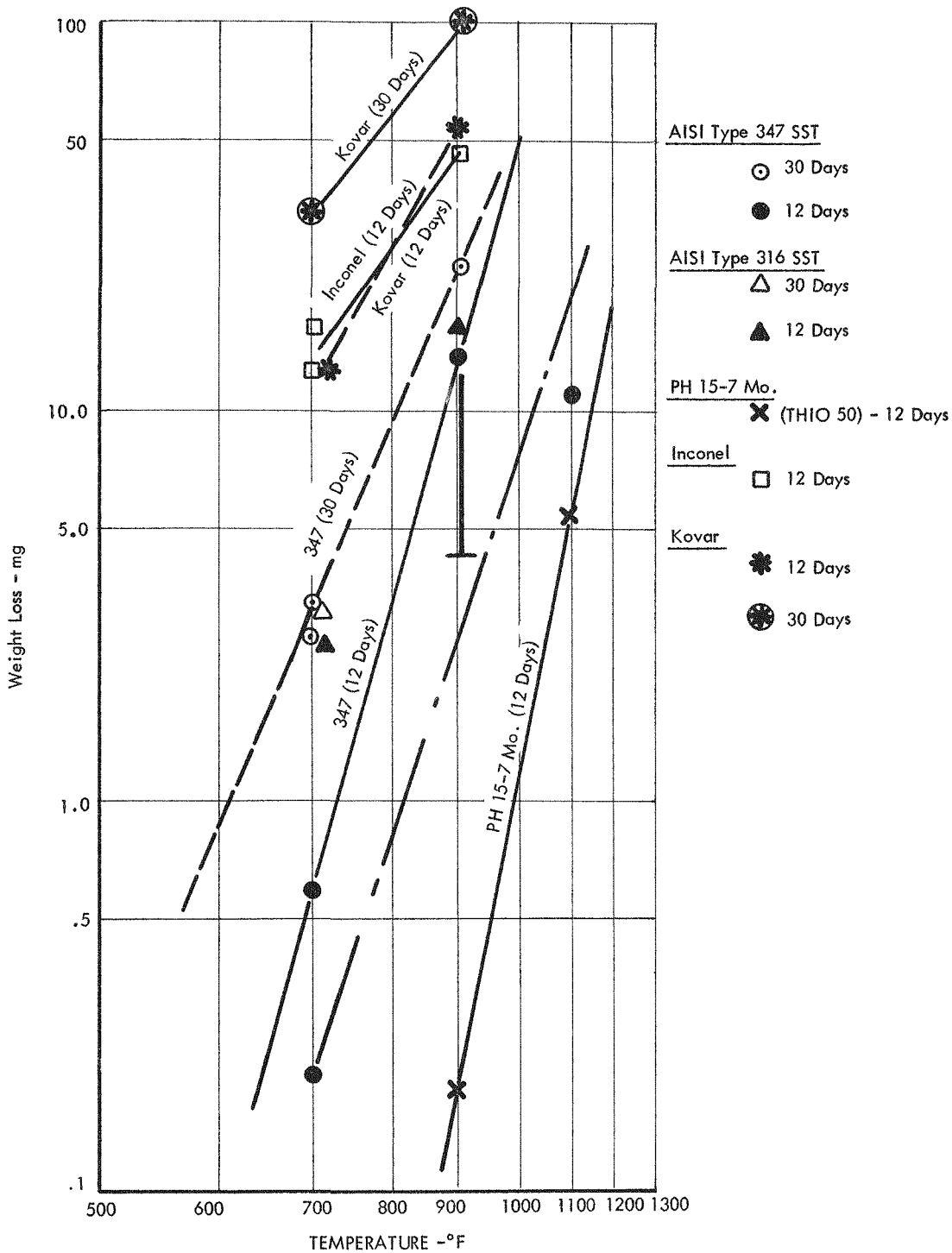
FIGURE 8

WEIGHT LOSS VERSUS TIME FOR TYPE 400 SERIES STAINLESS STEELS
IN REFLUXING LIQUID MERCURY AT 900°F

FIGURE 9

68
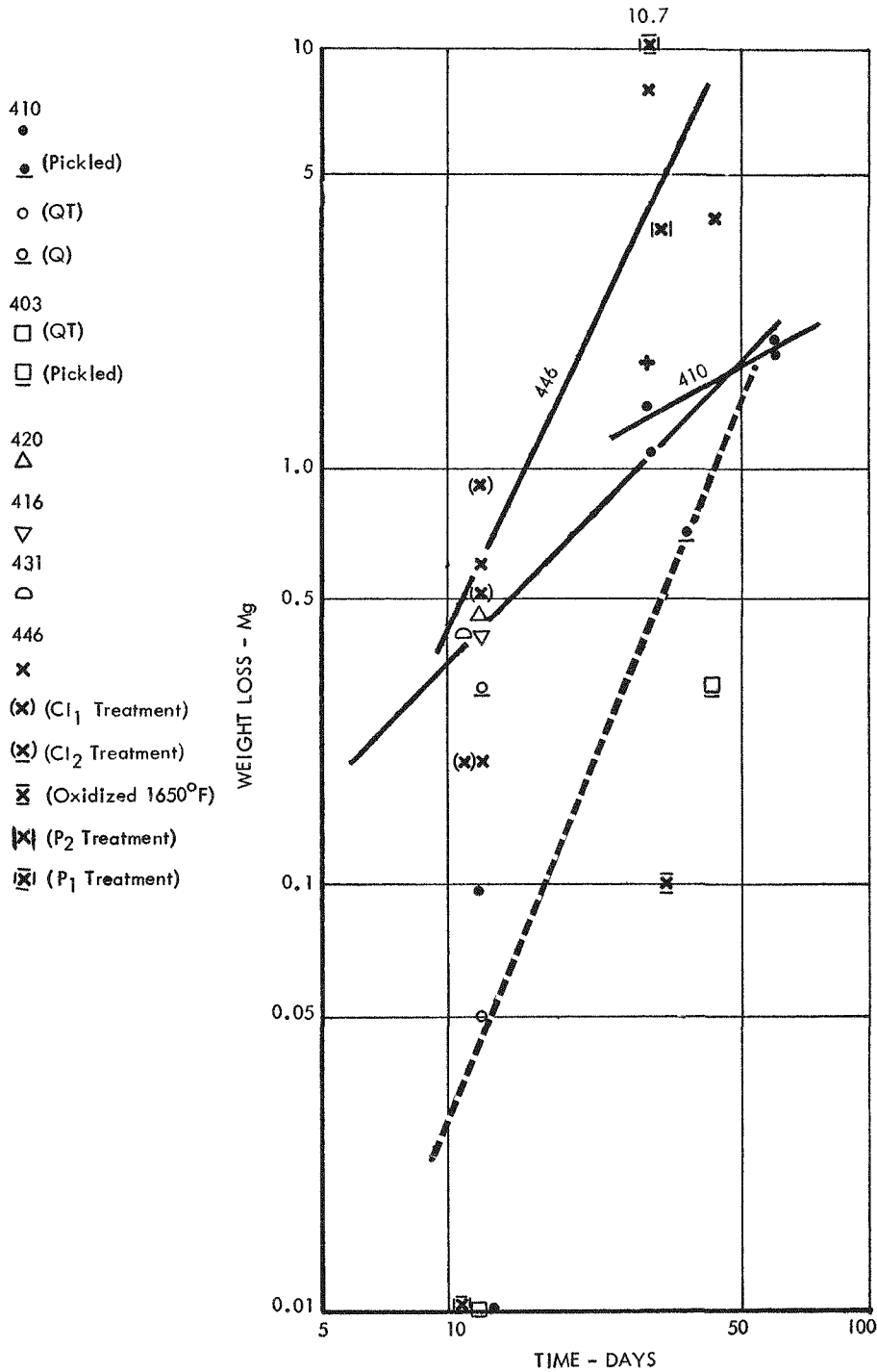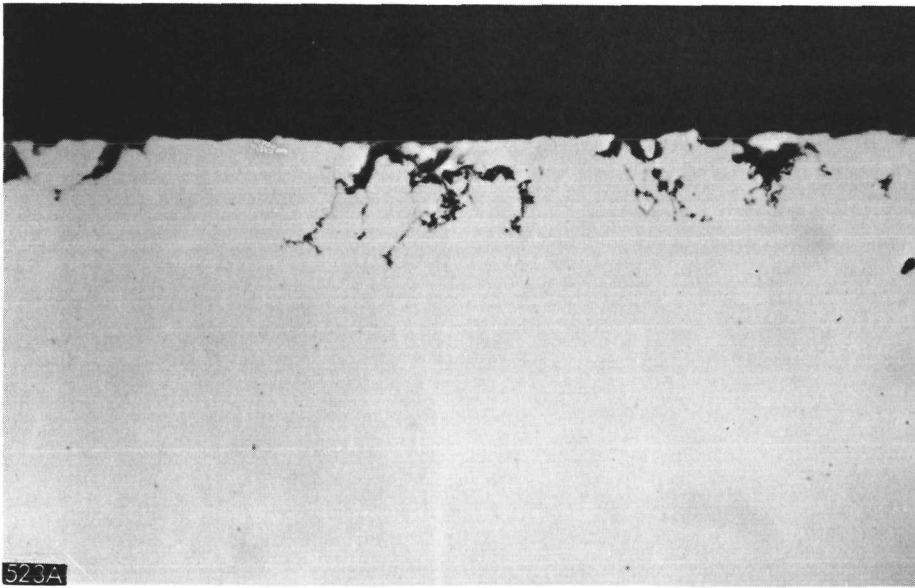
CROSS SECTION OF TYPE 410 STAINLESS STEEL AFTER   FIGURE 10
59 DAYS IN THE BENT REFLUX TUBE AT 900°F.

RDM 274   750 X

CORROSION PENETRATION VERSUS TIME FOR TYPE 400 SERIES
STAINLESS STEELS IN REFLUXING LIQUID MERCURY AT 900°F
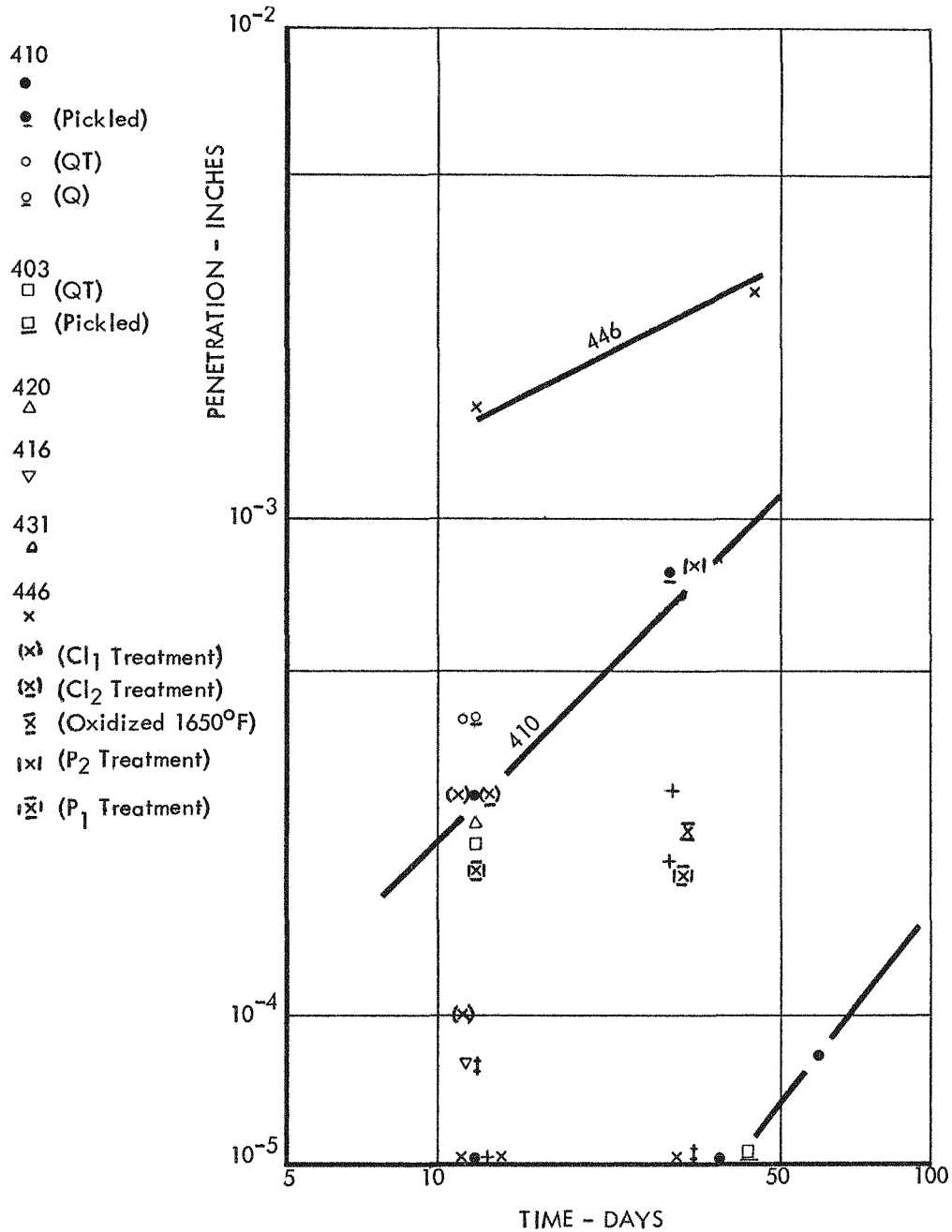
FIGURE 11

WEIGHT LOSS VERSUS TIME FOR TYPE 300 SERIES STAINLESS STEELS
IN REFLUXING LIQUID MERCURY AT 900°F
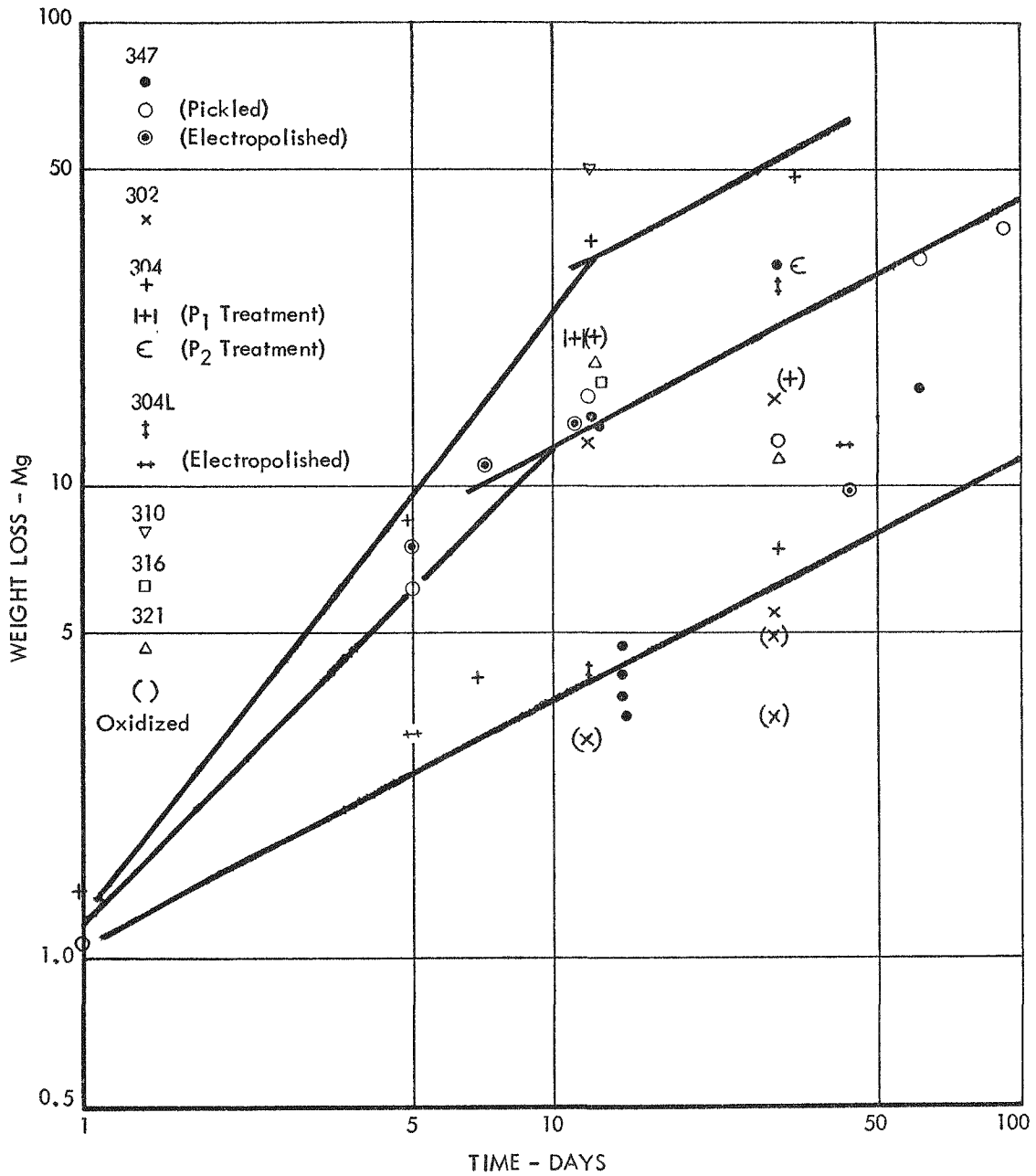
FIGURE 12
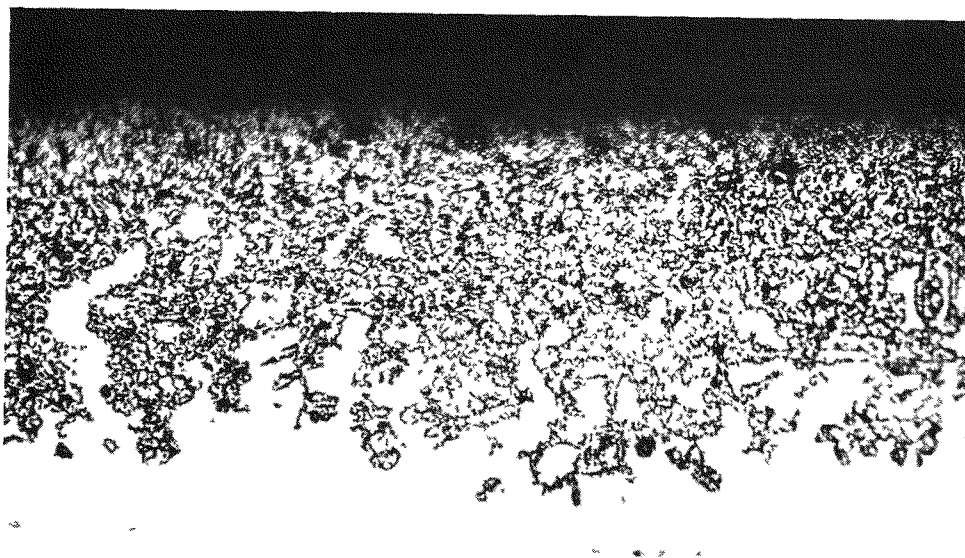
CROSS SECTION OF TYPE 347 STAINLESS STEEL AFTER
60 DAYS IN THE BENT REFLUX TUBE AT 900°F.   FIGURE 13

RDM 276   250 X

CORROSION PENETRATION VERSUS TIME FOR TYPE 300 SERIES
STAINLESS STEELS IN REFLUXING LIQUID MERCURY AT 900°F
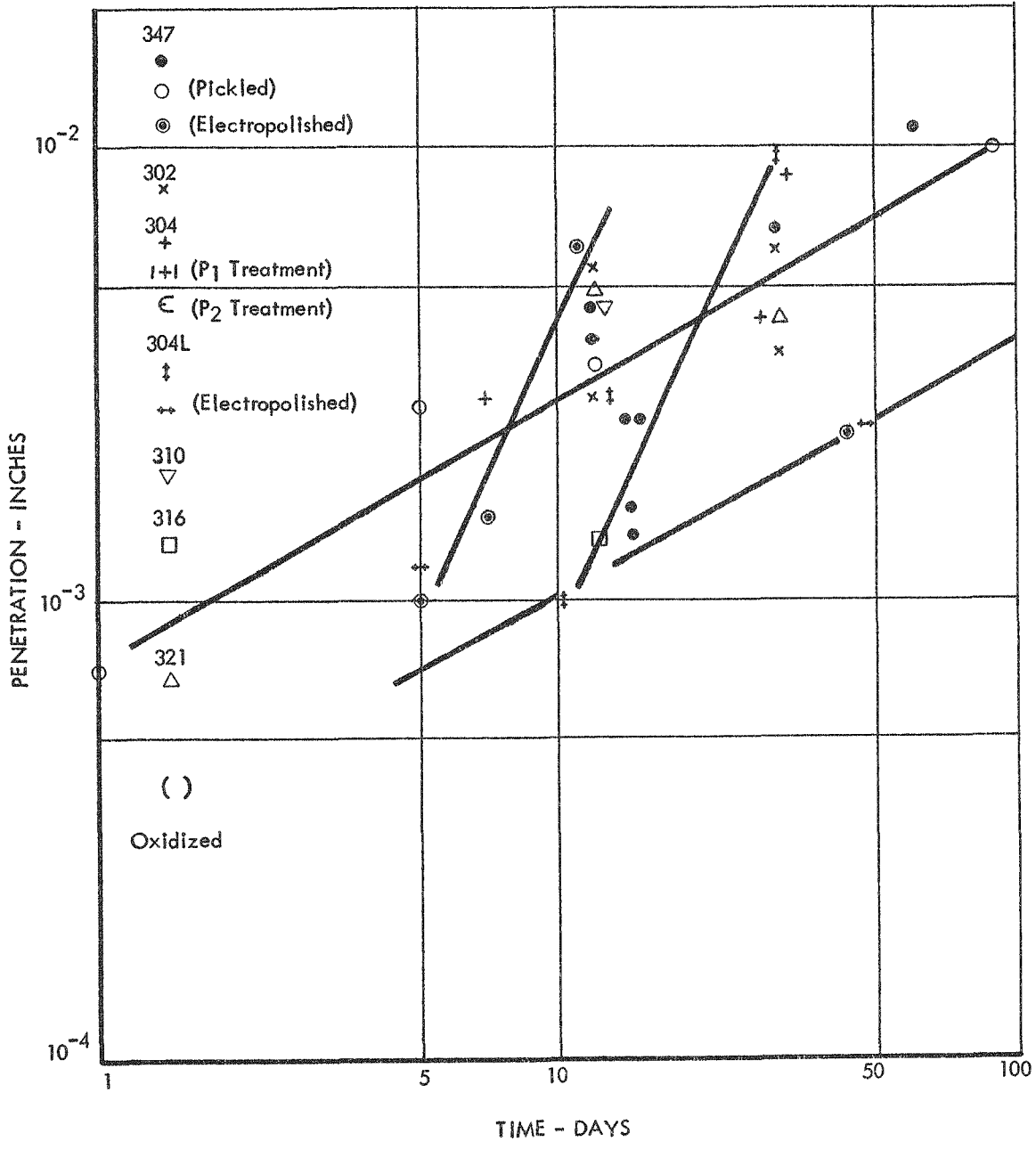
FIGURE 14

WEIGHT LOSS VS TIME FOR VARIOUS AUSTENITIC ALLOYS
IN REFLUXING LIQUID MERCURY AT 900°F

15 – 15N
△

19 – 9DL
×

Carp 20Cb
●

MS 201
○

XCR
□ (HT)

FIGURE 15

WEIGHT LOSS VS TIME FOR PRECIPITATION HARDENING STAINLESS STEELS
IN REFLUXING LIQUID MERCURY AT 900°F

17 – 4PH
● (TH 1050)
○ (Cond. A)

PH 15 – 7Mo
▲ (TH 1050)
△ (Cond. A)

17 – 7 PH
◆ (TH 1050)
◇ (Cond. A)

AM 350
▦ (DA)
☐ (Ann)

A 286
◆ (Aged)
◇ (Ann)

( ) Oxidized
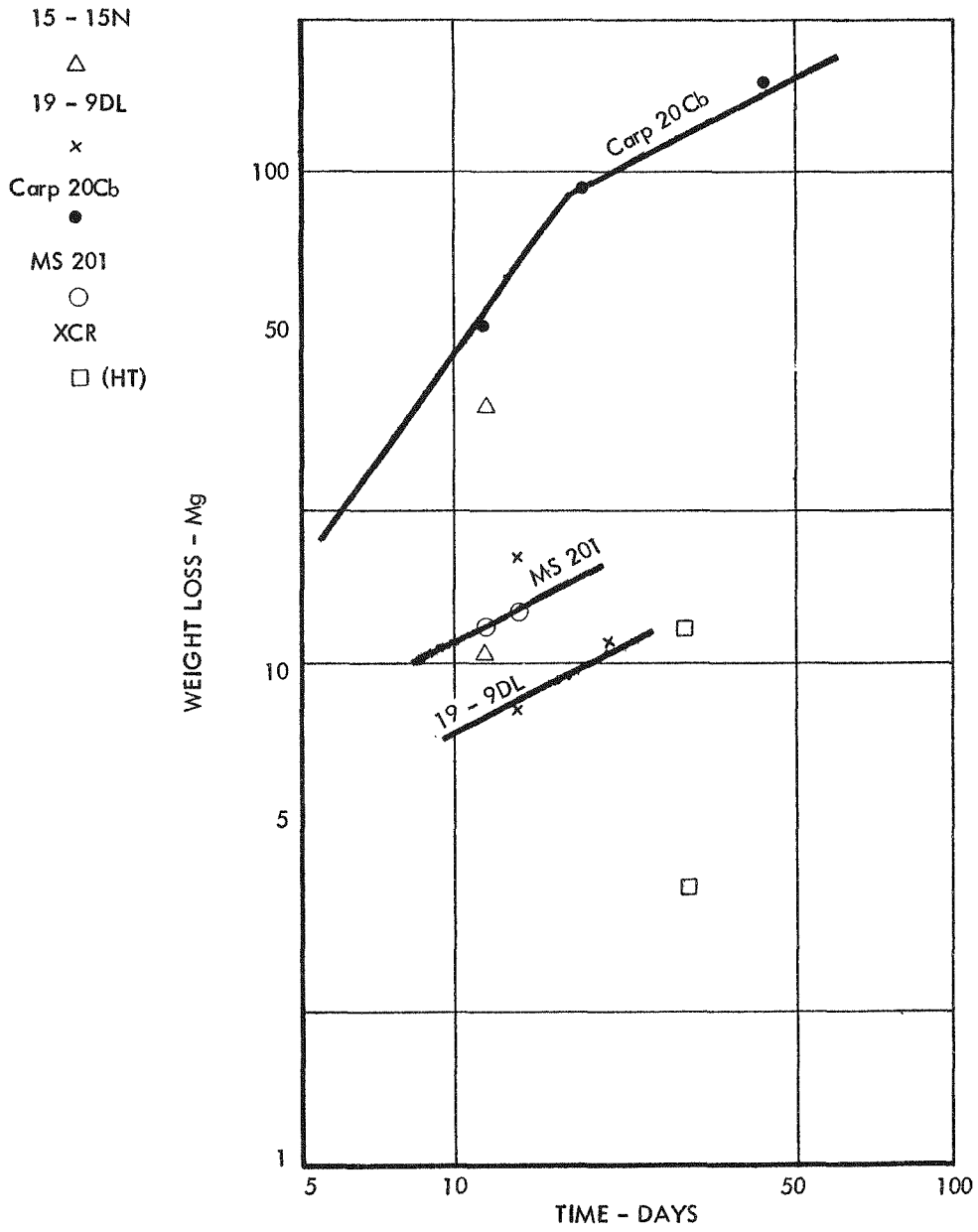
FIGURE 16

75
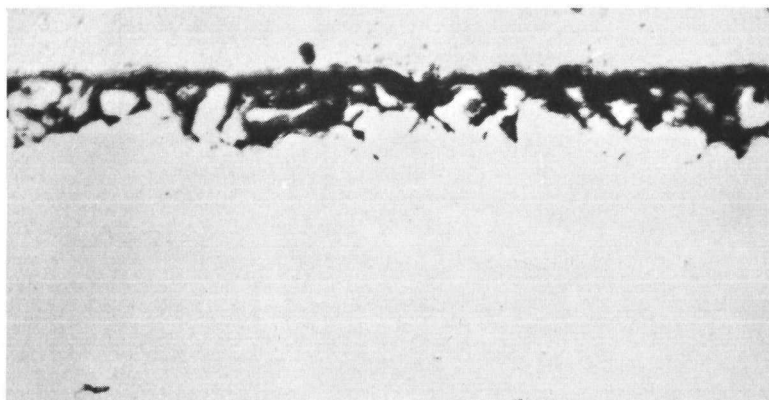
CROSS SECTION OF 17–4PH STAINLESS STEEL AFTER
59 DAYS IN THE BENT REFLUX TUBE AT 900°F.

FIGURE 17

RDM 275   750 X
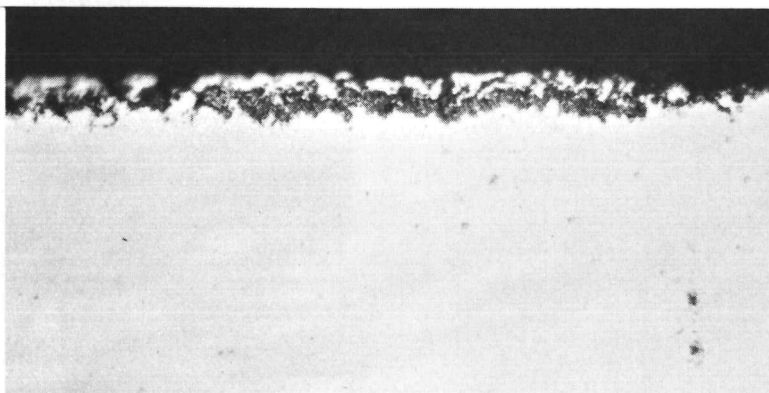
CROSS SECTION OF PH 15–7Mo STAINLESS STEEL AFTER
60 DAYS IN THE BENT REFLUX TUBE AT 900°F.

FIGURE 18

RDM 270   750 X
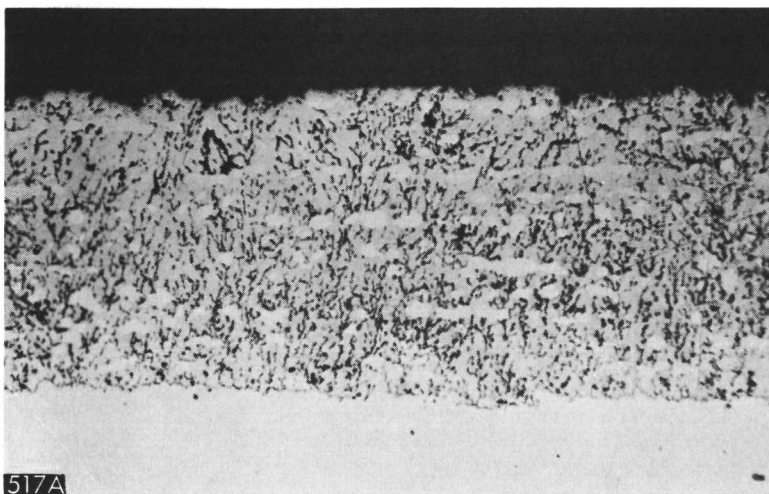
CROSS SECTION OF AM350 STAINLESS STEEL AFTER
60 DAYS IN THE BENT REFLUX TUBE AT 900°F.

FIGURE 19

RDM 267   250 X   7 6

PENETRATION VS. TIME FOR PRECIPITATION HARDENING STAINLESS STEELS
IN REFLUXING LIQUID MERCURY AT 900°F

17 - 4PH
     ⊛ (TH 1050)
     ○ (Cond. A)

PH 15 - 7 Mo
     ▲ (TH 1050)
     △ (Cond. A)

17 - 7PH
     ◆ (TH 1050)
     ◇ (Cond. A)

AM 350
     ■ (DA)
     ☐ (Ann)

A 286
     ◆ (Aged)
     ◇ (Ann)
     ( ) Oxidized

FIGURE 20

THuGROUP
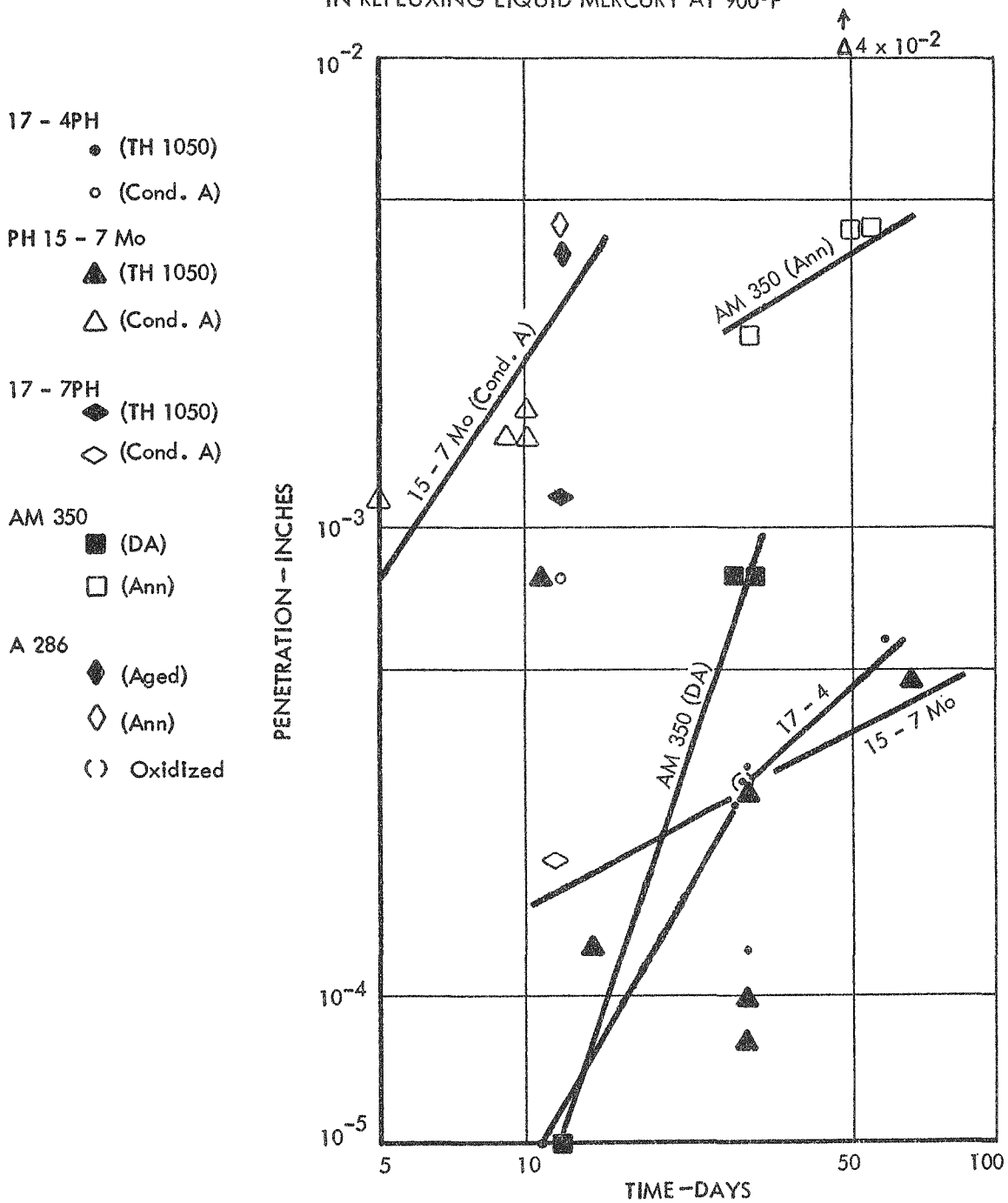
WEIGHT LOSS VS. TIME FOR VARIOUS NICKEL BASE ALLOYS IN
REFLUXING LIQUID MERCURY AT 900°F
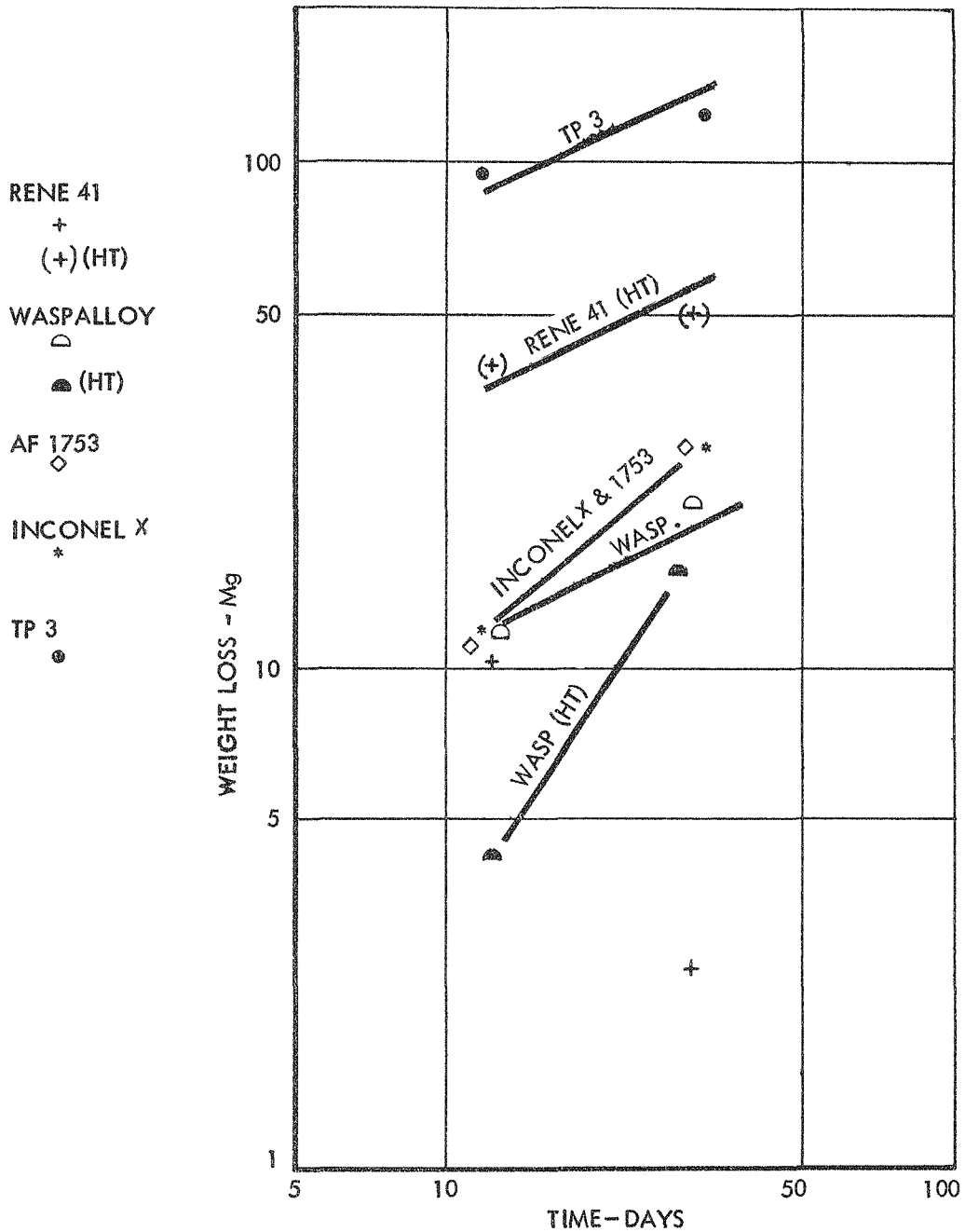
FIGURE 21

CORROSION PENETRATION VS. TIME FOR VARIOUS NICKEL
BASE ALLOYS IN REFLUXING LIQUID MERCURY AT 900°F.
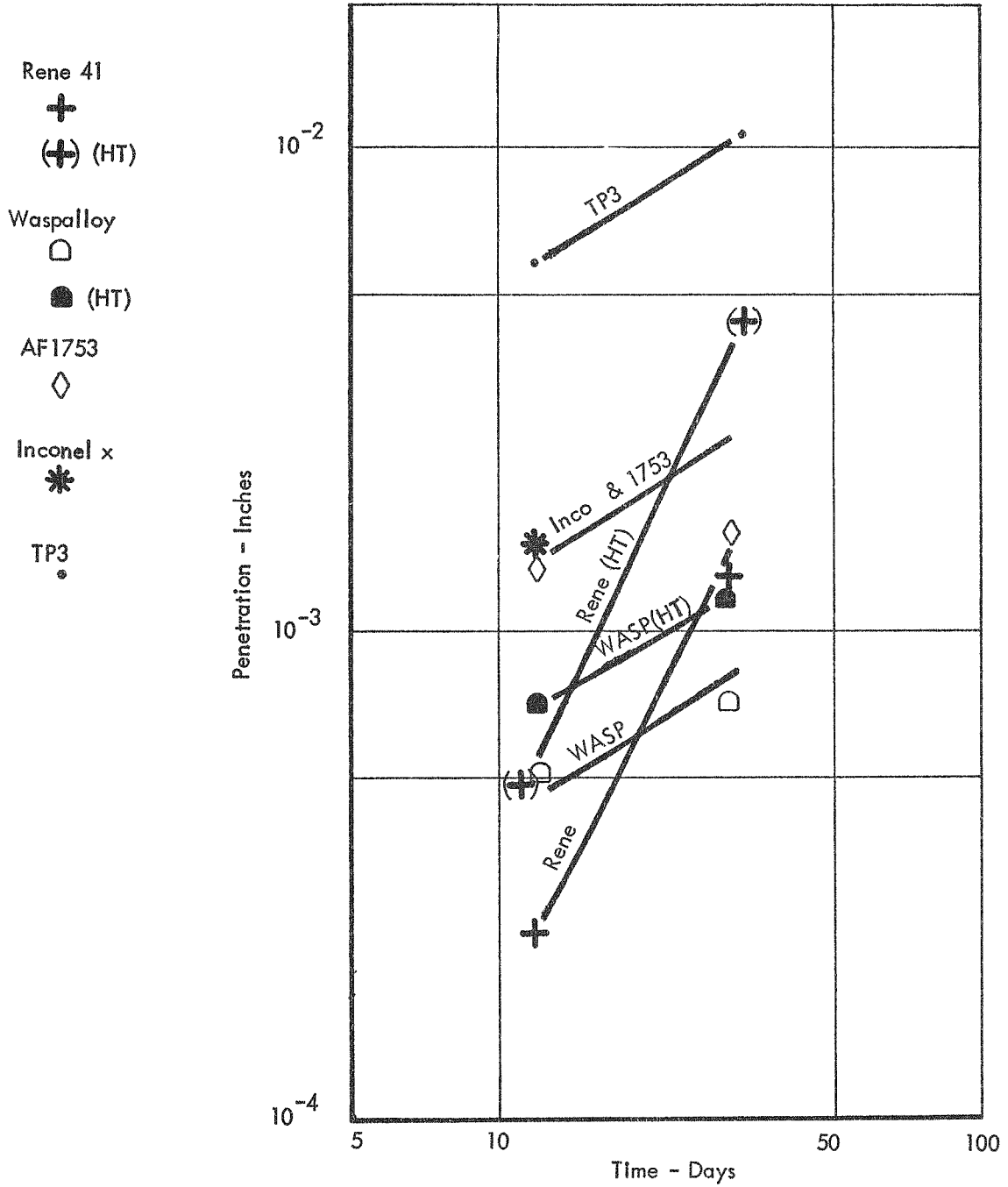
FIGURE 22

CROSS SECTION OF NICKEL-BASE ALLOY TP3 AFTER
32 DAYS IN THE BENT REFLUX TUBE AT 900°F.

FIGURE 23

RDM 268   250 X

CORROSION WEIGHT LOSS VERSUS TIME FOR COBALT BASE
ALLOYS IN REFLUXING LIQUID MERCURY AT 900°F
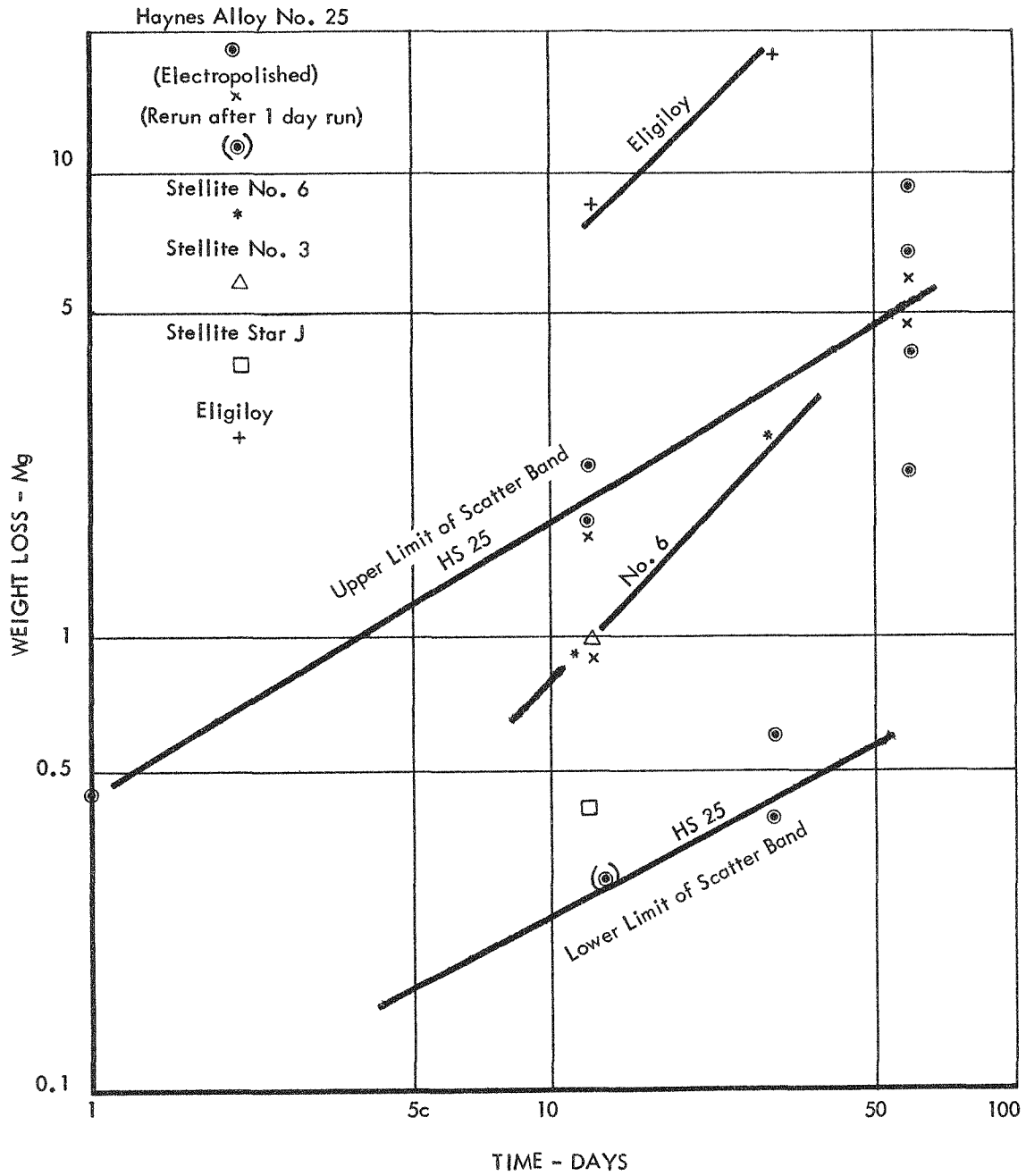
FIGURE 24

PENETRATION VS. TIME FOR COBALT BASE ALLOYS
IN REFLUXING LIQUID MERCURY AT 900°F

HAYNES ALLOY NO. 25

•

✘ (Electro polished)

(•) (Rerun after 1 day run)

STELLITE NO. 6
✳

STELLITE NO. 3
△

STELLITE STAR J
□

ELGILOY
✚
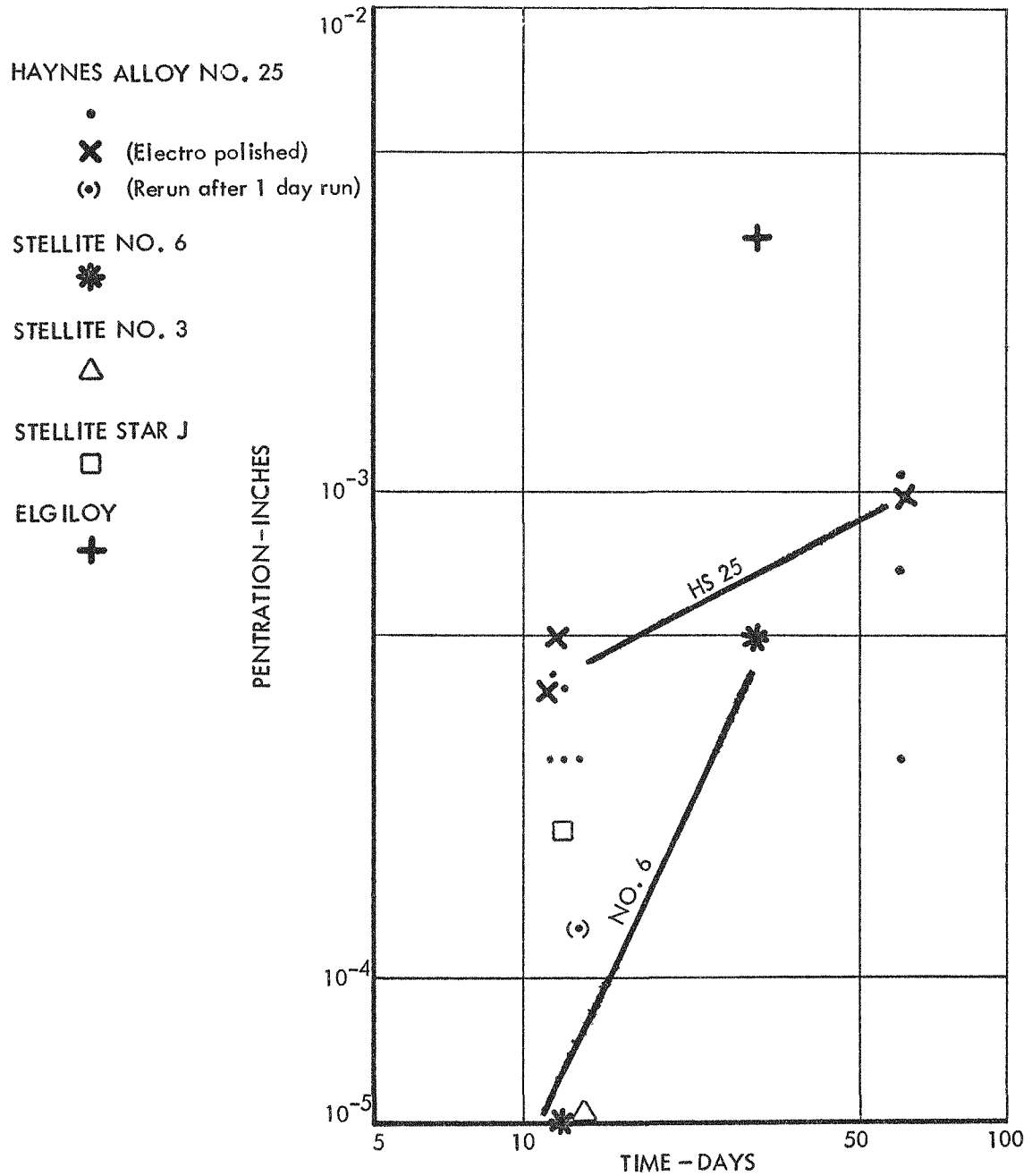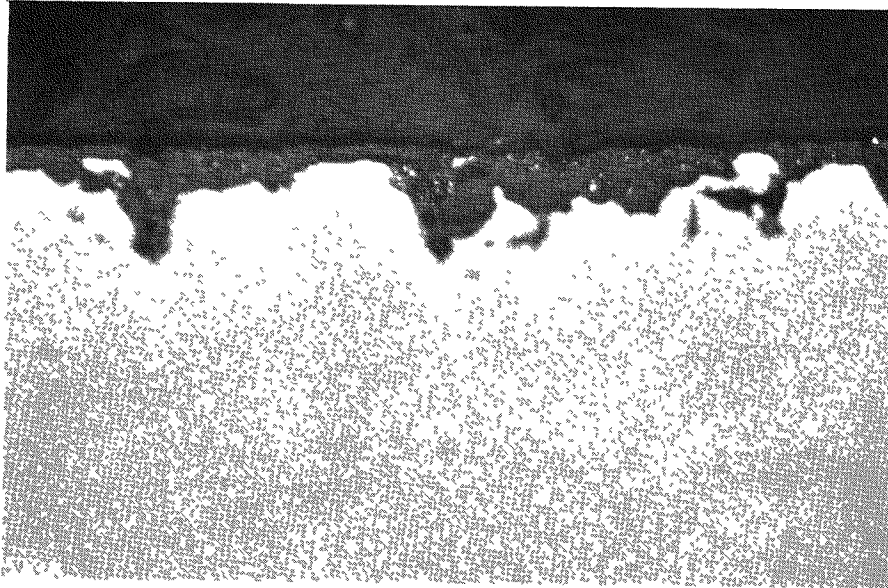
FIGURE 25

CROSS SECTION OF HAYNES ALLOY NO. 25 AFTER
 60 DAYS IN THE BENT REFLUX TUBE AT 900°F.

FIGURE 26

RDM 279   750 X

WEIGHT LOSS VS. RECIPROCAL ABSOLUTE TEMPERATURE FOR

HAYNES ALLOY NO. 25 IN REFLUXING LIQUID MERCURY
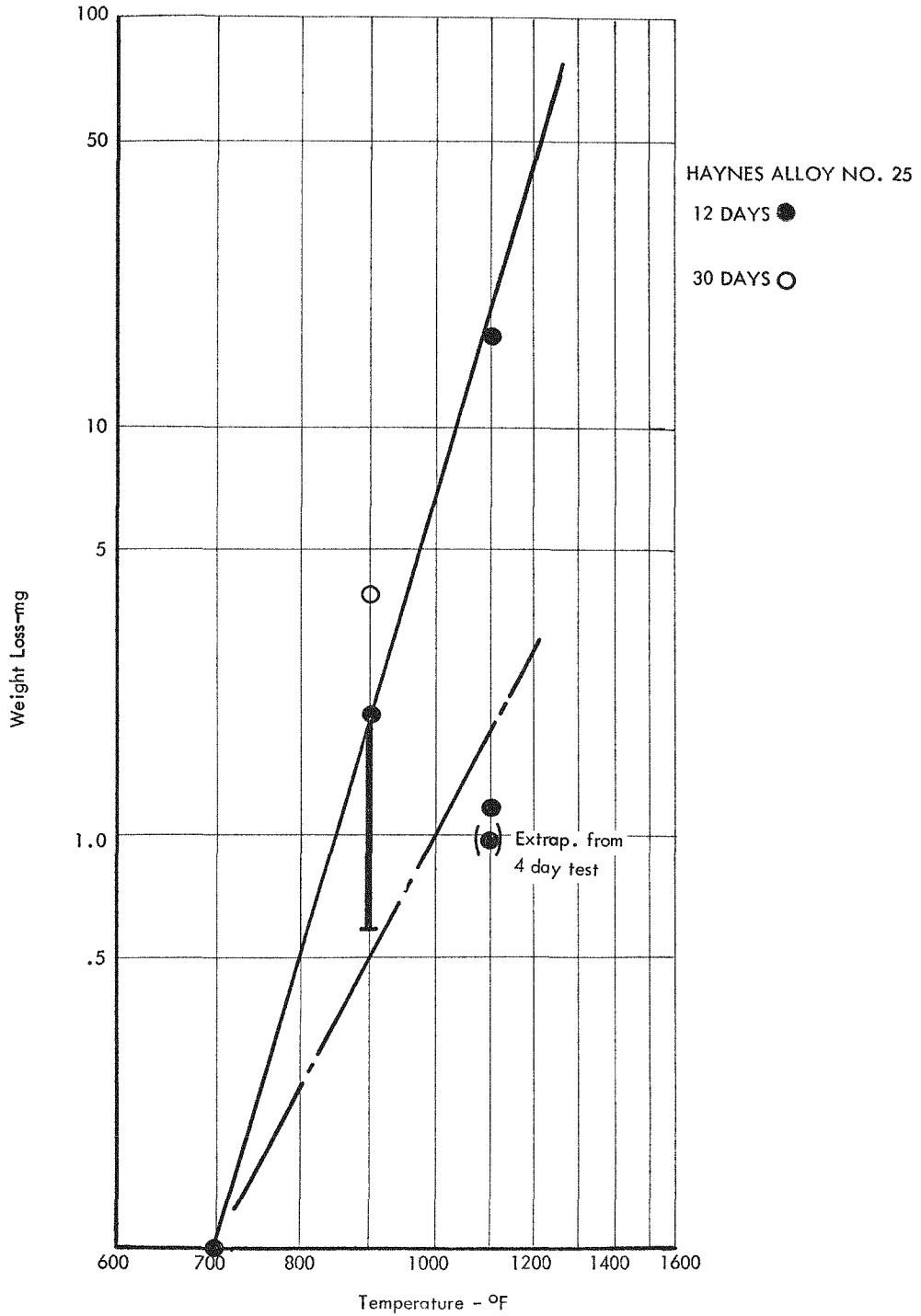
FIGURE 27
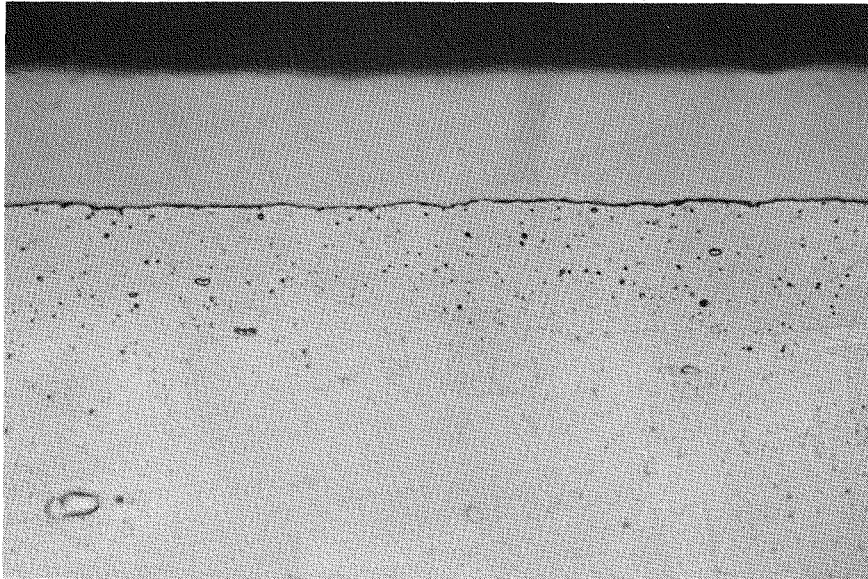
CROSS SECTION OF TYPE 347 STAINLESS STEEL AND HgCl$_2$ FIGURE 28
ADDITIVE FOR 11 DAYS IN THE BENT REFLUX TUBE AT 900°F.

Condenser Specimen   347 Type S.S.   Base Metal   Ni Plate
                                  X750
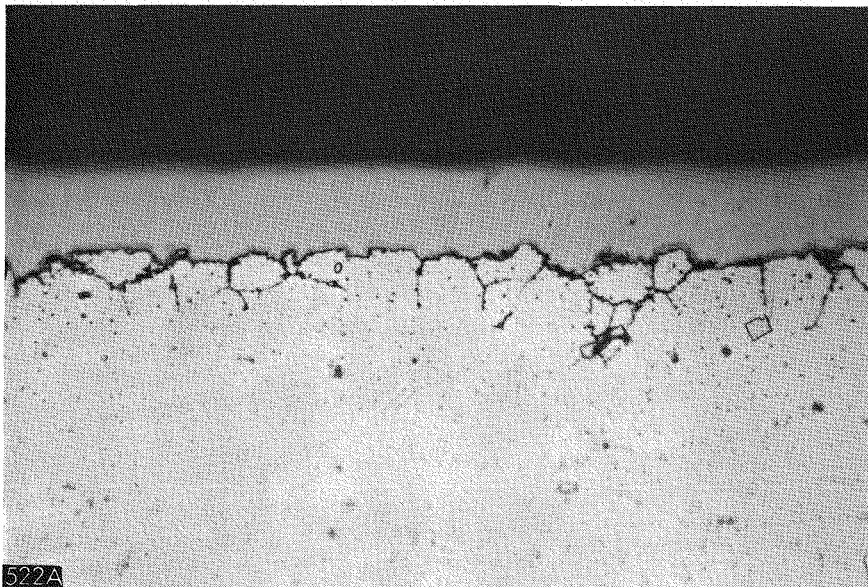
CROSS SECTION OF TYPE 347 STAINLESS STEEL BOILER SPECIMEN WITH   FIGURE 29
HgCl$_2$ ADDITIVE TESTED 11 DAYS IN THE BENT REFLUX TUBE AT 900°F.

Nb Etch   Boiler Specimen   347 Type S.S.   Base Metal   Ni Plate
                                      X750
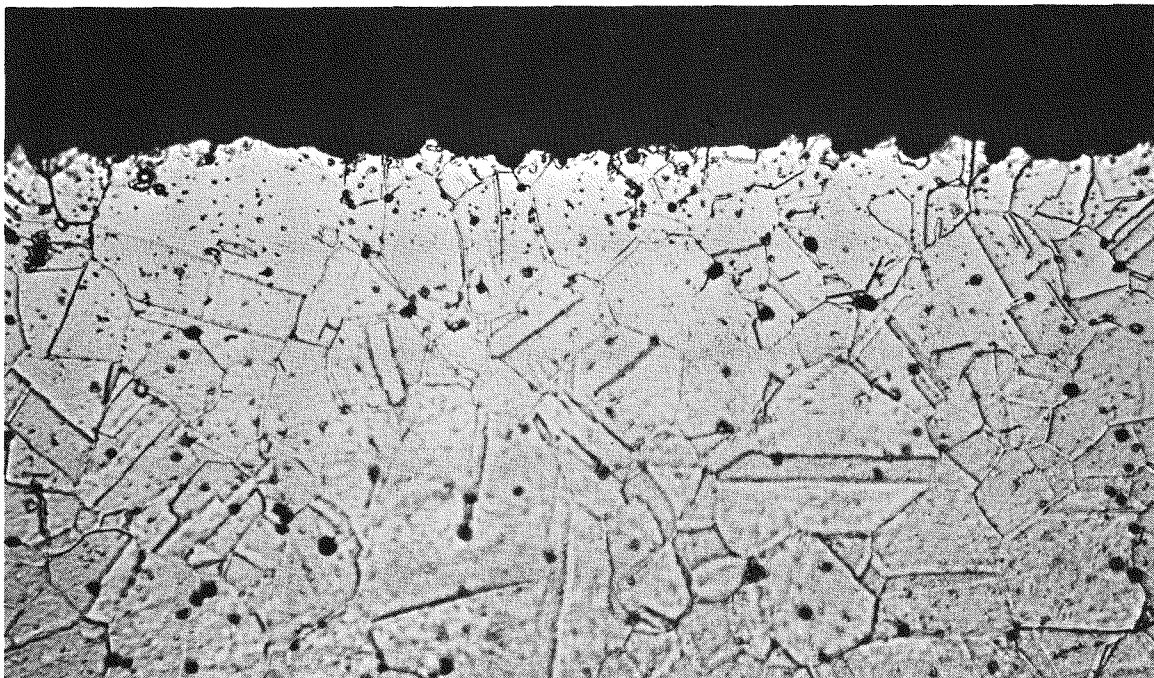
CROSS SECTION OF CARPENTER 20 Cb STAINLESS STEEL CONDENSER SPECIMEN
WITH HgO ADDITIVE AFTER TESTING 19 DAYS IN THE BENT REFLUX TUBE AT 900°F.

FIGURE 30
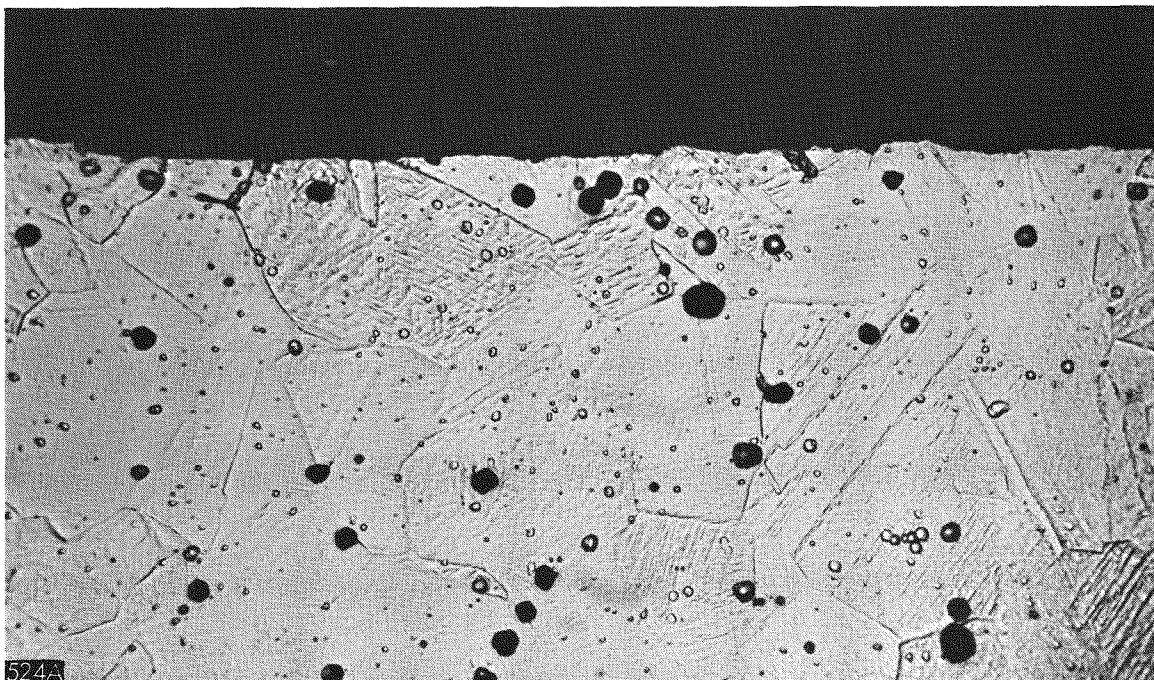
CROSS SECTION OF TYPE 304L STAINLESS STEEL CONDENSER SPECIMEN
AFTER 12 DAYS WITH Hg_2SO_4 ADDITIVE IN THE BENT REFLUX TUBE AT 900°F.

FIGURE 31
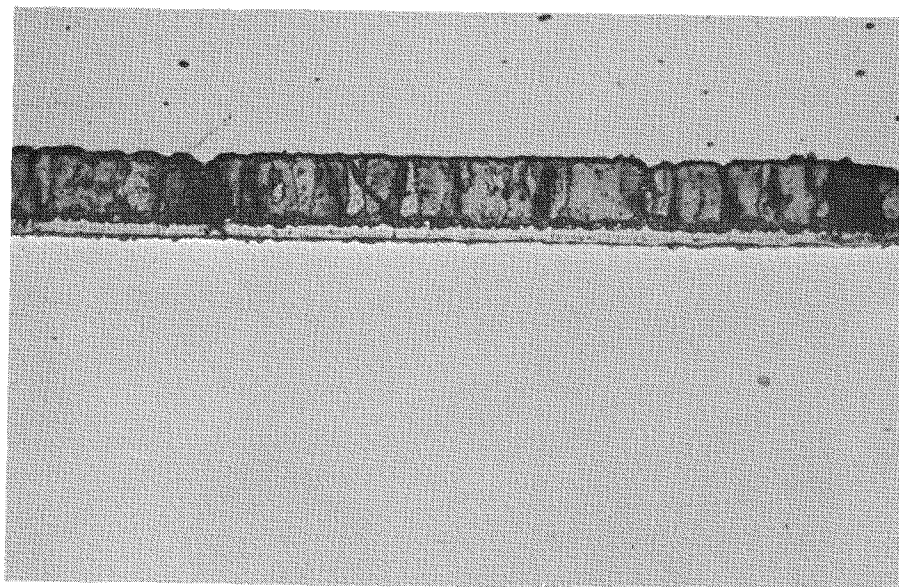
Edge Protection

Bakelite

Base Metal

CROSS SECTION OF TYPE 304 STAINLESS STEEL BOILER SPECIMEN AFTER 12 DAYS WITH Hg_2SO_4 ADDITIVE IN THE BENT REFLUX TUBE AT 900°F.

FIGURE 32   Nb Etch

X750
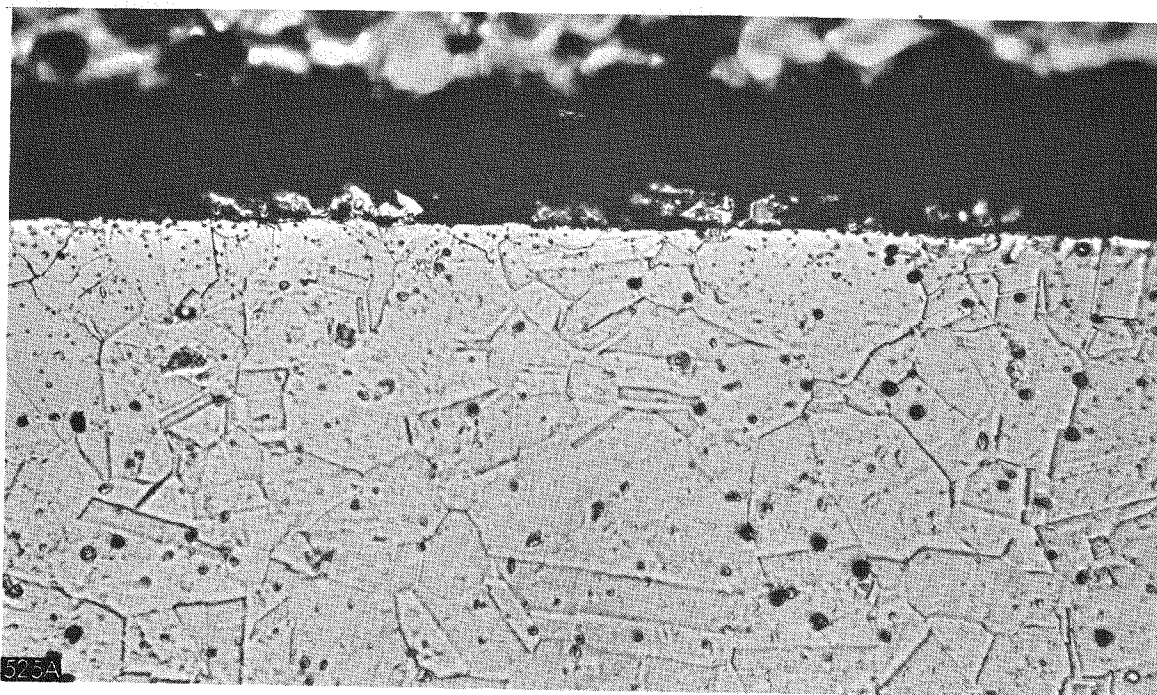
CROSS SECTION OF CARPENTER 20 Cb STAINLESS STEEL CONDENSER SPECIMEN WITH IODINE ADDITIVE AFTER 12 DAYS IN THE BENT REFLUX TUBE AT 900°F.

FIGURE 33   Hot Aqua Regia Etch

X750
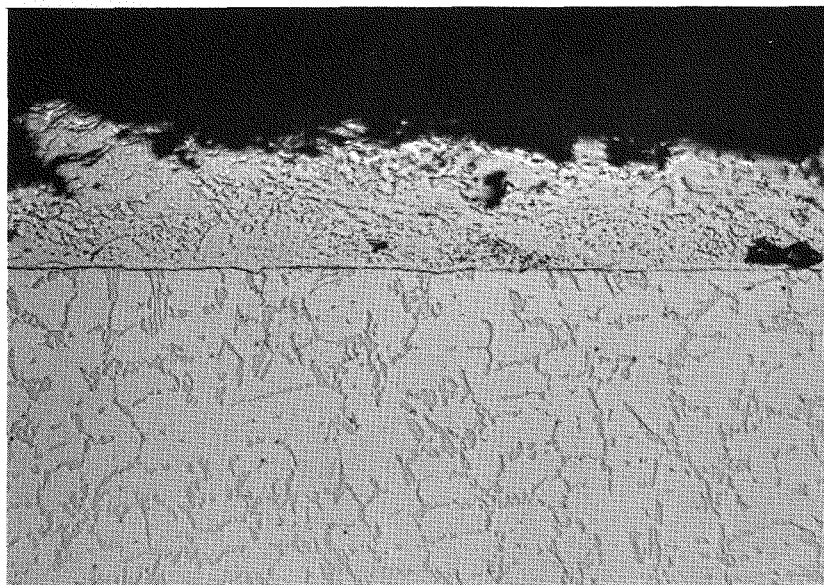
SURFACE DEPOSIT ON VALVE GUIDE.   FIGURE 34

RDM 102   250 X
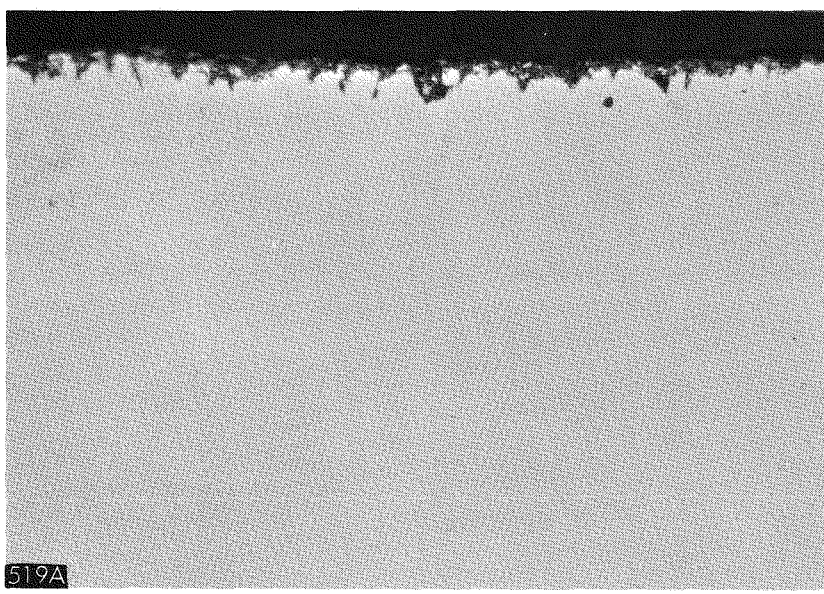
PH 15-7Mo STAINLESS STEEL NOZZLE BLADE SECTION.

RDM 180   750X   FIGURE 35
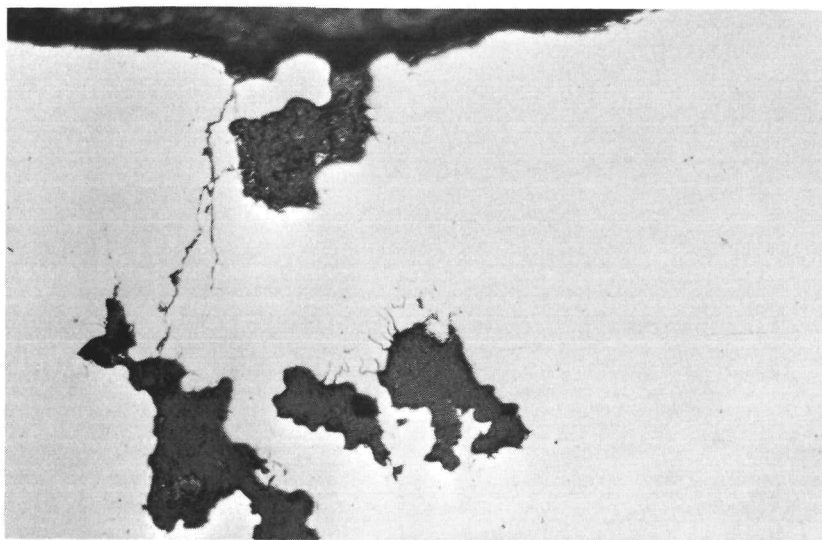
BRAZE REGION OF BEARING HOUSING.　　FIGURE 36　　RDM 172　　250 X
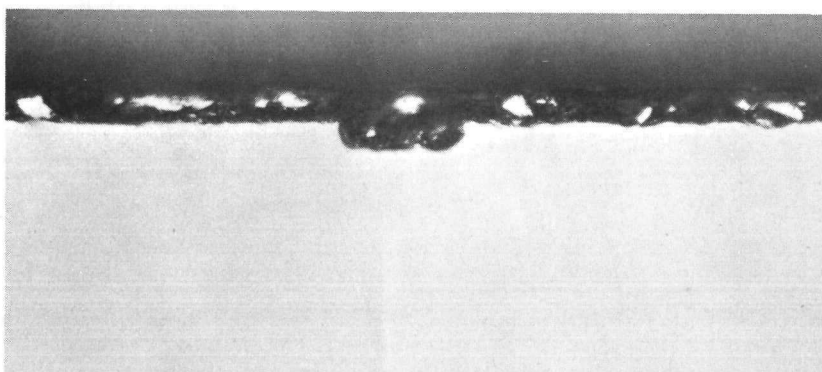
AUSTENITIC STEEL BALL VALVE SURFACE.　　FIGURE 37　　RDM 166　　750 X
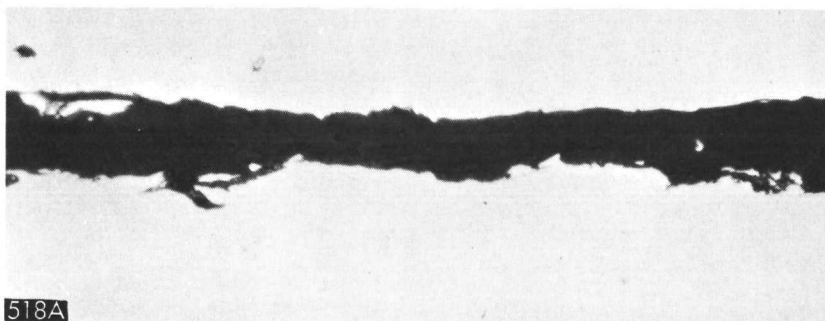
SECTION OF TYPE 316 STAINLESS STEEL TUBING SHOWING CORROSION.

RDM 185　　　　250 X　　　　FIGURE 38

CORROSION LOOP TRAP
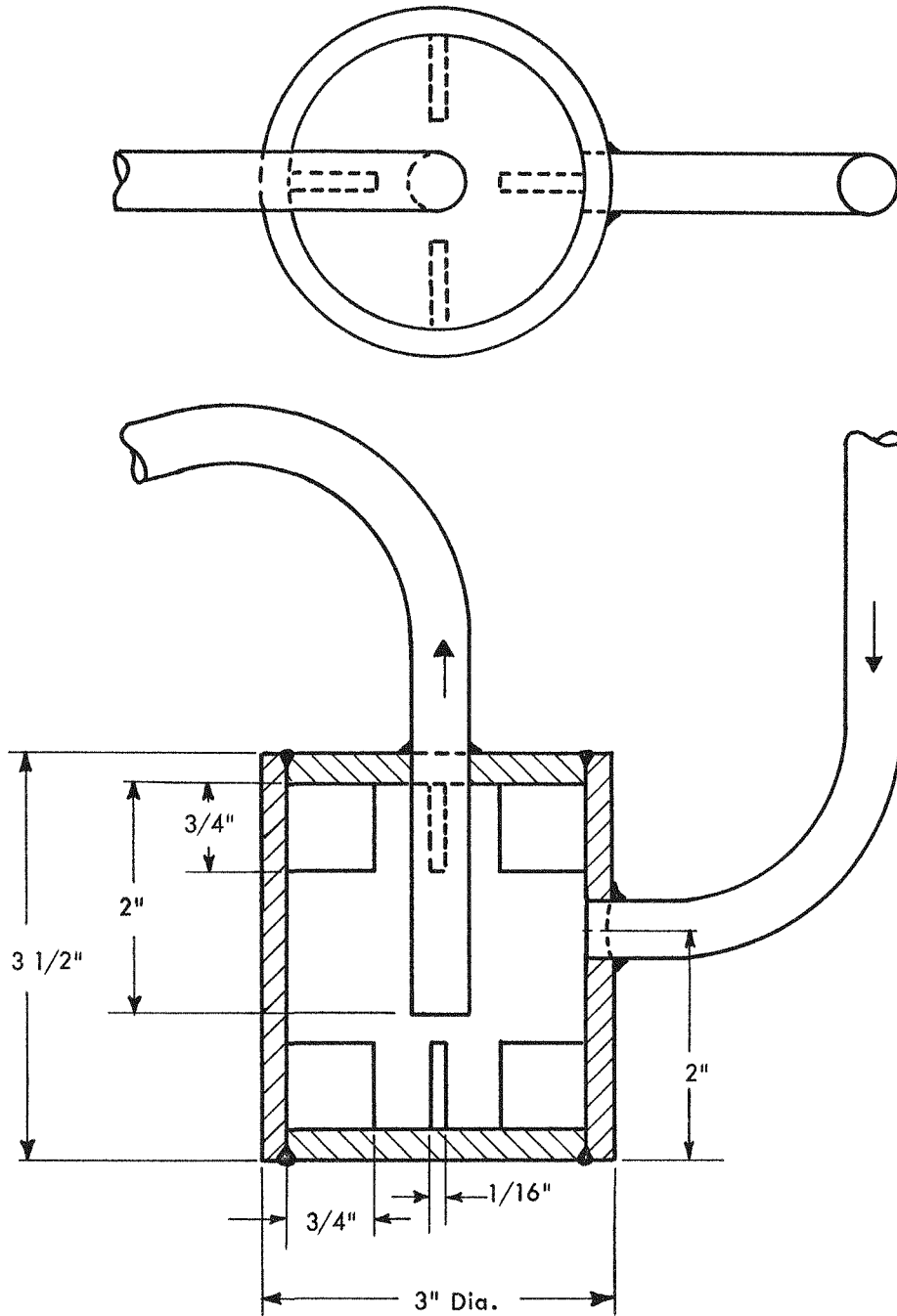
FIGURE 39

BENT REFLUX TUBE SET-UP

3/4" TRANSITE TOP

THERMOCOUPLE

5" OF MAGNESIA INSULATION BRICK

3/8" TRANSITE SHELL

CALROD RESISTANCE HEATERS
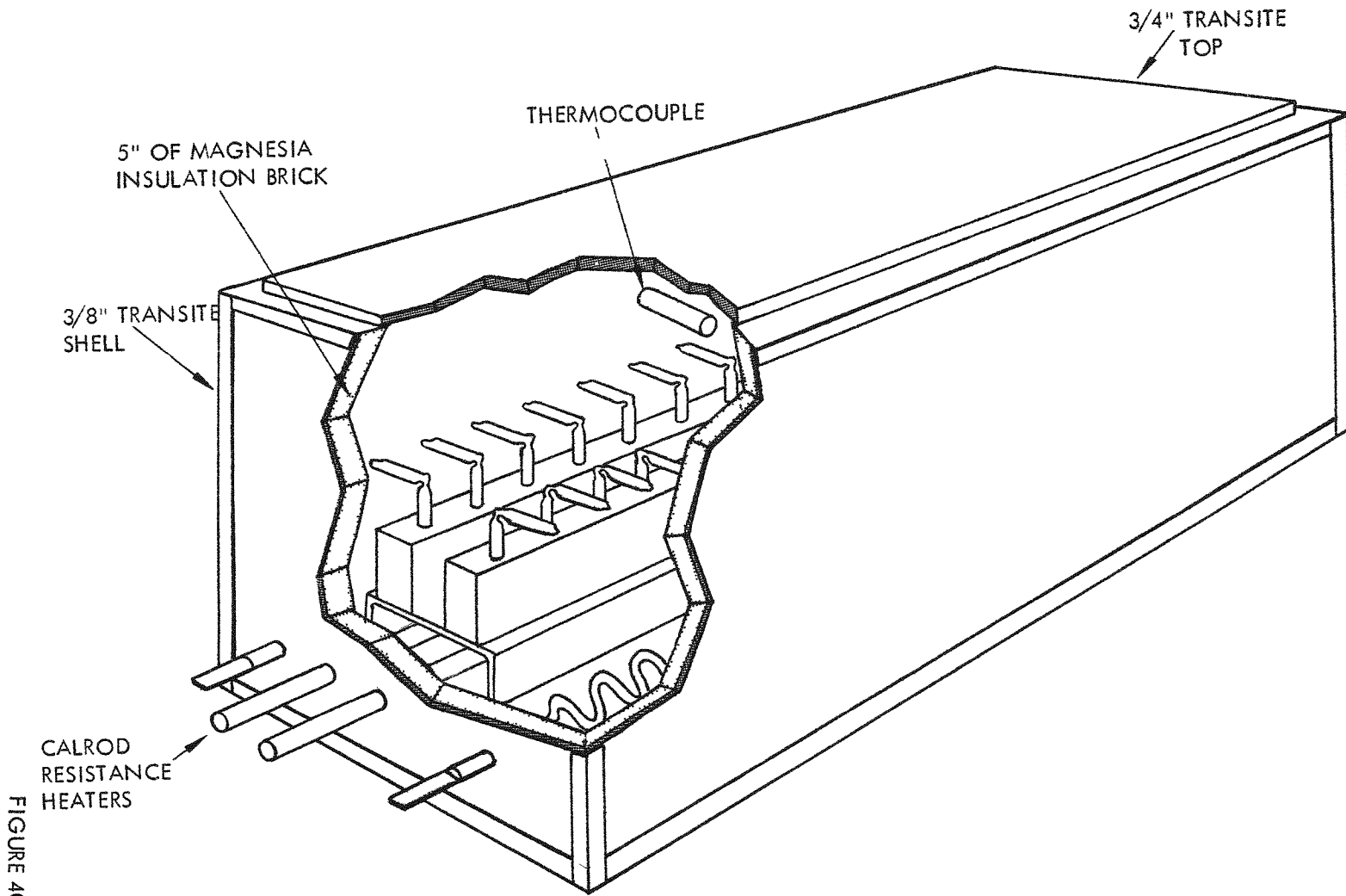
FIGURE 40

APPENDIX II: TABLES

TABLE 1

EQUILIBRIUM SOLUBILITY OF ELEMENTS IN LIQUID MERCURY AT
ROOM TEMPERATURE (17)

Element	Solubility, percent by weight
Mg	3.1×10^{-1}
Mn	1.7×10^{-3}
Mo	2×10^{-5}
Na	6.4×10^{-1}
Ni	$< 2 \times 10^{-6}$
Al	2×10^{-3}
Be	0.01×10^{-4} (100°C)
Co	$< 1 \times 10^{-6}$
Cr	$< 4 \times 10^{-7}$
Cu	2×10^{-3}
Fe	$< 5 \times 10^{-7}$
Ga	0.24
In	1.23
K	4.6×10^{-1}
Ti	1×10^{-5}
V	5×10^{-5}
W	1×10^{-5}
Zn	1.8

TABLE 1 - Page 2

Element	Solubility, percent by weight
Zr	5×10^{-4} (350°C)
Ge	2.7×10^{-2} (300°C)
Pt	0.1 (atomic %)
Rb	1.37
Sb	2.9×10^{-5}
Sn	6×10^{-1}
Th	1.6×10^{-2}
Ta	none
Si	none

TABLE 2

NOMINAL COMPOSITION OF ALLOYS

Nominal Composition, Percent

Material	C	Cr	Ni	Co	Fe	Mo	W	Mn	Si	Others
403	.15max	12	.5max	--	bal	--	--	1max	.5max	
410	.15max	12	.5max	--	bal	--	--	1max	1max	
416	.15max	13	.5max	--	bal	.6max	--	1.25max	1max	.15 min S
420	.15max	13	.5max	--	bal	--	--	1max	1max	
431	.2max	16	2	--	bal	--	--	1max	1max	
446	.2max	25	.5max	--	bal	--	--	1.5max	1max	.25max N
302	.15max	18	9	--	bal	--	--	2max	1max	
304	.08max	19	10	--	bal	--	--	2max	1max	
304L	.03max	19	10	--	bal	--	--	2max	1max	
309	.2max	23	13.5	--	bal	--	--	2max	1max	
310	.25max	25	20.5	--	bal	--	--	2max	1.5max	
316	.08max	17	12	--	bal	2.5	--	2max	1max	
321	.08max	18	10.5	--	bal	--	--	2max	1max	5xC min Ti
347	.08max	18	11	--	bal	--	--	2max	1max	10xC min Cb or Ta
19-9DL	.31	19	9.5	--	bal	1.4	1.4			.2 Ti, .4 Cb+Ta, .5 max Cu
Carp 20Cb	.07max	20	29	--	bal	2	--			3 Cu, 8xC min Cb + Ta
15-15N	.15max	16.4	15	--	bal	1.6	1.4	2max	.75max	.15 max N, 1 Cb + Ta
PH 15-7Mo	.09max	15	7	--	bal	2.5	--	1max	1max	1 Al
17-4PH	.07max	16.5	4	--	bal	--	--	1max	1max	4 Cu, .35 Cb + Ta
17-7PH	.07max	17	7	--	bal	--	--	1max	1max	1.1 Al
A286	.04max	15	25.5	--	bal	1.3	--	.2max	1max	.35 max Al, 2 Ti, .3 V, .005B
AM350	.10	16.5	4	--	bal	2.75	--	1max	.5max	.1 N
Waspalloy	.10max	1.9	bal	14	2max	4.3	--	1max	.75max	1.3 Al, 3Ti, .04 Zr, .006B
Rene 41	.09	19	bal	11	--	10	--			1.5 Al, 3.1 Ti
Inconel X	.08	15	70min	--	7	--	--			.7 Al, 2.4 Ti, 1 Cb
Inconel	.08	15.5	bal	--	7.5	--	--	--	--	
Sicromo 5S	.15max	5	--	--	bal	.55	--	.45	.5 max	

TABLE 2
Page 2

Material	C	Cr	Ni	Co	Fe	Mo	W	Mn	Si	Others
1095	.95	---	---	---	bal	---	---	.4	.1max	
1010	.10	---	---	---	bal	---	---	.4	.1max	
AF1753	.25	16.5	Bal	7.5	9.5	1.5	8.5	---	---	2Al, 3.2 Ti, .008 B, .05 Zr
Carp 42	---	---	42	---	bal	---	---	---	---	
Sylvania #4	---	6	42	---	bal	---	---	---	---	
18-4-1	.7	4	---	---	bal	---	18	.3	1	1 V
Vascojet 1000	.4	5	---	---	bal	1.3	---	.4	1	.5 V
XCR	.45	23.5	4.75	---	bal	2.75	---	1max	1max	
MS201	.5	20.5	4	---	bal	---	---	8.8	.14	.4 N_2
TP3	.5	20	bal	---	---	---	---	---		10.5 Al
Armco Tran-Cor T	.06	---	---	---	bal	---	---	---	1 1/2	
Thermanol	.06	---	---	---	bal	3.5	---	---	---	15 Al
Elgiloy	.15	20	15	40	bal	7	---	2	---	.04 Bi
Nichrome	.08	20	80	---	.5max	---	---	.15	1.3	
Haynes Alloy 25	.15max	20	10	bal	3max	---	15	---	---	
Stellite No. 3	2.45	30.5	3max	bal	3max	---	12.5	1max	1max	
Stellite No. 6	1.1	30	3max	bal	3max	---	4.5	1max	1max	
Stellite Star J	2.5	32	2.5max	bal	3max	---	17	1max	1max	
Kovar	.06max	---	29	17	bal	---	---	.5max	.2max	
Alnico VI	---	---	14	24	bal	---	---	---	---	8 Al, 1 Ti, 3 Cu
Titanium carbide (K150A)	---	---	10	---	---	---	---	---	---	80 TiC, 10 CbC
Titanium carbide (K151A)	15	---	19	---	---	---	---	---	---	58 Ti, 7.5 Cb, .5 Ta

TABLE 2
Page 3

Material	C	Cr	Ni	Co	Fe	Mo	W	Mn	Si	Others
Tungsten Carbide (CA8)	--	--	--	3	--	--	--	--	--	97 WC
Ferro-Tic, Grade C	7	2	--	--	bal	2	--	--	--	26 Ti
Molybdenum + 1/2 Ti	--	--	--	--	--	bal	--	--	--	.5 Ti
Nicrobraz AMS 4775	1	16.5	70	--	4	--	--	--	4	3.8 B
Zircaloy -1	--	--	--	--	--	--	--	--	--	2.5 Sn, bal Zr
Kanthal A-1	--	22	--	.5	bal	--	--	--	--	5 1/2 Al
Hoskins 875	.1	22.5	--	--	bal	--	--	--	.5	5.5 Al
Alfenol					bal					16 Al
Neatro	1.27	4.5	--	--	bal	4.5	5.5	.25	.3	4 V
Chromewear	2.3	5.3	--	--	bal	1.1	1.1	.7	.4	4.8 V
Hyperco 27				27	bal					

TABLE 3

HEAT TREATMENTS

Material	Designation	Heat Treatment
18-8 Type Stainless Steels	Ann	Annealed at 2000°F and water quenched.
17-7PH and PH15-7Mo	Cond A	Annealed 1/2 hour at 1950°F and water quenched.
	Cond TH1050	Subsequent to Cond A, 1-1/2 hours at 1400°F, air cooled and held 1/2 hour at 60°F. Aged 1-1/2 hours at 1050°F and air cooled.
17-4PH	Cond A	Annealed at 1900°F and water quenched.
	Cond TH1050	Cond A material aged at 1050°F for 1 1/2 hours and air cooled.
AM350	Ann	Annealed at 1950°F and water quenched.
	DA	Annealed at 1710°F and water quenched. Aged 2 hours at 1400°F and air cooled. Aged 2 hours at 1050°F and air cooled.
A286	Ann	Annealed at 1800°F and water quenched.
	Aged	After annealing, aged 16 hours at 1350°F and air cooled.
XCR	H.T.	Annealed at 2100°F and water quenched. Aged 14 hours at 1400°F and air cooled.
403 and 410	Q	Soaked at 1800°F and water quenched.
	QT	Tempered at 1350°F and air cooled.
1095	Q	Soaked at 1450°F and oil quenched.
	QT	Tempered at 1000°F for 1 hour and air cooled.

TABLE 3 - Page 2

Material	Designation	Heat Treatment
Vascojet 1000	QT	Preheated 1/2 hour at 1200°F and 1600°F. Soaked 1/2 hour at 1850°F and oil quenched. Tempered for 1 hour at 1000°F and air cooled.
18-4-1	QT	Preheated 5 minutes at 1550°F, soaked for 3 minutes at 2320°F and oil quenched. Tempered for 1 hour at 1100°F and air cooled.
410	Nitrided	Soaked for 1 hour at 1570°F and air cooled prior to nitriding to depth of 0.01-0.012 inches.
Nitralloy	Nitrided	Heat treated to core hardness of Rc 32-38. Nitrided to depth of 0.01-0.014 inches with case hardness of R15N92 min.
Rene 41	H.T.	Soaked 1/2 hour at 2150°F and air cooled. Aged 16 hours at 1400°F and air cooled.
Waspalloy	H.T.	Soaked 4 hours at 1975°F, air cooled. Soaked 24 hours at 1550°F and air cooled. Aged 16 hours at 1400°F and air cooled.
Haynes Alloy No. 25	Ag	Soaked 48 hours at 1350°F, air cooled.
Neatro	H.T.	Preheated at 1400 - 1500°F, soaked at 2200°F and oil quenched. Double tempered at 1040°F
Chromewear	H.T.	Preheated at 1400 - 1500°F, soaked 30 minutes at 1725°F and oil quenched. Tempered at 1000°F.

TABLE 4

SURFACE TREATMENTS

Designation	Procedure
Cl_1	Ultrasonically cleaned in trichloroethylene.
Cl_2	Same as above followed by acetone wash.
Cl_3	Soaked 5 minutes in 180°F No. 80A Oakite solution. Washed in running water followed by distilled water wash and ethyl alcohol dip.
P_1	Boiled 1 hour in 50% nitric acid, washed in running water.
P_2	Soaked 1/2 hour in a 140°F aqueous bath of 4% hydrofluoric acid and 4% chromic acid. Washed in running water.
P_3	Pickled in a mixture of 20% nitric acid and 2% hydrofluoric acid at 140°F. Washed in running water.
O_1	Oxidized 3 hours at 1050°F.
N_1	Coated and brazed with AMS 4775.

TABLE 5

CONDENSED SUMMARY OF RESISTANCE OF MATERIALS TO
ATTACK BY LIQUID MERCURY

Material	Resistance at 900°F
Ferrous Metals	
Low-carbon steel	Good
High-carbon steel	Good
Low-Chromium steels	Fair
Martensitic stainless steels	Good
Ferritic stainless steels	Good
Austenitic stainless steels	Poor
High-nickel steels	Poor
High-speed tool steel	Good
Precipitation-hardening stainless steels:	
Martensitic	Good
Semi-austenitic	Good
Austenitic	Poor
Non-Ferrous Metals	
Beryllium	Poor
Chromium	Poor
Nickel	Poor
Manganese	Non-resistant
Molybdenum	Good
Columbium	Good
Platinum	Non-resistant
Tantalum	Excellent
Tungsten	Excellent
Zirconium	Poor
Inconel, Nichrome	Poor
Haynes 25, Stellites	Good
Cobalt	Good
Titanium	Poor
Aluminum	Non-resistant
Non-Metals	
Graphite	Excellent
Alumina	Excellent
Pyroceram	Excellent
Carbides	Fair to Good

TABLE 6
PERIODIC TABLE OF THE ELEMENTS INDICATING PREDICTED AND EXPERIMENTALLY DETERMINED RESISTANCE TO LIQUID MERCURY*

Alkali Metals | Alkaline Earth Metals

H	
Li	Be_F^x
$Na_{(P)}^x$	$Mg_{(P)}^x$

LEGEND

Superscript:
x soluble (miscible)
v insoluble (immiscible)
‾ known intermetallic formation with Hg.

Subscript:
P poor resistance to attack.
F fair resistance to attack.
G Good resistance to attack.
E Excellent resistance to attack.
( ) Literature

Non-Metals | Halogens | Inert Gases

					He
B^v	C_E^v	N	O	F	Ne
Al_P^x	Si^v	P	S	Cl	A

Transition Metals Post-Transition Metals

K^x	$Ca_{(P)}^x$	Sc^x	Ti_F^{v-}	V^v	Cr_P^v	Mn_P^{x-}	Fe_G^v	Co_G^v	Ni_P^{v-}	$Cu_{(P)}^v$	$Zn_{(P)}^{x-}$	$Ga_{(P)}^x$	Ge^v	As^x	Se^x	Br	Kr
Rb^x	$Sr_{(P)}^x$	Y^x	Zr_F^{v-}	Cb_E^v	Mo_E^v	Tc^v	$Ru_{(P)}^v$	$Rh_{(P)}^v$	$Pd_{(P)}^v$	$Ag_{(\bar P)}^v$	$Cd_{(P)}^x$	$In_{(P)}^x$	$Sn_{(\bar P)}^v$	Sb^x	Te^x	I	Xe
Cs^x	$Ba_{(P)}^x$	Lanthanides	Hf^x	Ta_E^v	W_E^v	Re^v	Os^v	Ir^v	Pt_P^{v-}	$Au_{(\bar P)}^x$	Hg_P^x	$Tl_{(P)}^x$	$Pb_{(\bar P)}^x$	$Bi_{(P)}^x$	Po^x	At	Rn
Fr	Ra	Actinides															

*Superscripts refer to the calculated solubility in mercury at 1200°F as predicted by the Scott–Hildebrand –Mott miscibility index relationship. Subscripts refer to the experimentally determined dynamic corrosion resistance in mercury at 900°F.

TABLE 7

RELATIVE CORROSION OF SOME MATERIALS IN MERCURY AT 900°F
- BASED ON 12 DAYS TESTS -

Material	Relative Attack
Ta, W, T$_i$C, WC, Mo + 1/2% T$_i$	(NO MEASURABLE ATTACK)
CARBON STEELS 400 SERIES S.S.	▮
300 SERIES S.S. AND SIMILAR STEELS (EXCEPT 310 S.S.)	▰
HIGH NICKEL ALLOYS (20% UP) AND NICHROME	▰▰▰▰
T$_i$, Pt, Mn, Mg, Al, and Zr	▰▰▰▰▰▰▰▰

10   20   30   40   50   60   70   80   90   100

RELATIVE ATTACK
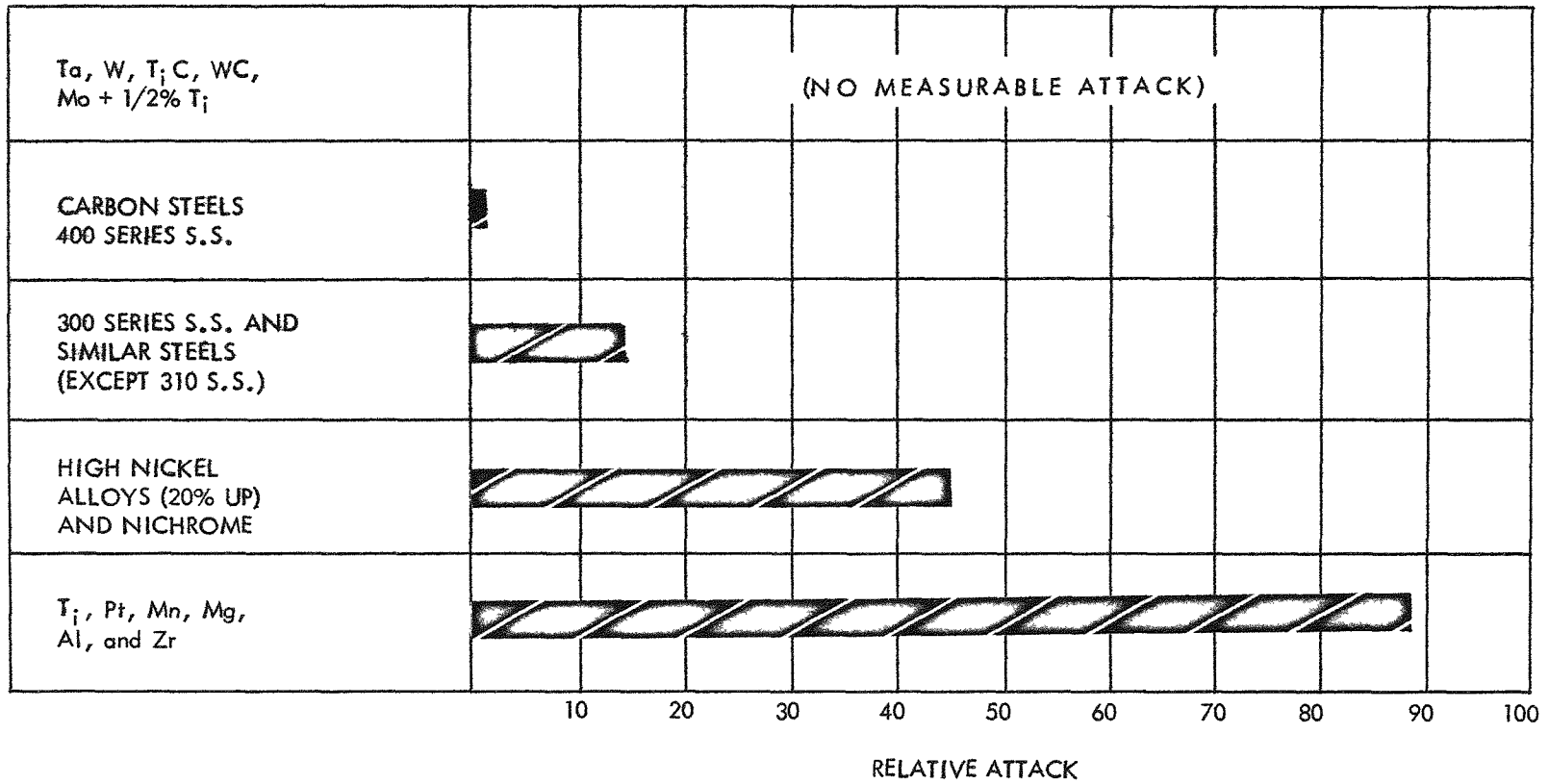
TABLE 8

BENT REFLUX TUBE TEST DATA AT 900°F FOR VARIOUS FERROUS ALLOYS

Test No.	Material and Condition*	Test Time, Days	Weight Change, Mg	Penetration, Inches	Wetted	Remarks
21	1010	12	-0.4	0	Slightly	---
336-39-1	Armco Iron	12	-0.3	---	Yes	Roughened surface. Some crystal deposition.
115	Armco iron (oxidized 1/2 hr 1650°F)	12	-0.4	0	No	Heavy oxide layer.
20	1095	12	-0.15	0	Slightly	
20A	1095 (QT)	12	-0.6	0.00008	No	
20C	1095 (QT)	33	-0.6	0.00005	Some	Surface roughening.
20D	1095	30	-1.8	0.0002	Some	Surface roughening. Crystal deposit.
20B	1095	30	-0.4	0.00028	No	Intergranular crevice attack.
132	Sicromo 5S	12	-0.1	0.00013	Partial	Slight crevice attack. Some deposition.
133	Sicromo 5S	30	-0.3	0.0004	Yes	Intergranular crevice attack.
80	Nitralloy-Nitrided	14	0	0.0015 0.00013	Partial	Intergranular attack of nitride layer. Base metal -surface roughened.
136	Armco Tran-Cor T (with core plate)	14	-0.2	0.0002	Slight	Surface roughened. Some deposition.
137	Armco Tran-Cor T	12	-0.2	0.0002	No	Surface roughened. Some deposition.
138	Armco Tran-Cor T (with core plate)	30	-0.5	0.0002		
139	Armco Tran-Cor T	30	-0.5	0.001		
159	Sylvania #4	12	-55.0	0.0042	Yes	Grains removed.
159A	Sylvania #4	12	-48.6	---	Yes	
160	Sylvania #4	30	-115.9		Yes	

*See Table 3 for heat treatment procedure.

TABLE 8   – Page 2

Test No.	Material and Condition*	Test Time, Days	Weight Change, Mg	Penetration, Inches	Wetted	Remarks
160A	Sylvania #4	30	-115.8		Yes	
17	Carp. Low Exp 42 (Ann)	12	-32.5	0.002	Yes	
18	Carp. Low Exp 42 (cold rolled)	12	-86.6	0.0044	Yes	
16	Carp. 42 (cold rolled)	37	-139.5	0.010	Yes	
52	TP3	12	-93.8	0.006	Yes	Intermetallic not attacked.
52A	TP3	32	-120.9	0.011	Yes	Gray-like deposit in leached zone.
27A	Thermanol	12	-0.8	0.0002	Yes	Roughened surface. Some crystal deposits.
27	Thermanol (Oxidized 2 1/2 hr 1100°F)	12	+0.4	0	No	
27B	Thermanol (Oxidized 2 1/2 hr 1100°F)	30	-0.4	0.0005	Pin-Point	Intergranular attack. Some crystal deposition.
64	Alnico VI	12	-0.4	0	Pin-Point	Magnetized
145	Kovar	12	-58.6	0.004	Yes	
145A	Kovar	12	-53.7	.004	Yes	Some crevice attack.
144	Kovar	30	-103.3	0.0095	Yes	Some cracks in corrosion layer.
144A	Kovar	30	-93.9	--	Yes	
40	Vascojet 1000	7	-0.3	0	No	
40A	Vascojet 1000	12	-1.4	0.0002	Yes	
44	Vascojet 1000 (QT)	12	-0.4	0	No	
40B	Vascojet 1000	30	-0.6	0	Yes	Roughened surface.
22B	18-4-1 (QT)	5	+0.3	0.0001	Some	Surface roughened.
22A	18-4-1	30	-0.2	0.00005	No	Intergranular attack.
22	18-4-1 (QT)	12	-0.4	--	No	---
		12	+0.3	0	No	Rerun #22

*See Table 3 for heat treatment procedure.

TABLE 8 - Page 3

Test No.	Material and Condition*	Test Time, Days	Weight Change, Mg	Penetration, Inches	Wetted	Remarks
229	1010	30	-1.3	0.00005	Yes	Pitting
230	1010	60	-2.7	0.00014	Yes	Crevice attack
166	1095 (QT) + 2 ppm Ti	12	-0.4		Yes	
166	Rerun above in clean Hg	30	-1.2	0.00028	No	Layer deposition and crevice attack.
166A	1095 (QT) + 2 ppm Ti	12	-0.2		Yes	
166A	Rerun above in clean Hg	30	-0.9	0.00028	No	Crevice attack
167	1095 (QT) + 2 ppm Ti	12	0		Yes	
167	Rerun above in clean Hg	60	-4.6	0.00028	Yes	Crevice attack
167A	1095 (QT) + 2 ppm Ti	12	0		Yes	
167A	Rerun above in clean Hg	60	-4.7	0.00028	Yes	Crevice attack
233	1095 (QT)	30	-0.7	0.0008	Yes	Crevice attack
234	1095 (QT)	60	-1.6	0.00013	Yes	Crevice attack
225	Vascojet 1000 (QT)	30	-0.3	0	No	
226	Vascojet 1000 (QT)	18	-1.4	0	No	Exploded
270	Neatro	13	-0.8	0.00013	Slight	
270A	Neatro	13	-0.9		Slight	
271	Neatro	30	-1.3	0.00028	Yes	
271A	Neatro	30	-1.2		Yes	
295	Neatro (HT)	12	-0.2	0.00014	Slight	Crevice attack (?)
295A	Neatro (HT)	12	-0.2	0.00028	Slight	
273	Chromewear	13	-0.3	0.00005	Slight	
273A	Chromewear	13	-0.3		Slight	
275	Chromewear	30	-1.8	0.00028	Yes	
275A	Chromewear	30	-1.7		Yes	
278	Chromewear (HT)	12	-0.3	0.00013	Yes	
278A	Chromewear (HT)	12	-0.2		Yes	

*See Table 3 for heat treatment procedure.

TABLE 8 - Page 4

Test No.	Material and Condition*	Test Time, Days	Weight Change, Mg	Penetration, Inches	Wetted	Remarks
168	18-4-1 (QT) + 2ppm Ti	12	0		No	
168	Rerun above in clean Hg	30	-0.4	0.00013	No	Crevice attack
168A	18-4-1 (QT) + 2ppm Ti	12	-0.1		No	
168A	Rerun above in clean Hg	30	-0.2	0.00026	No	Crystal deposition
169	18-4-1 (QT) + 2 ppm Ti	12	0		No	
169	Rerun above in clean Hg	60	-1.0	0.0005	No	Some pitting
169A	18-4-1 (QT) + 2 ppm Ti	12	0		No	
169A	Rerun above in clean Hg	60	-0.9		No	
227	18-4-1 (QT)	30	-0.7	0.00013	Yes	
228	18-4-1 (QT)	60	-2.1	0.0005	Yes	
249	18-4-1 (QT)(Cl$_3$ Treatment)	12	-0.6	0.00028	Partial	Pitting and intergranular attack. Vapor Test.
206	Kovar	12	-29.5		Yes	Vapor Test.
206A	Kovar	12	-29.0	0.0044	Yes	Vapor Test. Cracks in layer.
276	Hyperco 27	14	-0.3	0.00005	Slight	Crevice attack. Cracks
276A	Hyperco 27	14	-0.2		Slight	
277	Hyperco 27	30	-0.9	0.00027	Slight	Intergranular crevice. Cracks
277A	Hyperco 27	30	-0.6		Slight	
250	Alnico VI (demagnetized)	12	-0.2	0	Yes	

* See Table 3 for heat treatment procedure.

TABLE 9

BENT REFLUX TUBE TEST DATA AT 900°F FOR TYPE 400 SERIES STAINLESS STEELS

Test No.	Material & Condition*	Test Time, Days	Weight Change, Mg	Penetration, Inches	Wetted	Remarks
82	410	12	-1.0	0.00028	Yes	Some crystal deposits· Intergranular penetration.
10	410 (Q)	12	-0.3	0.0005	Yes	Integranular penetration
11	410	12	-0.5	0.0005	No	
12	410	12	0	0	Slight	
49	410 (Coated and nicrobrazed with AMS 4775)	12	-3.0	0.0041	Yes	410-roughened & grey layer.
100	410 (Stressed)	14	0	0.00002 tension 0.001 compression	Yes	Roughened surface.
142	410	30	-1.1	0.0008	Yes	Intergranular attack.
142A	410	30	-1.4		Yes	
33	410 (P$_3$ Treatment)	37	-0.7	0	Yes	
143	410	59	-1.9	---	Yes	
143A	410	59	-2.0	0.0008	Yes	Intergranular attack.
79	410 Nitrided-(Nitride surface)	12	+0.3	0.0006	Yes	Cracked deposit on surface.
	(Base metal surface)			0.00028	Yes	Intergranular attack.
82A	410 + 0.0002% Ti added	12	-1.5	0.00014	Yes	Some intergranular attack. Crystal deposit.
34A	403 (Q.T.)	12	+0.2	0	No	
34	403 (Q.T.) (P$_3$ Treatment)	43	-0.3	0	Yes	
57	416	12	-0.4	0.00008	No	
56	420	12	-0.45	0.00025	No	
59	431 (P$_3$ Treatment)	12	0.4	0.00022	Slightly	Intergranular attack in vapor.
31	446 (P$_3$ Treatment)	12	-0.2	0.0017	No	
31A	446	12	-0.6	0	Slight	
31B	446	30	-1.8	0.00005	Yes	Some intergranular crevice attack.
135	446 (Carburized)	30	-3.5	0.00005	Yes	Deposit
32	446 (P$_3$ Treatment)	43	-1.4	0.0029	Yes	
108	446 (P$_1$ Treatment)	12	0	0.0002	Yes	Deposit layer.
108A	446 (P$_1$ Treatment)	30	-10.7	0.0002	Yes	Crevice attack. Layer deposit.
101	446 (Stressed)	14	-0.2	0.00014 tension 0.00028 compression	Yes	
107	446 (P$_2$ Treatment)	12	-0.5	0.0001	Yes	
107A	446 (P$_2$ Treatment)	32	-3.7	0.0008	Yes	Some intergranular attack.
31C	446 (Oxidized 3 hrs 1000°F)	33	-0.1	0.00024	Slightly	Crystal deposits. Roughened surface.
76	446 (Cl$_1$ Treatment)	12	-0.9	0.00028	Yes	Intergranular attack.
76A	446 (Cl$_2$ Treatment)	12	-0.2	0.00028	Yes	Intergranular attack.
217	410 (Stressed)	30	-0.6	0.00005	No	
218	410 (Stressed)	23	-0.9	0.00005	No	Some intergranular attack.
245	410 (Cl$_3$ Treatment)	12	-1.4	0.00028	Yes	Crevice attack.

*See Table 3 for heat treatment procedure and Table 4 for surface treatment.

TABLE 10

BENT REFLUX TUBE TEST DATA AT 900°F FOR TYPE 300 SERIES STAINLESS STEELS

Test No.	Material & Condition*	Test Time, Days	Weight Change, Mg	Penetration, Inches	Wetted	Remarks
65	302	12	-12.95	0.0028	Yes	
65B	302	30	-5.5	0.0035	Yes	
77	302	30	-16.3	0.0060	Yes	
77A	302 (O$_1$ Treatment)	30	-4.9	0.0052	Yes	
65A	302 (O$_1$ Treatment)	12	-2.9	0.0025	Spotty wetting	0.1 mg wt. gain by oxidation
50	302 (N$_1$ Treatment)	13	-11.5	0.0027	Yes	
50A	302 (N$_1$ Treatment)	30	-54.4	0.0095	Yes	
42	304	7	-4.0	0.0028	No	
53A	304	12	-34.65	0.0055	Yes	
42A	304	30	-7.6	0.0042	Yes	
78	304	32	-48.5	0.0085	Yes	
53	304 (O$_1$ Treatment)	12	-21.55	0.0039	Partial	
78A	304 (O$_1$ Treatment)	30	-3.4	0.0036	Yes	Crystal deposit.
112	304 (Oxidized 1/2 hr 1650°F)	14	-9.8	0.0046	Pin Point	
110	304 (P$_1$ Treatment)	12	-21.0	0.0067	Yes	
110A	304 (P$_1$ Treatment)	32	-18.3	0.0016	Yes	
109	304 (P$_2$ Treatment)	12	+1.2	0.0044	Yes	Some Crystal deposition. Unknown phase in corrosion layer.
109A	304 (P$_2$ Treatment)	32	-42.1	0.0040	Yes	
105	304 (After run washed with 10% HNO$_3$ + 1% Na NO$_2$)	1	-1.4	---	No	
105	304 (After run washed with 10% HNO$_3$ + 1% Na NO$_2$)	12	-8.9	0.0035	Yes	Rerun #105. Some crystal deposits.
6V	347 (Ann) (P$_3$ Treatment)	5 hrs	+0.1	0.00019	No	Intergranular attack -0.00028".
7V	347 (Ann) (P$_3$ Treatment)	1	-1.1	0.0007	Yes	
8V	347 (Ann) (P$_3$ Treatment)	5	-6.1	0.0027	Yes	
12V	347 (Ann) (P$_3$ Treatment)	12	-16.4	0.0033	Yes	Some crystal deposition.
336-6-1	347 (Ann) (P$_3$ Treatment)	30	-13.1	0.0027	Yes	Some intergranular attack.
336-7-1	347 (Ann) (P$_3$ Treatment)	60	-32.4	0.0258	Yes	Intergranular attack

*See Table 3 for heat treatment procedure and Table 4 for surface treatment.

TABLE 10
Page 2

Test No.	Material & Condition*	Test Time, Days	Weight Change, Mg	Penetration, Inches	Wetted	Remarks
336-8-1	347 (Ann) (P$_3$ Treatment)	90	-36.9	0.01	Yes	Intergranular attack, some cracks in corrasion layer. Roughened surface
41	347 (Ann)	1	-0.5	---	No	
		5	-0.8	0.00069	No	Rerun #41
303-156-1	347 (Electropolished)	5	-7.7	0.0010	---	
37	347	12	-14.8	0.0044	Yes	
75	347 (Cl$_1$ Treatment)	12	-14.2	0.0037	Yes	Intergranular attack
75A	347 (Cl$_2$ Treatment)	12	-11.7	0.0030	Partial	Some crystal deposits. Intergranular attack.
303-142	347 (Electropolished)	11	-14.0	0.0060	---	
303-135	347 (Electropolished)	7	-11.7	0.0016	---	
303-160-1	347 (Electropolished)	43	-9.7	0.0024	---	Oxidation.
37A	347	30	-36.2	0.0065	~~Wetted~~	Some intergranular attack.
29A	347	60	-17.2	0.011	Yes	Oxidized slightly.
2A	347 (Stressed)	12	---	0.002	---	---
336-62-1	347 (Ann)	14	-3.8	0.0025	Yes	Intergranular cusps.
336-65-1	347 (Ann)	14	4.7	0.0014	Yes	Some intergranular cusps.
336-66-1	347 (Ann)	14	-4.1	0.0025	Yes	Some intergranular cusps.
336-64-1	347 (Ann)	14	-3.4	0.0016	Yes	Some intergranular cusps.
106	304	5	-8.9	---	Yes	
		13	-5.1	0.0033	Yes	Rerun #106
134	304 (Carburized)	14	-8.7	0.0052	Yes	No carburization noted.
102	304 (Stressed)	12	-13.5	0.0038	Yes	.0047" corrosion one side. Crystal deposition.
303-156-4	304L (Electropolished)	5	-3.0	0.0012	---	---
303-136	304L (Electropolished)	10	-5.4	0.001	---	---
1A	304L (Stressed)	12	---	0.0032-42	---	---
36	304L	12	-4.1	0.0028	Slightly	---
36A	304L	30	-28.0	0.0096	Yes	
303-160-2	304L (Electropolished)	43	-12.7	0.0024	---	
66	304L (Stressed-compression)	12	-2.45	0.0014	Wetted	0.0038 and 0.002" corrosion on sides.
43	304L (Oxidized 3 hr 1000°F)	1	0	---	No	
	304L (Oxidized 3 hr 1000°F)	12	-0.5	0.00008	Pin Point	Rerun #43

*See Table 3 for heat treatment procedure and Table 4 for surface treatment.

TABLE 10
Page 3

Test No.	Material & Condition*	Test Time, Days	Weight Change, Mg	Penetration, Inches	Wetted	Remarks
61	310	12	-49.7	0.0044	Yes	Some crystal deposition
54	316	12	-16.6	0.0014	Yes	
54A	316 (Polished side)	12	-2.0	0.0028	Yes	
	(Passivated side- P₁ Treatment)			0.0016	Yes	Intergranular attack
83	321	12	-19.3	0.0047	Pin point	
83A	321	30	-11.85	0.0042	Yes	
81	15-15N	12	-10.55	0.0027	Yes	Some crystal deposits.
62	15-15N	12	-33.95	0.0038	Yes	Crystal deposit.
81A	15-15N + .0002% Ti added	12	-0.7	0.0008	Yes	Some deposits.
86	19-9DL	14	-16.7	0.0035	Yes	
97	19-9DL	14	-8.3	0.004	Yes	
86A	19-9DL	21	-11.3	0.0063	Yes	Oxidized slightly.
98	19-9DL + .0002% Ti added	14	+0.4	0.0008	Yes	Some crystal deposition.
99	19-9DL + .0002% Ti added	14	+0.4	---	Yes	
		14	-0.5	0.00028	No	Rerun #99. Slight corrosion. Crystal deposit.
84	Carp 20Cb	12	-48.7	0.0040	Yes	
303-162-1	Carp 20Cb	19	-92.5	0.0054	Yes	
303-160-4	Carp 20Cb	43	-148.0	0.0620	Yes	
84A	Carp 20Cb + 0.0002% Ti added	12	-0.5	0.0013	Yes	Intergranular attack, partially.
51	MS-201	12	-10.9	0.0033	Yes	
51A	MS-201	14	-12.0	0.004	Yes	

*See Table 3 for heat treatment procedure and Table 4 for surface treatment.

TABLE 10
Page 4

Test No.	Material & Condition*	Test Time, Days	Weight Change, Mg	Penetration, Inches	Wetted	Remarks
220	347 (Stressed)	30	-2.8	0	Slight	Corrosion on side of specimen.
221	347 (Stressed)	60	-11.7	0.0014	Yes	
255A	347 (Ann) Hg with 1.9 mg Co	14	-6.9	0.0008	Yes	Intergranular layer and crevice attack.
231	347 (Ann) + 380 ppm graphite	12	-3.9	0.0005	Slight	
232	347 (Ann) + 380 ppm graphite	30	-1.6	0.0007	Slight	
237	347 (Ann) + 9mm Hg-H_2	13	-1.9	0	Yes	Grey layer.
238	347 (Ann) + 9mm Hg-O_2	13	-2.7	0.0033	Slight	Intergranular leached attack.
244	347 (Cl_3 Treatment)	12	-5.3	0.0016	Yes	
266	347 (Ann)	14	-6.2	0.0014	Yes	Also intergranular layer.
239	347 (Ann) + 9mm Hg-N_2	13	-0.5	0.0011	Yes	One area.
266A	347 (Ann)	14	-6.6		Yes	
267	347 (Ann) -1/2 size specimen	14	-3.1	0.0016	Yes	Also intergranular layer & deposition.
276A	347 (Ann) -1/2 size specimen	14	-3.2		Yes	
268	347 (Ann)	30	-6.7	0.0033	Yes	
268A	347 (Ann)	30	-7.5	0.0024	Yes	Some intergranular attack.
269	347 (Ann) -1/2 size specimen	30	-4.8	0.0012	Yes	Some deposition & intergranular attack.
269A	347 (Ann) -1/2 size specimen	30	-4.8	0.0012	Yes	Intergranular attack.
161	304L + 2 ppm Ti	12	0			
161	Rerun above in clean Hg	30	-3.5		Yes	
161	Rerun "rerun" above in clean Hg	30	-1.5	0.0014*	Yes	*One area. Pitting .0003" deep.
243	310 (Cl_3 Treatment)	12	-45.1	0.0052	Yes	
242	316 (Cl_3 Treatment)	12	-26.1	0.0055	Yes	
241	321 (Cl_3 Treatment)	12	-7.5	0.0016	No	Halfmoons started from pits.
152	304 + 2 ppm Ti	12			Yes	
	Rerun above in clean Hg	21	-16.9	0.0085	Yes	Many small areas of attack.
161	304L + 2 ppm Ti	12	-0.4		Yes	
161A	Rerun above in clean Hg	30	-4.6	0.003	Yes	Few areas of attack.

*See Table 3 for heat treatment procedure and Table 4 for surface treatment.

TABLE 11

BENT REFLUX TUBE TEST DATA AT 900°F FOR PRECIPITATION HARDENING STAINLESS STEELS

Test No.	Material and Condition*	Test Time, Days	Weight Change, Mg	Penetration, Inches	Wetted	Remarks
94	PH15-7Mo (Cond TH1050)	14	-0.1	0.00013	YES	
303-151	PH15-7Mo (Cond A)	10	-1.1	0.0018		
303-154	PH15-7Mo (oxidized 24 hr 900°F)	10	-0.2	0.0016		
303-155	PH15-7Mo (Cond A)	10	0	0.0006		Not vacuum annealed
303-150	PH15-7Mo (Cond A)	10	-0.9	0.0016		
303-164-1	PH15-7Mo (Cond TH1050)	11	-0.2	0.0008		
303-156-5	PH15-7Mo (Cond A)	5	0	0.0012		
303-164-2	PH15-7Mo (Cond TH1050)	67	-2.9	0.0005		
3A	PH15-7Mo (Cond A) (Stressed)	12	---	0.0012		
303-160-3	PH15-7Mo (Cond A)	43	-4.7	0.04		
63	PH15-7Mo (Cond TH1050)	30	-1.1	0.00028	YES	Some crystal deposits. Intergranular attack.
95	PH15-7Mo (Cond TH1050) ÷ .0002% Ti added	12	0	0	YES	
155	PH15-7Mo (Cond A)	30	-1.2	0.0001	YES	

*See Table 3 for heat treatment procedure and Table 4 for surface treatment.

TABLE 11 – Page 2

Test No.	Material and Condition*	Test Time, Days	Weight Change, Mg	Penetration, Inches	Wetted	Remarks
155A	PH15-7Mo (Cond A)	30	-0.7	----	YES	
157	PH15-7Mo (Cond TH1050)	30	-0.5	0.00008	YES	
157A	PH15-7Mo (Cond TH1050)	30	-1.4	----	YES	
156	PH15-7Mo (Cond A)	60	-3.5	0.00017	YES	Crevice-like attack.
156A	PH15-7Mo (Cond A)	60	-3.4	----	YES	
158	PH15-7Mo (Cond TH1050)	60	-1.5	0.0003	YES	Intergranular cusps. Deposition.
158A	PH15-7Mo (Cond TH1050)	60	-1.6	----	YES	
96	PH15-7Mo (Cond TH1050) + 0.002% Ti	12	0	----	YES	
		12	0	0.00005	NO	rerun #96
23	AM350 (DA)	12	-0.3	0	SLIGHTLY	
72	AM350 (DA)	30	-1.7	0.0008	YES	
72A	AM350 (DA) (Oxidized 3 hr 1000°F)	30	-0.8	0.0008	PIN POINT	
153	AM350 (Ann)	30	-2.8	----	YES	
153A	AM350 (Ann)	30	-1.5	0.0027	YES	
154A	AM350 (Ann)	60	-4.4	0.0042	YES	
154	AM350 (Ann)	60	-6.2	0.0042	YES	Crevice and pitting attack.
45	A286 (Ann)	12	-45.2	0.0045	YES	
46	A286 (Aged)	12	-49.5	0.0039	YES	
13	XCR (HT)	12	+0.1	----	SLIGHTLY	
13A	XCR (HT)	30	-12.0	0.002	YES	Sigma phase not attacked.
13AA	XCR (HT)	30	-3.5	0.002	YES	
14	17-4 PH (Cond TH1050)	12	-0.8	0	NO	
15	17-4 PH (Cond A)	12	-0.7	0.0008	NO	

*See Table 3 for heat treatment procedure and Table 4 for surface treatment.

TABLE 11 - Page 3

Test No.	Material and Condition*	Test Time, Days	Weight Change, Mg	Penetration, Inches	Wetted	Remarks
303-109-1	17-4PH (Cond TH1050)	12	-0.8			
14A	17-4PH (Cond TH1050)	30	-0.2	0.00013	PARTIAL	
14AA	17-4PH (Cond TH1050)	30	-1.8	0.00027	YES	Partial crevice attack. Some crystal deposit.
140	17-4PH (Cond TH1050)	30	-1.1	0.0003	YES	Some crevice attack.
140A	17-4PH (Cond TH1050)	30	-1.4		YES	
14B	17-4PH (Cond TH1050)**	30	-0.7	0.00028	PIN POINT	Intergranular crevice attack.
141	17-4PH (Cond TH1050)	59	-1.5	0.0006	YES	Intergranular and crevice attack.
141A	17-4PH (Cond TH1050)	59	-2.1	---	YES	
60	17-4PH (Cond TH1050)	12	-1.4	0.0012	YES	Intergranular attack. Crystal deposit.
60A	17-7PH (Cond A)	12	-3.5	0.0002	YES	
164	PH15-7Mo (TH1050) + 2ppm Ti	14	-0.6		YES	
164	Rerun above in clean Hg	30	0	0.00028	NO	Intergranular attack.
164A	PH15-7Mo (TH1050) + 2ppm Ti	14	-0.2		YES	
164A	Rerun above in clean Hg	30	0	0.0002	NO	Wedge layer and crevice attack.
165	PH15-7Mo (TH1050) + 2ppm Ti	14	-0.3		YES	
165	Rerun above in clean Hg	58	-0.5	0.00013	NO	Few Areas - intergranular attack.
165A	PH15-7Mo (TH1050) + 2ppm Ti	14	-0.6		YES	
165A	Rerun above in clean Hg	58	-0.6	0.00013	NO	Some pitting.

*See Table 3 for heat treatment procedure and Table 4 for surface treatment.
**(O_1 Treatment)

TABLE 11 - Page 4

Test No.	Material and Condition*	Test Time, Days	Weight Change, Mg	Penetration, Inches	Wetted	Remarks
197	PH15-7Mo (TH1050) + 2ppm Ti	30	-0.5	0.0005	YES	Pits. Layer deposition.
247	PH15-7Mo (TH1050) (Cl$_3$ treatment)	12	-1.5	0.00012	YES	Crevice attack.
248	17-4PH (TH1050) (Cl$_3$ treatment)	12	-0.1	0.0001	PARTIAL	Crevice attack.
198	AM350 + 2ppm Ti (Ann)	30	-1.5	0.0005	YES	.00014" crevice attack.
198A	AM350 + 2ppm Ti (Ann)	62	-1.3	0.00028	YES	
197A	PH15-7 Mo (TH1050) + 2ppm Ti	43	-2.4			Exploded

*See Table 3 for heat treatment procedure and Table 4 for surface treatment.

TABLE 12

BENT REFLUX TUBE TEST DATA AT 900°F FOR NON-FERROUS METALS AND ALLOYS

Test No.	Material & Condition *	Test Time, Days	Weight Change, Mg	Penetration, Inches	Wetted	Remarks
71	Aluminum (O_1 Treatment)	12	−555.9	—	Yes	Completely dissolved.
73	Beryllium	12	−7.0	0.0016	Yes	Crevice attack
35	Cobalt (As cast)	12	+0.1	0	Yes	
35A	Cobalt (As cast)	32	−4.8	0	Yes	Some crystal deposition
38	Chromium (As cast)	1	−0.4	—	Yes	
38 336−	Chromium	13	−0.6	0.0004	No	Rerun. Crevice attack
41−1	Chromium	2	−4.1	—	Yes	
38A	Chromium	12	−26.7	0.0022	Yes	Crevice attack
113	Chromium (Oxidized 1/2 hr 1650°F)	14	−3.6	0	Pin-point	Surface roughened
39	Haynes Alloy No. 25	1	−0.45	—	—	
39	Haynes Alloy No. 25	13	−0.75	0.00013	—	Rerun. Some crystal deposition
117	Haynes Alloy No. 25	12	−0.6	0.00028	Yes	Crevice attack
117A	Haynes Alloy No. 25	30	−0.4	0.00028	Yes	Crevice attack. Some crystal deposition
146	Haynes Alloy No. 25	60	−4.1	—	Yes	
146A	Haynes Alloy No. 25	60	−6.7	0.00028	Yes	Surface roughened to 0.00014"
170	Haynes Alloy No. 25 (Electropolished)	12	−0.9	0.0004	Yes	Intergranular attack
170A	Haynes Alloy No. 25 (Electropolished)	12	−1.6	0.0005	Yes	Intergranular attack. Some crystal deposition
171	Haynes Alloy No. 25 (Electropolished)	60	−5.8	—	Yes	
172	Haynes Alloy No. 25	12	−2.3	0.00028	Yes	Some intergranular attack
172A	Haynes Alloy No. 25	12	−1.7	0.0004	Yes	Some intergranular attack
173	Haynes Alloy No. 25	60	−9.2	0.0011	Yes	Crevice attack
9	Inconel	12	−49.4	0	Yes	Surface eaten away in part
68	Manganese (Electrolytic)	12	−1393.0	—	Yes	Completely amalgamated

* See Table 3 for heat treatment procedure and Table 4 for surface treatment.

TABLE 12
Page 2

Test No.	Material & Condition*	Test Time, Days	Weight Change, Mg	Penetration, Inches	Wetted	Remarks
47	Molybdenum	12	-0.2	0	Yes	
30A	Molybdenum	30	+0.25	0	No	
30AA	Molybdenum	35	+0.46	0	No	
30	Molybdenum (.5% Ti)	73	0	0	No	
116	Nichrome (oxidized 1/2 hr 1650°F)	12	-305.7	0.0015	Yes	Pitting
	Nickel (electrolytic)	8	-358	—	Yes	
70	Nickel (electrolytic)	12	-46.4	0.0025	Yes	Crevice attack. Black powder on surface.
114	Nickel (electrolytic, Oxidized 1/2 hr. 1650°F)	12	-56.6	0.0055	Pin-point	Crevice attack.
7	Columbium (cold rolled)	12	-0.9	0	Yes	Laminated coupon. Results may be erroneous
7C	Columbium (cold rolled)	30	+0.2	None	Partial	
7B	Columbium (Temescal ingot)	12	-0.2	0	No	
7A	Columbium (Temescal ingot)	30	0	0	No	
7AA	Columbium (Temescal ingot)	33	+0.5	0	Yes	
69	Platinum	13	-383.3	—	Yes	Completely dissolved
55	Stellite No. 3	12	-0.9	0	Yes	
26	Stellite No. 6 (cast)	12	-0.9	0	Yes	
26A	Stellite No. 6 (cast)	30	-2.7	0.0005	Yes	
58	Stellite Star J	12	-0.4	0.0002	No	Surface roughened. Some crystal deposition
8	Tantalum	26	0	0	No	
8A	Tantalum	30	0	0	No	
8AA	Tantalum	34	0	—	Slightly	
25	Titanium	12	-33.5	0.0014	Yes	Pitted to depth of 0.03"
24	Tungsten	12	0	0	No	
24A	Tungsten	30	0	0	No	
19	Zircaloy-1	12	-223.0	0.046	Yes	

* See Table 3 for heat treatment procedure and Table 4 for surface treatment.

TABLE 12
Page 3

Test No.	Material & Condition*	Test Time, Days	Weight Change, Mg	Penetration, Inches	Wetted	Remarks
48	Zirconium (reactor grade)	12	---	---	Yes	Appeared to be severely attacked. Burned upon exposure to air.
180	Rene 41	12	-10.0	0.00024	Yes	Crevice attack parallel to surface.
180A	Rene 41	30	-2.5	0.0013	Yes	Some crevice attack.
179	Waspalloy	12	-11.4	0.0005	Yes	Some Intergranular and crevice attack.
179A	Waspalloy	30	-20.6	0.0007	Yes	
178	AF1753	11	-11.0	0.0014	Yes	Intergranular attack.
178A	AF1753	30	-26.8	0.0016	Yes	Some intergranular and crevice attack.
177	Inconel X	12	-10.9	0.0015	Slightly	Cracks at layer-base metal interface.
177A	Inconel X	30	-26.4	0.0025	Yes	Intergranular cusps. Cracks as in Test 177.
189	Haynes Alloy No. 25 + 2ppm Ti	30	-0.1	0.00029	Slightly	Deposit and pitting.
236	Haynes Alloy No. 25 + H_2 at 9mm Hg Pressure	30	-1.8	0.0005	Yes	Crevice attack.
211	Haynes Alloy No. 25 (Stressed)	29	-2.3	0.0004		.0006" on compression side. Tube Exploded.
212	Haynes Alloy No. 25 (Stressed)	60	-2.1	0	Yes	
171A	Haynes Alloy No. 25 (Electro-polished)	60	-4.5	0.001	Yes	Crevice attack.
173A	Haynes Alloy No. 25	60	-2.2	0.0007	Yes	Crevice attack.
189A	Haynes Alloy No. 25 + 2ppm Ti	30	-0.2	0.00028	Slightly	Crevice attack.
190	Haynes Alloy No. 25 + 2ppm Ti	60	-1.9		Slightly	
190R	Rerun 190 in Clean Hg	60	-0.3	0.0004	No	Crevice attack - slight
190A	Haynes Alloy No. 25 + 2ppm Ti	60	-1.5	0	Slightly	
213	Haynes Alloy No. 25 + 0.1% Cerro-bend	30	-1.7	0	Yes	

* See Table 3 for heat treatment procedure and Table 4 for surface treatment.

TABLE 12
Page 4

Test No.	Material & Condition*	Test Time, Days	Weight Change, Mg	Penetration, Inches	Wetted	Remarks
214	Haynes Alloy No. 25 + 0.1% Cerro-band	12	-1.1	0.00026	Yes	Crevice attack. More attack than usually visible.
215	Haynes Alloy No. 24 + 1/2% Na	39	-0.3	0	Yes	Deposition.
216	Haynes Alloy No. 25 + 1/2% Na	12	-1.2	.00026	Yes	Parallel surface crevice attack.
222	Haynes Alloy No. 25	12	-1.2	0.0007	Yes	Intergranular attack.
223	Haynes Alloy No. 25	30	-2.6	0	Yes	
224	Haynes Alloy No. 25 (Oxidized 1650°F)	30	-0.4	0.00014	No	Roughening.
235	Haynes Alloy No. 25 (No polish)	30	0	0	Slightly	Wedge penetration of I.D. due to acid pickle at mill.
253	Haynes Alloy No. 25 (Ag)	13	-0.6	0	Yes	
254	Haynes Alloy No. 25 (Ag)	30	-2.1	0.0008	Yes	Intergranular crevice attack and grain removal.
246	Haynes Alloy No. 25 (Cl$_3$ treatment)	12	-2.1	0.0005	Yes	Crevice attack.
128	Elgiloy	12	-8.6		Yes	
129	Eligiloy	30	-18.7	0.0034	Yes	One phase corrosion resistant.
196	Tantalum	62	0		No	
196A	Tantalum	62	0		No	
219	Tantalum (Stressed)	30	-0.3	0.00005	No	Crevice attack?
240	Nichrome	12	-56.9	0.0004	Yes	Pitted. Crystal deposition.
255	Cobalt	20	-1.9		Yes	

* See Table 3 for heat treatment procedure and Table 4 for surface treatment.

TABLE 12
Page 5

Test No.	Material & Condition	Test Time, Days	Weight Change, Mg	Penetration, Inches	Wetted	Remarks
261	Rene 41(HT)	12	-38.9	0.0005	Yes	Pitted. Black powder.
261A	Rene 41(HT)	29	-49.3	0.0045	Yes	Pitted. Black powder.
262	Waspalloy (HT)	12	-4.1	0.0007	Yes	
262A	Waspalloy (HT)	29	-14.8	0.0012	Yes	Crevice - like layer.
162	Haynes Alloy No. 25 + 2ppm Ti	14	0		Slight	
162R	Rerun 162 in clean Hg	30	0	0.00005	No	Crevice attack and deposition.
162A	Haynes Alloy No. 25 + 2ppm Ti	14	0		Slight	
162AR	Rerun 162A in clean Hg	30	0	0.00017	No	Crevice attack and deposition.
163	Haynes Alloy No. 25 + 2ppm Ti	12	-0.1		Slight	
163R	Rerun 163 in clean Hg	60	-0.3	0	No	
163A	Haynes Alloy No. 25 + 2 ppm Ti	12	-0.1		Slight	
163AR	Rerun 163A in clean Hg	60	-0.6	0.00005	No	Slight crevice attack.

* See Table 3 for heat treatment procedure and Table 4 for surface treatment.

TABLE 13

BENT REFLUX TUBE TEST DATA AT 900°F FOR NON-METALS

Test No.	Material and Condition	Test Time, Days	Weight Change, Mg	Penetration, Inches	Wetted
5	Titanium Carbide (K162B)	12	0	0	No
6	Titanium Carbide (K150A)	12	0	0	No
1	Titanium Carbide (K150A)	26	0	0	No
6A	Titanium Carbide (K150A)	32	-0.4	0.00028	No
111	Titanium Carbide (K151A)	32	-7.9	0.00035	No
2	Tungsten Carbide (CA-8)	12	+0.2	0	No
2A	Tungsten Carbide (CA-8)	31	0	0	No
4	Tungsten Carbide (K96)	12	+0.1	0	No
3	Ferro-Tic	12	+0.2	0	No
3A	Ferro-Tic	32	-0.6		No
28	Pyroceram (#9608)	12	+0.1	---	No
67	ATJ Graphite	12	-0.2	---	No
130	Alumina (99.9%)	12	0	---	No
131	Alumina (99.9%)	30	+0.5	---	No

TABLE 14

BENT REFLUX TUBE TEST DATA AT 900°F FOR VARIOUS BIMETALLIC COMBINATIONS (SAME COMPARTMENT)

Test No.	Material and Condition	Test Time, Days	Weight Change, Mg	Penetration, Inches	Wetted	Remarks
118	17-4PH 18-4-1	12	-0.8 -0.6	0.00005 0.0002	No No	
119	17-4PH 19-9DL	12	-0.4 -12.3	0 0.004	Yes Yes	Some deposit and pitting.
120	17-4PH Titanium Carbide (K151A)	12	-1.6 -2.9	0.00028 0.002	Yes Yes	Crevice attack.
121	17-4PH Inconel	12	0 -21.3	0 0.0007	Yes Yes	Irregular surface. Deposit. Surface eaten away.
122	17-4PH 347	12	-1.0 -9.1	0 0.0036	Yes Yes	Surface roughening. Deposit. Intergranular attack.
123	17-4PH PH15-7Mo	12	-1.3 -1.0	0 0.001	Yes Yes	
124	17-4PH 321	12	-0.4 -2.0	0 0.004	Yes Yes	Irregular surface deposit. Some crystal deposits.
125	17-4PH Ferro-Tic	12	-1.5 -0.7	0.00028 0.00023	Pin-point Pin-point	Crystal deposit.
126	17-4PH Tungsten carbide (CA8)	12	-0.5 -0.3	0.00028 0.0003	Yes No	Some deposits. Some deposits.

TABLE 14 - Page 2

Test No.	Material and Condition	Test Time, Days	Weight Change, Mg	Penetration, Inches	Wetted	Remarks
127	17-4PH	12	-1.1	0.00005	Yes	
	431		-1.5	0.00022	Yes	Surface roughened
147	17-4PH	13	0	0.00014	Yes	Crevice attack, deposit.
	Haynes Alloy No. 25		-0.6	0.00017	Yes	Some intergranular attack. Deposit.
148	Haynes Alloy No. 25	13	-1.4	0.0002	Yes	Some crystal deposits.
	304		-14.4	0.0043	Yes	Some crystal deposits.
149	Haynes Alloy No. 25	13	-1.2	0.0003	Yes	Crevice attack
	410		0	0.00008	Yes	Some intergranular attack.
174	Tantalum	12	+0.3	0	Yes	Diffused layer.
	347		-5.6	0.0005	Yes	
175	Tantalum	11	+0.3	0.00028	Yes	Crevice attack. Crystal deposition.
	410		-0.4	0.0002	Yes	Crevice attack.
176	Haynes Alloy No. 25					
	+ 2ppm Ti	12	-0.3	---		
	410 + 2ppm Ti	12	-0.3			
	Rerun above in clean Hg:					
	Haynes Alloy No. 25	12	0	0.00075	No	Crevice attack and deposition.
	410	12	0	0.0004	Slight	Crevice attack.
182	PH15-7Mo Welded to	30	-0.8	0.0003	Yes	Weld attacked -.0003 inch layer.
	Hayes Alloy No. 25	--	---	0.0005	-	Deposit.

TABLE 14 - Page 3

Test No.	Material and Condition	Test Time, Days	Weight Change, Mg	Penetration, Inches	Wetted	Remarks
187	17-4PH welded to Haynes Alloy No. 25	30 --	-1.0 ---	0.0006 0.0004	Yes --	Crevice attack and deposition, Weld attack-.0004 inch.
187A	17-4PH welded to Haynes Alloy No. 25	30 ---	-1.6 ----	0.00005 0.00028	Yes --	Weld attacked. Deposition on both.
191	Haynes Alloy No. 25 W	12	-0.3 0	0.00013 0	No No	Crevice attack and deposit. Deposit layer.
192	Haynes Alloy No. 25 Cb	12 --	-2.6 +1.0	0.0003 0	Yes Yes	.0004 intergranular attack. Diffusion of material. Attack?
193	Haynes Alloy No. 25 Ta	12 --	-2.5 +0.3	0.00014 0	Yes Yes	Diffusion of material.
194	347 (Ann) TiC (K150A)	12 ---	-14.4 -0.1	0.0032 0.0005	Yes Yes	Intergranular layer.
195	347 (Ann) WC (CA8)	12 ---	-6.0 0	0.0003 0.00028	Yes Yes	Intergranular and crevice attack. Cracked layer. Deposition.
182A	PH15-7 Mo welded to Haynes Alloy No. 25	30	0	0.00012 0.000025	Slight	Weld attack .0003"

TABLE 15

BENT REFLUX TUBE TEST DATA AT 900°F FOR VARIOUS BIMETALLIC COMBINATIONS (Separate Compartments)*.

Test No.	Material & Condition	Test Time, Days	Weight Change, Mg	Penetration, Inches	Wetted	Remarks
10V	Nickel	12	-52.5	0.0037	Yes	
10VA	Nichrome		+11.4	0.0023	Yes	Crystal deposit 0.002" thick.
11V	Nichrome	12	-23.8	0.0005	Yes	Crystal deposit 0.0008" thick.
11VA	Nickel		-83.5	0.0013	Yes	Crystal deposit
87	Nickel	14	-779.5	0.090	Yes	Dissolved
87A	Nickel		-104.3	0.0044	Yes	Crystal deposit
88	Nickel	14	-480.8	0.0082	Yes	
	Armco Iron		+8.4	0	Yes	Crystal deposit
89	Armco Iron	14	+4.5	0	Yes	Crystal deposit. Attack on deposit
	Nickel		-835.5	0.096	Yes	Dissolved
90	Nickel	14	-605.8	0.0027	Yes	
	Chromium		-21.4	0.001	Yes	Crystal deposit on uncorroded side.
91	Chromium	14	-17.5	0	Yes	Surface roughened.
	Nickel		-518.5	0	Yes	Surface roughened. Crystal deposits.
92	Armco Iron	14	-0.1	0	Yes	Surface roughened, Crystal deposit.
	Chromium		-14.6	0	Yes	Surface roughened. Crud layer.
93	Chromium	14	-16.2	0	Yes	Crystal deposits. Surface crud.
	Armco Iron		-0.2	0	Yes	Surface roughened. Some crystal deposits
150	Haynes Alloy No. 25	13	+0.6	0.00013	Yes	Crystal deposits.
	410		-0.3	0.00028	Yes	Crevice attack. Some deposits
151	410	16	0	0.0003	Yes	Intergranular attack. Grey deposit.
	Haynes Alloy No. 25		-1.2	0.0004	Yes	Some intergranular attack.

*First material listed of each pair placed in upper condenser compartment.

TABLE 16

. BENT REFLUX TUBE TEST DATA AT 700°F FOR VARIOUS MATERIALS AND BIMETALLIC COMBINATIONS

Test No.	Materials and Condition*	Test Time, Days	Weight Change, Mg	Corrosion Layer, Inches	Wetted	Remarks
208A	A286 (Ann)	12	0	--	No	
208	A286 (Ann)	12	0	0.00008	No	Crystal deposition.
209A	347 (Ann)	12	-0.2	--	Yes	
209	347 (Ann)	12	-0.6	0.00018	Yes	Pitting in corrosion interface.
336-103-1	310	12	-1.3	0.00028	Yes	Some crevice attack.
336-104-1	310	12	-1.4	0.00028	Yes	Some crevice attack.
202	Carp. 20 Cb	12	-0.5	--	Yes	
202A	Carp. 20 Cb	12	-0.5	0	Yes	
204	316	12	-3.1	0.0008	Yes	
204A	316 (Electropolished)	12	-2.6	0.0012	Yes	Intergranular cusps.
205	Haynes Alloy No. 25	12	-0.1	0.00005	Slight	Crevice attack.
210	347 (Ann)	30	-3.3	0.0007	Yes	Some crevice-intergranular attack.
210A	347 (Ann)	30	-2.7	--	Yes	

* See Table 3 for heat treatment procedure.

TABLE 16
Page 2

Test No.	Materials and Condition*	Test Time, Days	Weight Change, Mg	Corrosion Layer, Inches	Wetted	Remarks
336-						
107-1	Zr	12	+247.5	0.0038	Yes	Amalgam layer.
108-1	Zr	12	+240.6	--	Yes	
183	Kovar	12	-13.0	0.0015	Yes	Vapor. Cracks in layer.
183A	Kovar	12	-13.3	--	Yes	
184	Kovar	30	-11.6	0.003	Yes	Vapor. Cracked. Some deposition.
184A	Kovar	30	-33.5	0.0041	Yes	
185	Hoskins 875	12	-0.2	0.011	Yes	Vapor. Crack-like penetrations.
185A	Hoskins 875	12	-0.2	--	Yes	
188	Kanthal A-1	12	+0.5	--	Yes	Vapor.
188A	Kanthal A-1	12	+0.5	--	Yes	Slight crevice attack and deposition.
203	Alfenol	12	+0.5	--	No	Pitting.
203A	Alfenol	12	+0.5	--	Yes	
207	Kovar	12	-5.0	0.0016	Yes	Vapor. Half-moon layer.
251	Inconel	12	-9.7	0.0005	Yes	Vapor. Pitting attack.
251A	Inconel	12	-8.4	--	Yes	Vapor.
252	Inconel	12	-12.7	0.00013	Yes	Wedge attack.
252A	Inconel	12	-16.8	0.0006	Yes	Pitting, crevice & wedge attack.

*See Table 3 for heat treatment procedure.

TABLE 16
Page 3

Test No.	Materials and Condition*	Test Time, Days	Weight Change, Mg	Corrosion Layer, Inches	Wetted	Remarks
199	Haynes Alloy No. 25 brazed with AMS4778 to Tran-Cor T	12	+0.8	0	No	Roughening of braze & H.S. 25. Some deposits on H.S. 25.
199A	Haynes Alloy No. 25 brazed with AMS4778 to Tran-Cor T	12	+0.2	0	No	Vapor.
200	17-4PH brazed with AMS4778 to 17-4PH	12	0	0.0002	No	Attack on braze and 17-4PH. Grey Layer.
200A	17-4PH brazed with AMS4778 to 17-4PH	12	+0.3	--	No	Vapor.
201	17-4PH brazed with AMS4778 to Tran-Cor T	12	+0.3	0	No	Roughening of all components. Deposits and grey layer on 17-4 PH and Tran-Cor T
201A	17-4PH brazed with AMS4778 to Tran-Cor T	12	+0.4	--	No	Vapor.

*See Table 3 for heat treatment procedure.

TABLE 17

BENT REFLUX TUBE TEST DATA AT 1100°F FOR VARIOUS MATERIALS

Test No.	Materials and Condition*	Test Time, Days	Weight Change, Mg	Corrosion Layer, Inches	Wetted	Remarks
181D	Haynes Alloy No. 25	12	-16.9	0.0008	Yes	Dark layer.
181	Haynes Alloy No. 25	12	-1.2	0.00028	No	Questionable.
258	PH15-7Mo (TH1050)	12	-5.5	0.0005	Yes	Crevice attack.
260A	Cb	12	+0.5	0.00028	Yes	Crevice layer(?)
281	347 (Ann)	12	-11.5	0.0016	Yes	Crevice attack.

*See Table 3 for heat treatment procedure.

TABLE 18

BENT REFLUX TUBE TEST DATA AT 900°F FOR VARIOUS MATERIALS AND ADDITIVES

Test No.	Material and Additive	Test Time, Days	Weight Change, Mg		Corrosion Layer, Inches		Remarks
			Condenser	Boiler	Condenser	Boiler	
303-144	304L + 0.5g $HgCl_2$	11	-36.6	-70.7	0.0016	0.00028	Deposit in condenser.
303-138	304L + HgO	10	- 0.3	- 3.7			
303-147	304L + $HgNO_3$	12	- 0.9	-56.8	0		
303-148	304L + Hg_2SO_4	12	- 0.4	+ 2.8	0.0008		
303-145	304L + Cu	12	- 2.7	+ 1.4	0.0016		
303-146	304L + S_n	12	- 2.6	+70.8	0.002		
303-174-1	304L + Cd	12	- 3.1	+ 1.4	0.00011	0	Crystal deposit in boiler.
303-174-2	304L + Cd	13	- 3.5	+ 2.2			
336-9-1	304L + Cd	50	-21.1	+21.9	0.005	0	Crystal deposit in boiler.
336-2	304 + 0.5g Hg_2SO_4	12	0	- 2.3		0	Deposit in boiler.
336-20	304 + 0.001g Hg_2SO_4	5	- 5.0				
336-22	304 + 0.01g Hg_2SO_4	5	- 0.6				
336-30	304 + 0.1g Hg_2SO_4	5	- 2.0				
336-21	304 + 0.001g Hg_2SO_4	12	- 0.4	- 3.0	0.0034	0.0008	Slight deposit in boiler.
336-32	304 + 0.01g Hg_2SO_4	12	- 5.3	- 2.1	0.0023		
336-27	304 + 0.1g Hg_2SO_4	12	- 0.1	- 1.9	0.0033	0.00028	Deposition in condenser. Deposition in boiler.
336-51	304 + 0.001g Hg_2SO_4	12	- 0.9		0.002		
336-52	304 + 0.01g Hg_2SO_4	12	- 0.6		0.0025		
336-53	304 + 0.1g Hg_2SO_4	12	- 0.2		0.00015		
336-23	304 + Mineral Oil	12	-28.4		0.0042		
336-28	304 + Mineral Oil	12	- 0.2	- 1.4	0.0013		
336-25	304 + GE-9996 Silicone Oil	12	- 1.2		0.0043		
336-29	304 + GE-9996 Silicone Oil	12	- 2.7	+ 1.4	0.0035	0.0014	Deposit in boiler.
336-35	304 + 0.1g B_2O_3	14	+ 0.3		0		

TABLE 18
Page 2

Test No.	Material and Additive	Test Time, Days	Weight Change, Mg Condenser	Boiler	Corrosion Layer, Inches Condenser	Boiler	Remarks
336-57	304 + 0.1g B_2O_3	12	- 1.0	+ 2.3	0	0.00028	Crevice attack in boiler.
336-36	304 + 0.1g As_2O_3	14	+ 3.1		0.0006		Deposit in condenser.
336-37	304 + 0.03ml H_2O	14	- 0.3		0.0011		
336-59	304 + 0.03ml H_2O	12	-11.1	+ 7.4	0.003	0	Deposition in boiler.
336-38	304 + Te power	14	- 0.3		0.0007		
336-42	304 + 0.1g BaO_2	14	- 1.6		0.00015		Deposit in condenser.
336-43	304 + Sb	14	-12.5		0.0027		Sb located in condenser.
336-54	304 + As	14	+39.5		0.002		As in condenser layer deposit.
336-55	304 + As	14	+62.1		0.0033		As in boiler layer deposit.
336-9	304 + Cd	50	-21.1	+21.9			Cd in boiler.
336-56	304 + Mineral Oil	14	-13.0		0.005		
303-143	347 + 0.5g $HgCl_2$	11	-37.7	-78.6			
303-172	347 + Cd	12	- 6.9	+ 6.2	0.00083	0	Deposit in condenser. Deposit in boiler.
303-174	347 + Cd	12	+68.8	+12.7			
336-10	347 + Cd	43	- 4.6	+ 0.5	0.0033	0	Intergranular layer in condenser. Deposit in boiler.
303-162-3	Carp. 20 Cb + HgO	19	- 0.4	+ 0.8			
303-162-4	Carp. 20 Cb + Hg_2SO_4	19	+ 0.2	- 2.0	0	0	
336-1-1	Carp. 20 Cb + Hg_2SO_4	12	+ 0.1	- 2.9	0	0	Crystal deposit in condenser. Crystal deposit in boiler.
303-173-2	Carp. 20Cb + Cd	12	-33.1	+19.2	0.0039	0	Crystal deposit in boiler.
303-188-1	Carp. 20Cb + Cd	43	-80.6	+ 4.0	-	0.0058	Deposition in condenser.
303-162-2	Carp. 20Cb + Mg	19	-44.8	+34.2	-	0	Deposit in boiler.
303-189-1	Carp. 20Cb + FeSe	12	+ 2.1				
303-187-1	Carp. 20Cb + Al	12	-63.7				

TABLE 18
Page 3

Test No.	Material and Additive	Test Time, Days	Weight Change, Mg Condenser	Boiler	Corrosion Layer, Inches Condenser	Boiler	Remarks
303-185-1	Carp. 20 Cb + S	12	-57.8				
303-186-1	Carp. 20 Cb + I$_2$	12	- 2.9				
303-190-1	Carp. 20 Cb + 0.5g Ti	12	+ 0.2				
303-155	PH15-7Mo + Mg	10	0	- 0.6	0.0006		
303-159-1	PH15-7Mo + 0.5g HgO	20	0	- 1.5			
303-159-2	PH15-7Mo + 0.5g Hg$_2$SO$_4$	20	+ 0.2	- 6.2			
303-158-1	PH15-7Mo + 0.5g HgCl$_2$	20	-54.3	-98.4			
303-158-2	PH15-7Mo + 0.05g HgCl$_2$	20	- 7.0	-22.8			
303-158-3	PH15-7Mo + 0.005g HgCl$_2$	20	- 0.7	- 1.4			
303-158-4	PH15-7Mo + 0.0005g HgCl$_2$	20	- 3.2	+ 2.3			
303-173-1	PH15-7Mo + Cd	12	- 0.1	- 0.2			
303-174-3	PH15-7Mo + Cd	43	- 1.2	- 0.7			

TABLE 19

SUMMARY OF OBSERVATIONS MADE ON FLAT SPECIMENS CONTAINED IN TEST G-4,
TYPE 316 STAINLESS STEEL LOOP

| Material | Boiler | | Condenser | |
	Total Weight Change, Mg.	Observations	Total Weight Change, Mg.	Observations
AM 350	+24.7	Crystalline surface deposit.	+ 2.2	No appreciable attack.
PH 15-7 Mo	+14.0	Crystalline surface deposit.	+ 3.4	No appreciable attack.
Type 347 SS	+ 6.4	Crystalline surface deposit. Tendency towards intergranular penetration.	-28.1	Discontinuous depleted corrosion layer. Tendency towards intergranular penetration.
Type 316 SS	+14.2	Crystalline surface deposit. No tendency towards intergranular penetration	-44.7	Discontinuous depleted corrosion layer. No tendency towards intergranular penetration.
Molybdenum	- 3.5	Cavity-type of dissolution.	- 4.1	Cavity-type of dissolution.
Type 446 SS	+46.2	Crystalline surface deposit.	+ 0.4	No appreciable attack.
Type 420 SS	+19.8	Crystalline surface deposit. Corrosion layer with severe intergranular penetration. Depletion of carbides adjacent to corrosion layer and patches of precipitation of carbides.	- 6.1	Corrosion layer. Depletion of carbides adjacent to corrosion layer.

TABLE 20

FREE ENERGY OF AMALGAMATION AS CALCULATED FROM CATHODIC HALF-WAVE REDUCTION POTENTIALS FOR A NUMBER OF ELEMENTS*

Element	Free Energy of Amalgamation, cal/mole		Element	Free Energy of Amalgamation, cal/mole
Ba	-53,300		Sn	+ 2,760
Mn	-52,800		Pb	+ 2,760
Mg	-33,200		Sb	+ 2,760
Rb	-26,000		Bi	+ 2,760
Ca	-21,200		Cu	+ 7,600
Al	-19,300		Cr	+24,800
Na	-19,100		Ni	+26,700
TL	- 3,800		Fe	+28,600
In	- 2,070		Ga	+31,100
Zn	+ 1,380		Co	+31,400
Cd	+ 1,840		W, Mo, Ta	Not reducible

*Positive values indicate that deposition is associated with marked irreversible polarization (large overpotential).

SNAP II

TOPICALS DISTRIBUTION LIST

Copy No.

Advanced Research Projects Agency   1
The Pentagon
Washington 25, D. C.
     Attn: Dr. Nathan Snyder

Aerospace Technical Intelligence Center   2
The Pentagon
Washington 25, D. C.

Air Force Ballistic Missile Division, Commander   3
Commander, Air Force Ballistic Missile Division
Hq., Air Research and Development Command, USAF
P.O. Box 262
Inglewood, California
     For: Major George Austin

Air Force Special Weapons Center, Commander   4
Commander, Air Force Special Weapons Center
Technical Information & Intelligence Office
Kirkland Air Force Base, New Mexico
     Attn: Delmer J. Trester

Argonne National Laboratory   5
Argonne National Laboratory
Lemont, Illinois

Atomic Energy Commission, Washington   6-10
U.S. Atomic Energy Commission
Technical Reports Library
Washington 25, D. C.
     Attn: J. M. O'Leary
       For: Lt. Col. G. M. Anderson, DRD
            Capt. John Wittry, DRD
            Lt. Col. Robert D. Cross, DRE
            R. G. Oehl, DRE
            Technical Reports Library

<u>Copy No.</u>

Bureau of Naval Weapons   11-14
Chief, Bureau of Naval Weapons
Washington 25, D. C.

Bureau of Ships, Chief   15
Chief, Bureau of Ships
Code 1500
Department of the Navy
Washington 25, D. C.
     Attn: Melvin L. Ball

Canoga Park Office (AEC)   16-17
U.S. Atomic Energy Commission
Canoga Park Area Office
P.O. Box 591
Canoga Park, California
     Attn: S. Stamp

Chicago Operations Office (AEC)   18-19
U.S. Atomic Energy Commission
Chicago Operations Office
P.O. Box 59
Lemont, Illinois
     Attn: D. Reardon and George H. Lee

Chief of Naval Operations   20
Office of the Chief of Naval Operations
Department of the Navy
Washington 25, D. C.

Convair, San Diego   21
Astronautics, Division of General Dynamics
3302 Pacific Highway
San Diego, California
     Attn: F. J. Dore

Department of the Army   22
Atomic Division
Office of Chief of Research and Development
Department of the Army
Washington 25, D. C.

	Copy No.
Diamond Ordnance Fuse Laboratories	23-24
Diamond Ordnance Fuse Laboratories	
Washington 25, D. C.	
Attn: ORDTL 06.33, Mrs. M. A. Hawkins	

Lawrence Radiation Laboratory   25
University of California
Livermore, California

Lockheed Missile Systems Division   26-29
Missile Systems Division
Lockheed Aircraft Corporation
P.O. Box 504
Sunnyvale, California
    Attn: Asst. AF Plant Representative

Los Alamos Scientific Laboratory   30
Los Alamos Scientific Laboratory
P.O. Box 1663
Los Alamos, New Mexico

Marshall Space Flight Center   31-32
National Aeronautics and Space Administration
Huntsville, Alabama
    Attn: Dr. Ernst Stuhlinger

National Aeronautics and Space Administration, Ames   33
Ames Aeronautical Laboratory
Moffett Field, California
    Attn: Smith J. deFrance, Director

National Aeronautics and Space Administration, Cleveland   34
Lewis Flight Propulsion Laboratory
21000 Brookpark Road
Cleveland 35, Ohio
    Attn: Richard Geye

National Aeronautics and Space Administration, Langley   35
Langley Aeronautical Laboratory
Langley Field, Virginia
    Attn: Henry J. E. Reid, Director

Copy No.

National Aeronautics and Space Administration, Washington   36-40
National Aeronautics and Space Administration
1512 H Street, N.W.
Washington 25, D. C.
    Attn: Dr. Addison M. Rothrock

Naval Ordnance Laboratory   41
Commander, U.S. Naval Ordnance Laboratory
White Oak, Silver Spring, Maryland
    Attn: Eve Liberman, Librarian

Naval Research Laboratory   42
Director, Naval Research Laboratory, Code 1572
Washington 25, D. C.
    Attn: Mrs. Katherine H. Cass

Oak Ridge National Laboratory   43
Oak Ridge National Laboratory
Oak Ridge, Tennessee

Office of Naval Research   44
Office of Naval Research
Department of the Navy, Code 735
Washington 25, D. C.
    Attn: E. E. Sullivan
      For: Code 429

Project RAND   45
Director, OSAF Project Rand
Via AF Liaison Office
The Rand Corporation 1
1700 Main Street
Santa Monica, California
    Attn: F. R. Collbohm
      For: Dr. Huth

Rome Air Development Center, Commander   46
Commander, Rome Air Development Center
Griffiss Air Force Base, New York
    Attn: RCSG, Mr. J. L. Briggs

	Copy No.
School of Aviation Medicine, Randolph AFB	47
School of Aviation Medicine, Randolph AFB	
Randolph Air Force Base, Texas	
Attn: Col. J. E. Pickering, Department of Radiobiology	
Thompson Ramo Wooldridge	48,49
Thompson Ramo Wooldridge Inc.	
Staff Research and Development	
New Devices	
P.O. Box 1610	
Cleveland 4, Ohio	
Attn: D. L. Southam	
Wright Air Development Center, Commander	50-52
Commander, Wright Air Development Center	
Wright-Patterson Air Force Base, Ohio	
Attn: WCACT	
For: G. W. Sherman, WCLEE	
Capt. Clarence N. Munson, WCLPS	
WCOS	
Technical Information Service Extension	53-77
U.S. Atomic Energy Commission	
Reference Branch	
Technical Information Service Extension	
P.O. Box 62	
Oak Ridge, Tennessee	
AI Library	78-97
Atomics International	
P.O. Box 309	
Canoga Park, California	
Thompson Ramo Wooldridge Library	98-100